Gene expression analysis for assessment of lymph node metastasis in head and neck squamous cell carcinoma

Genexpressieprofielen voor het vaststellen van halsklier metastase bij hoofd-halsplaveiselcelcarcinoom

(met een samenvatting in het Nederlands)

Proefschrift

ter verkrijging van de graad doctor aan de Universiteit Utrecht
op gezag van de rector magnificus, prof. dr. W.H. Gispen,
ingevolge het besluit van het college voor promoties
in het openbaar te verdedigen op
vrijdag 8 december 2006 des middags te 12.45 uur

door

Paul Roepman

geboren op 18 augustus 1979 te Oosterhout

Promotoren: Prof. dr. F.C.P. Holstege
Prof. dr. P.J. Slootweg

The research presented in this thesis was performed at the Department of Physiological Chemistry and the Department of Pathology, University Medical Center Utrecht, The Netherlands, within the Utrecht Graduate School for Developmental Biology (OOB) and the Centre for Biomedical Genetics (CBG). Financial support for the publication of this thesis by the J.E. Jurriaanse Stichting, University Medical Center Utrecht and Merck B.V. is gratefully acknowledged.

Science is a wonderful thing if one does not have to earn one's living at it
- Albert Einstein

ISBN-10: 90-393-4391-8
ISBN-13: 978-90-393-4391-3

Druk: Ponsen & Looijen b.v., Wageningen

Contents

1

General introduction

General Introduction

Head and neck squamous cell carcinoma

Cancer is an uncontrolled proliferation of cells that can in principle arise from every tissue. Cancer currently accounts for one-fifth of the total mortality in high-income countries and is the second leading cause of death after cardiovascular diseases (1, 2). The incidence of neoplastic disease increases with age and the current increase in life expectancy will unavoidably enlarge the population at risk and increase the prevalence of cancer (3).

Head and neck cancer consists of a heterogeneous group of lesions that arise in the upper aerodigestive tract which includes the oral cavity, pharynx, larynx and sinonasal cavities. The majority of these neoplasms (90 percent) are head and neck squamous cell carcinomas (HNSCC) that develop in the squamous layer of the mucosal lining (Fig. 1.1).

Epidemiology

With about 500,000 new cases each year, HNSCC is the fifth most common malignancy worldwide, with incidence increasing in Western countries (4, 5). In the Netherlands, HNSCC accounts for approximately 2000 new patients every year (6). Occurrence is much higher in certain regions such as South Asia, where it is the most common malignancy and includes up to 50 percent of all cancer related deaths (7). Additionally, incidence is higher for Afro-Americans compared to the Caucasian population (8). The patterns of occurrence reflect the prevalence of the main risk factors of this type of cancer; high tobacco use and alcohol consumption in rich countries as well as chewing of betel quid in Asia (9).

Head and neck cancer occurs 2–3 times more frequently in men compared to women. However, during the last decade the 3.5% yearly increase in oral cancer in the Netherlands is mostly caused by an increased occurrence for women, while the incidence for men remains relatively stable (10). Like most cancers, risk for HNSCC increases with age and is most commonly diagnosed in older patients (2), generally between the 50^{th} and 60^{th} year of age. Less than 10 percent of the patients is initially diagnosed under an age of 45 (10). With the current increasing life expectancy, cancers, including HNSCC, are expected to become an increasing cause of mortality and morbidity. HNSCC is associated with severe disease- and treatment-related morbidity and has a 5-year survival rate of approximately 50%. Although our knowledge about this disease had increased significantly, the survival rate has not improved during the last 20 years (11).

Etiology

Tobacco use and alcohol consumption are the main risk factors for HNSCC. A number of epidemiological studies have established a strong correlation between these two factors and an increased risk for HNSCC. Ninety percent of HNSCC occurs in individuals who are

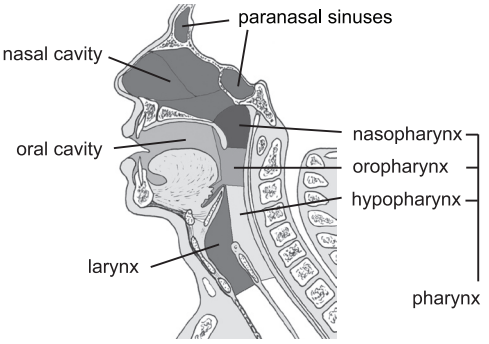

Figure 1.1 | Anatomical subsites of HNSCC. Head and neck squamous cell carcinoma arise in the upper aerodigestive tract which includes the oral cavity, nasal cavity and paranasal sinuses, oropharynx, nasopharynx, hypopharynx and the larynx.

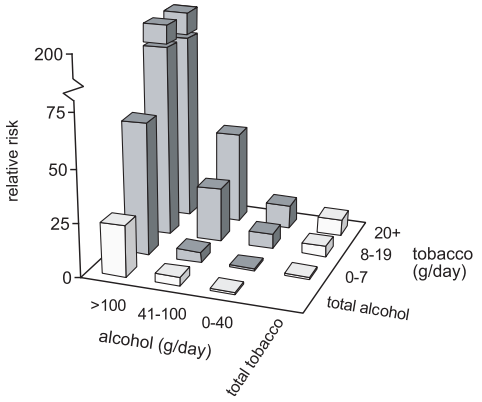

Figure 1.2 | Risk factors for HNSCC. Tobacco use and alcohol consumption are the two main risk factors for HNSCC and give a synergistic effect when combined. Based on Andre *et al*. (13).

heavy smokers or drinkers (12-18). Tobacco use, both smoking and chewing (betel quid), and alcohol consumption are independent risk factors but have a synergistic effect when combined (19, 20). The risk for development of oral cancer is about 3 to 9 times greater in individuals who smoke or drink compared to those who neither smoke nor drink and increases dramatically for persons who smoke and drink heavily (21) (Fig. 1.2). Twenty-five cigarettes and ten glasses of alcohol per day increase the risk for HNSCC up to 200 fold (13). Furthermore, those who started with smoking before an age of 18 have an additional 1.5 times greater risk for developing HNSCC (13). The risk decreases upon ending of smoking and is related to the time span that has passed since stopping (16, 20). Stopping alcohol consumption does not seem to reduce the risk for developing oral cancer (22). Mutations of p53 have been frequently found in HNSCC of smokers and drinkers and suggests that the inactivation of the tumor suppressor gene p53 is important for the cancerous effects of tobacco and alcohol consumption (23).

Although a strong link exists between smoking, drinking and the risk for HNSCC, not all smokers develop this type of cancer. In addition there is a group of HNSCC patients that have neither smoked nor drunk alcohol. The human papillomavirus (HPV) may play a role in the origin of HNSCC, especially for tumors of the oropharynx which show HPV infection in about 25% of the cases (24). Also, HNSCC development might be associated with inherited mutagen hypersensitivity as familial predisposition to HNSCC has been reported (25). Hereditary polymorphisms associated with familial predisposition (26), might contribute to the mutagenic effect of carcinogens from tobacco smoke and alcohol consumption.

Histological and clinical classification

The location of the HNSCC lesion is important for treatment planning since HNSCCs originating at different locations within the upper aerodigestive tract are genetically different, show a different clinical course and thus require different treatment policies (27, 28) For

example, hypopharyngeal tumors have a higher chance to metastasize compared to oral cavity and oropharyngeal tumors (29). In contrast, laryngeal tumors rarely metastasize and these patients often receive only irradiation therapy to retain their speech function (30).

HNSCCs are histologically graded as being well, moderately or poorly differentiated carcinomas. Well differentiated tumors still show an orderly stratification and keratinization of the skin squamous layers and bear a strong resemblance to normal squamous cells. Poorly differentiated tumor cells are difficult to identify as of squamous origin, have clear nuclear pleomorphisms and show atypical mitotic figures. Although histological grading is compulsory for classification of HNSCC, this information is not very useful for treatment planning since clinical outcome or treatment response of HNSCC is not strongly associated with differentiation grade (31).

The standard TNM staging system for classification and clinical treatment selection of cancer patients is based on tumor size and invasion characteristics (T), presence of regional lymph node metastasis (N) and spread to distant sites (M) (32). For HNSCC patients, TNM staging is strongly associated with survival but patients with similar TNM stage may differ significantly in clinical outcome and response to specific treatment. This all clearly indicates the need for another staging system, one that is perhaps based on molecular instead of classical assessment to accurately predict disease progression and treatment response.

HNSCC tumorigenesis

Head and neck squamous cell carcinoma originates from the squamous epithelium lining of the upper aerodigestive tract. Like most cancers, HNSCC develops through the accumulation of genetic and epigenetic alterations and acquires a set of essential cancer specific characteristics that includes self-sufficiency in growth signals, insensitivity to anti-growth signals, evading apoptosis, limitless replicative potential, angiogenesis and finally tissue invasion and metastasis (33). Deletions and amplifications of specific chromosomal regions, mutations in tumor suppressor genes and amplification of oncogenes have been detected throughout multistep HNSCC development (34). Although the precise nature of all genetic aberrations occurring at each step are still unclear, Califano *et al*. have proposed a HNSCC molecular progression model for various stages of tumorigenesis (35) (Fig. 1.3).

Chromosomal regions

Deletion of the chromosomal regions 3p14 and 9p21 are frequently associated with development of head and neck lesions and are events that occur early during tumorigenesis, sometimes in normal appearing squamous cells (36, 37). These two chromosomal regions harbor multiple tumor suppressor genes such as *FHIT* at 3p14 and $p16^{INK4a}$ at 9p21, and deletion of these regions might effect a higher risk for malignant transformation (36). Amplification of chromosomal region 11q13 is found in 70% of primary HNSCC tumors and includes the cell cycle regulator gene *cyclin D1* (38). Increased production of cyclin D1 protein significantly

Figure 1.3 | HNSCC tumorigenesis. Important genetic changes that are associated with HNSCC tumorigenesis (34, 35).

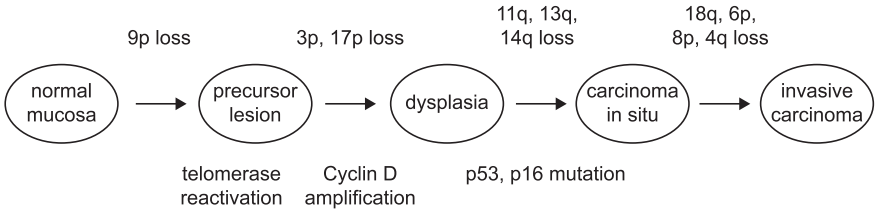

reduces the 5-year survival rate of HNSCC patients compared to that of patients with low cyclin D1 levels (39). Another important event during early HNSCC tumorigenesis is the reactivation of telomerase activity thereby extending the survival of aberrant tumor cell and facilitating the accumulation of multiple other genetic defects (37, 40).

Tumor suppressor genes and oncogenes

The tumor suppressor gene p53 is most frequently mutated in HNSCC with an incidence reported to be around 50-60% for all HNSCC (23, 37, 41). The p53 gene is located on the short arm of chromosome 17 (17p13) and is important for maintaining genomic stability. Mutations in p53 are the most frequent genetic alterations in human cancers (42, 43) and p53 is the most frequently studied molecular marker in HNSCC (41, 42, 44). Mutant p53 protein has a much longer half-life than the wild-type protein and accumulates in the cell. Inactivation of p53 leads to a loss of the G_1/S phase cell cycle checkpoint and as a result cells continue dividing without pausing to repair DNA damage (45). Besides increasing the risk for developing HNSCC, inactivation of p53 makes the tumor less sensitive to radiotherapy and chemopreventive strategies (46, 47). p63, a p53 homologue with oncogenic properties is frequently amplified in HNSCC (48).

Inactivation of the tumor suppressor gene p16 is commonly found in oral cancers (49). Normally, this cyclin-dependent kinase inhibitor negatively regulates cell proliferation mediated through the retinoblastoma protein (Rb). Alterations in the p16 protein result in an inactivation of Rb, thereby allowing uncontrolled cell proliferation (50). Overexpression of epidermal growth factor receptor (EGFR) and its ligands is an important feature of HNSCC cancer with up to 80% of HNSCC showing elevated EGFR mRNA levels compared to normal mucosa (41, 51).

Field cancerization

Another aspect of HNSCC development is the high prevalence of multiple primary tumors in the upper aerodigestive tract. The concept of field cancerization was firstly introduced in 1953 (52) to explain this higher-than-expected degree of primary HNSCC tumors and is based on the fact that a large area of epithelium surrounding the initial tumor is chronically exposed to carcinogens, such as due to smoking and heavy drinking (35, 53). As a result, multiple squamous cell lesions develop independently of each other. An alternative theory for

the development of multiple oral lesions is clonal spread of HNSCC lesions due to migration of transformed cells by for example saliva or via intraepithelial migration of progenitor cells (54). A recent study indicated that the majority of multiple oral lesions are clonally independent and arise likely due to field cancerization, although the probability of clonal spread increases with tumor progression (55).

HNSCC metastasis

Clinical prognostic factor

Metastasis is the process by which primary tumor cells migrate to other sites in the body. After development into solid tumors, metastases are the leading cause of cancer-related deaths and the presence of metastases can predict the survival rate for most, if not all, cancer patients. It is therefore of great importance to timely detect metastatic disease and intervene with appropriate therapy to prevent further spread and development of distant metastasis in vital organs such as the lungs and the liver. For HNSCC, distant metastasis is strongly linked to the presence of regional lymph node metastasis (56, 57). Only 7% of the HNSCC patients without lymph node metastasis develop distant metastasis versus 50% when neck node metastases are present (57). Consequently, lymph node metastatic status (N-status) is one of the most important prognostic factors for HNSCC patients, halving the survival rate if positive (11, 58). Treatment of patients with head and neck cancer depends heavily on staging of the disease to determine whether the tumor has already spread to the regional lymph nodes.

Development of metastasis

In the long-established metastasis model, initially proposed by Filder and Kripke in 1977 (59), metastases are thought to originate from individual cells or small subpopulations within the primary tumor that arise late during tumorigenesis due to subsequent genetic alterations (59, 60). Lately, this traditional metastasis model has been challenged by gene expression profiling studies of metastatic primary tumors (e.g. 61, 62). These studies have identified metastasis associated gene expression patterns using complete primary tumors and indicate that most primary tumor cells contribute to a metastatic phenotype. The specific metastatic signatures indicates that metastatic capacity is probably acquired early in tumorigenesis and sustained throughout tumor growth and development (63).

Tumor cells have to acquire a variety of capacities that are needed for dissemination and development into full-blown metastases. A growing primary tumor mass needs to produce angiogenic factors to stimulate growth of blood and lymph vasculature for providing sufficient oxygen and nutrition and to gain access to the blood and lymph circulation (33). Next, tumor cells need to invade through their surrounding tissue to reach the vasculature, detach and survive in the blood or lymph circulation, arrest and extravasate at the site of metastasis, evade the host immune system and finally be able to proliferate to form solid metastases

(33, 64). Since cancer cell spread can be blocked at each critical stage, this suggests that metastasis is a highly selective process and that only a small fraction of all disseminated tumor cells will finally develop into metastases (64). Moreover, it has been implied that certain tumor types specifically target towards certain organs to form metastases (59, 64), a process in which the disseminated cancer cells interact with and exploit factors produced by their target organs, such as growth factors and chemokines (65, 66).

Metastatic tumor-microenvironment

According to the newly proposed metastasis model, most cells within metastatic primary tumors contribute to the metastatic phenotype (63). This suggests that both the tumor cells and the surrounding tissue are involved in development of metastasis. It is now generally believed that cancer is not solely caused by the tumor cells but that malignancy is a state that emerges from a tumor-host microenvironment (33, 67, 68). Throughout the entire process of survival, proliferation, invasion and metastatic spread of cancer cells, the surrounding microenvironment plays an active role and includes the extracellular matrix, blood vessel cells, fibroblasts and immune and inflammatory cells such as lymphocytes and macrophages (65, 69-73). Since the tumor microenvironment organization resembles that of granulation tissue during typical wound healing, tumors have been defined as wounds that never heal (74).

It has been suggested that cancer cells can actively alter their surrounding tissue into a 'reactive' stroma, which supports proliferation, invasion and metastasis of tumor cells (71). Communication between metastatic tumor cells and the tumor stroma facilitates tumor cell motility and metastasis because of stromal production of growth and angiogenic factors, chemokines, extracellular matrix components and matrix metalloproteinases (70, 75). Skobe *et al.* have shown that normalization of the 'reactive' stroma by specific blocking of angiogenic factors could revert the metastatic microenvironment into a non-invasive phenotype and reduced the malignancy and invasive growth (76).

Haematogenous and lymphatic spread

Neither the traditional models in which metastases arise from small subpopulations of primary tumor cells (59) nor the newly proposed model wherein most primary tumor cells show a metastatic phenotype (63) make a distinction between lymph node and distant metastasis. Distant spread of certain tumor types depends greatly on prior involvement of the regional lymph nodes, while other types can spread directly to distant sites. This indicates that the cascade of metastatic spread might predominantly follow different routes for different tumor types. Many of the expression profiling studies have been performed on breast cancer (61, 77-79), which is only moderately dependent on involvement of the lymph nodes and can disseminate directly to distant sites via the blood (80). Distant spread of a tumor that heavily depends on intermediate lymph node metastasis, such as head and neck cancer (57), may follow an alternative route.

Pantel and Brakenhoff have proposed a model for development of distant metastases

that discriminate two specific complementary routes for metastatic spread (56) (Fig. 1.4). In the first route, tumor cells disseminate into the lymph and blood circulation early during tumorigenesis. The disseminated cells are able to survive and proliferate at the lymph nodes but die or remain dormant in the blood. After development in the lymph nodes, metastatic cells can subsequently disseminate from the solid lymph node metastases to distant sites through the blood to form distant metastases. Possibly, properties needed for survival in the blood and at distant sites are acquired during development in the lymph nodes. In the second route, cancer cells primarily metastasize via haematogenous dissemination and are directly able to survive in the blood and to form distant metastases without involvement of the lymph nodes. Distant spread of tumor cells via the second route is independent of intermediate lymph node metastases and occurs predominantly in cancer types that show no strong correlation between lymph node and distant metastasis. HNSCC disseminates almost exclusively via lymphatic spread and so obviously requires an intermediate station at the lymph nodes (56, 57). This indicates that if tumor cells first spread to the regional lymph nodes, removal of the neck nodes in patient with head and neck cancer before secondary haematogenous spread to distant organs will likely prevent future spread of the disease

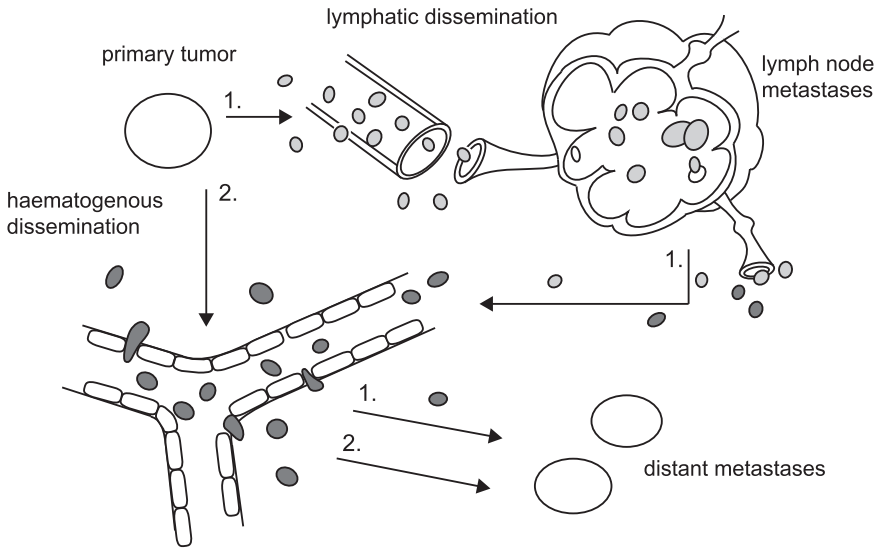

Figure 1.4 | Model of metastatic routes to distant spread of tumor cells. Model for distant metastatic spread proposed by Pantel and Brakenhoff (56). Disseminated primary tumor cells can follow two routes for distant spread: one which is dependent on lymphatic dissemination and another wherein haematogenous spread predominantly occurs without involvement of the regional lymph nodes. In the first route (**1.**) tumor cells spread to lymph and blood vessel but die or remain dormant in the blood while being able to form solid metastasis in the lymph nodes. After development in the lymph nodes, tumor cells subsequently spread to distant sites through the blood and form solid distant metastasis. In the second route (**2.**) disseminated cancer cells predominantly spread via the haematogenous route and are able to survive and develop into solid metastases without requirement of intermediate development in the regional lymph nodes. In breast cancer patients the second metastatic route is more common while head and neck cancer almost exclusively progresses via the lymph node dependent route. Adapted from Pantel *et al*. (56).

Diagnosis and treatment of HNSCC lymph node metastasis

The presence of cervical lymph node metastasis in HNSCC patients is an important prognostic factor for disease outcome. For accurate treatment of the patient, it is of great importance to know the regional lymph node status (N-status) since removal of affected lymph nodes will reduce the chance of distant spread to other organs. Within the group of HNSCC patients, accurate diagnosis of the neck nodes is particularly important for treatment policy in individuals with oral cavity or oropharynx tumors, as in this group the chance that metastatic lesions are present is highly variable among individual cases. In contrast, laryngeal lesions rarely metastasize whilst tumor in the hypopharynx very frequently spread to the cervical lymph nodes (29, 30). Therefore, treatment of laryngeal cancer may assume absence of metastasis unless evidently shown, while in case of hypopharyngeal cancer treatment will routinely include the neck. For oral and oropharyngeal cancer, treatment should preferably be more individually tailored to avoid over- or under-treatment.

Diagnosis and treatment of neck node metastasis

Lymph node metastatic disease in the neck is classified according to a level system that delineates the location of the metastases. The neck lymph node groups are classified into 6 levels that encompass the complete anatomy of the neck. The six neck lymph node levels are outlined as submental (IA) and submandibular (IB), upper jugular (II) which is divided in jugulogastric (IIA) and suprspinal accessory (IIB), middle jugular (III), lower jugular (IV), posterior cervical (V) which is divided in spinal accessory nerve nodes (VA) and transverse cervical nodes (VB), supraclavicular (SC) and anterior group (VI) (81, 82) (Fig. 1.5 A). For patients with oral cavity cancers, levels I to III are at greatest risk for metastases. In patients with oropharyngeal, hypopharyngeal and laryngeal cancers, metastasis most often occur in levels II to IV, whereas level VI nodes are mostly at risk for thyroid cancers (81).

Diagnosis of neck nodes in patients with HNSCC is performed by clinical examination (palpation) of the neck region followed by bilateral ultrasound examination, computed tomography (CT) and/or magnetic resonance imaging (MRI) (83-85). Suspected nodes are subjected to aspiration cytology (86). In this way, patients are preoperatively classified as N0; without lymph node metastases or as N+; with lymph node metastatic disease, the latter in the case of aspirates yielding metastatic tumor cells. Only in the case of obvious neck involvement, as shown by huge swelling, are the patients classified as N+ without additional efforts to prove the presence of metastasis.

Surgical treatment of oral cavity and oropharynx cancer is aimed at complete removal of the primary tumor. With respect to the neck, N+ patients additionally receive a radical neck dissection which encompasses uni- or bilateral removal of all lymph nodes from levels I to V (81) (Fig. 1.5 B). Neck node level VI is only removed in case of thyroid cancer (81). Postoperative irradiation is administered depending on tumor margin status, tumor growth features, number of positive nodes and extracapsular growth. However, upon histological examination of removed lymph node tissue about 10% of clinically diagnosed N+ patients

turn out to be metastasis-free (N0) and thus unnecessarily received a comprehensive neck dissection (87), which leads to severe morbidity especially concerning the shoulder and neck (88, 89).

Treatment of the N0 neck

Besides false assessment of 10% of the clinical N+ patients, current diagnosis is especially inaccurate for clinically diagnosed N0 patients. Postoperative histological examination of lymph node tissue indicates that about one-third of the clinically assessed N0 patients have metastasis-positive lymph nodes in the neck (90, 91). Inaccurate diagnosis of the presence of lymph node metastasis will lead to a high number of clinically false negative patients whose undetected neck node metastases can, if left untreated, further spread to distant sites such as the liver and the lungs. Different strategies exist for treatment of clinically diagnosed N0 patients (92). Following a 'watch-and-wait' approach patients do not undergo an elective neck dissection but instead are followed under careful clinical observation (93). This approach risks fatality by allowing overlooked metastases to spread further and is therefore only acceptable if the change for development of neck node metastasis is less than 20% (94, 95).

Since the prevalence of false negative patients is very high, elective neck dissection is preferred for all clinical N0 patients (92, 94). For patients with oral cavity or oropharynx cancer, selective neck dissection encompasses removal of the upper three lymph node levels, also called a supraomohyoid neck dissection (SOHND) (81, 96) (Fig. 1.5 C). As a consequence of avoiding undertreatment due to false negative diagnosis, two-thirds of the N0 patients, which were retrospectively accurately diagnosed to have no node metastasis, receive unnecessary surgery since their removed lymph nodes indeed do not show any sign of metastasis. Although a SOHND is less severe than a radical neck dissection, it still results in disfigurement, long-term discomfort and pain and can lead to additional complications such as shoulder disability (97, 98).

Figure 1.5 | Neck lymph node levels and enclosure of radical and selective neck dissection. (**A**) Cervical nodes by levels and sublevels. IA, submental; IB, submandibular; II, upper jugular divided into IIA, jugulogastric and IIB, supraspinal accessory; III, midjugular, IV lower jugular; posterior cervical V, divided in VA, spinal accessory nerve nodes and VB, transverse cervical nodes; SC, supraclavicular; and VI anterior group. (**B**) A radical neck dissection encompasses all lymph node levels from I to V. Neck level VI is only includes for thyroid and larynx cancer (81) (**C**) Selective neck dissection for oral cancer, or supraomohyoid neck dissection (SOHND), only covers removal of levels I to III that are at greatest risk for metastases. Based on Robbins *et al*. (81).

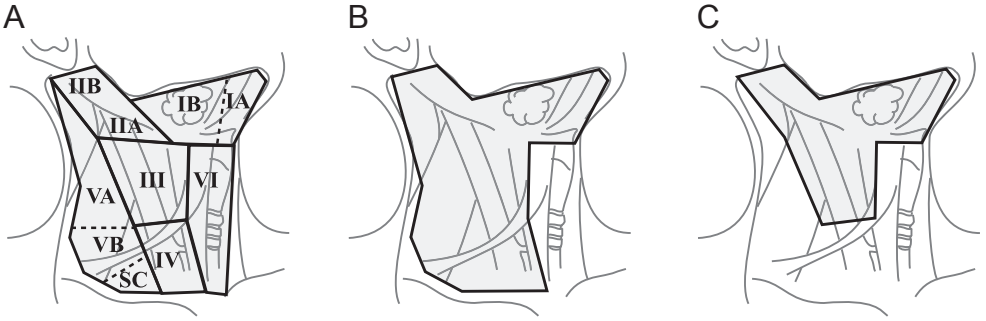

Improved diagnostics

Due to inaccurate preoperative diagnosis of neck node metastasis a large proportion of clinically N0 patients receive an unnecessary surgical treatment, whereas for the falsely diagnosed N0 patients the current selective neck dissection is too restricted. It is clear that new or improved techniques are needed for accurate diagnosis to reduce the number of HNSCC patients that unnecessary receive a treatment which is associated with severe side effects and morbidity. Techniques such as ultrasound-guided aspiration cytology and sentinel node diagnostics (99, 100) will likely improve diagnosis of regional lymph node metastasis, making a wait-and-wait approach more appropriate for clinically diagnosed N0 patients. Improvements in imaging techniques such as CT, MRI and ultrasound examination as well as new techniques such as RadioImmuno Scintigrapy (RIS) (101) and Positron Emission Tomography (PET) (102) will likely improve the diagnosis of metastases within the neck lymph nodes, but detection of small positive nodes will remain difficult, especially if the metastatic tumor is in an pre-macroscopic stage of development (103).

Biomarkers

As mentioned, the standard TNM staging system and histological grading for HNSCC tumor are not able to accurately predict the tumor behavior or disease outcome. Classification of primary tumors based on biomolecular characteristics might enable better estimations of disease progression such as development of lymph node metastatis. During the last few years multiple biomarkers have been tested for their association with development of metastasis (104). Although in some studies an association was found between expression of certain biomarkers, such as Cyclin D1, EGFR, p53, E-cadherin, CD44 and uPA/PAI, none showed significant concordance between different studies (reviewed in 104). Apparently, measurement of individual biomarkers is not sufficient for accurately prediction. Likely, a broader, genome-wide view into the activity of multiple metastasis related genes is needed to elucidate the molecular mechanisms behind development of metastasis. For this, analyses using genome-wide techniques, such as DNA microarrays, are required.

Gene expression microarrays to study human cancer

DNA microarrays

The Human Genome Project has provided an enormous amount of knowledge about the genes that are present in our genome (105, 106). Identification of the function and activity of all these genes and their relevance to human disease and cancer has put great emphasis on transcriptional genomics to examine gene expression in a comprehensive and high-throughput manner (107-109). Traditional techniques for assessment of gene expression, such as Northern blotting and quantitative PCR, can measure only a single or a few genes at a time and do not measure up against the complexity of human cancers (110). In a remarkably short time microarrays have become the main technology for studying gene expression,

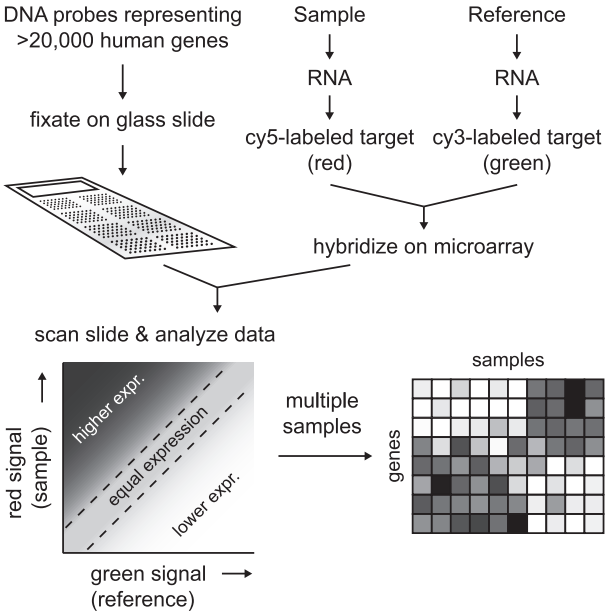

Figure 1.6 | Microarray procedure. DNA microarrays are generated by fixation of a collection of DNA probes on a glass surface. Each feature on the microarray represents one human gene. For the analyzed samples, i.e. primary tumors, RNA is isolated and subsequently labeled with a fluorescent group, such as cy5 (red) or cy3 (green). The sample target is combined with a reverse labeled reference target and hybridized on a DNA microarray. After quantification of the sample and reference signal channels on the array, a sample–reference ratio is calculated by which genes can be identified that are higher or lower expressed in the analyzed samples compared to the reference. By combining the results of multiple samples, a specific set of genes can be identified that is able to discriminate the analyzed samples in specific groups.

whereby thousands of DNA probes that represent genes are fixated on a glass surface and hybridized against fluorophore-labeled RNA targets from various sources (111-113) (Fig. 1.6). The power of DNA microarray technology is that the simultaneous measurement of thousands of genes will uncover higher-order organization in complex gene transcription regulation. The more genes and biological samples are studied, the more obvious underlying biological properties or processes become in complex gene expression behavior. The gene expression data generated by microarrays should therefore not be considered a collection of separate "Northerns" but as a composite snapshot of gene expression in the analyzed cells or tissues. Thorough analysis of the complex gene expression data will be the most critical issue in microarray studies to identify underlying biological patterns and mechanism (114-116).

Diagnostic gene expression signatures

In cancer research, DNA microarrays have initially been used for molecular classification of tumors into known or newly identified subtypes (117-120). In a landmark study, van't Veer *et al*. have used gene expression profiling to predict the clinical outcome of breast cancer patients (61). Van't Veer and colleagues identified a 70-gene signature that could distinguish between good prognosis and poor prognosis patient groups based on the gene expression profiles of primary breast tumors, where classical predictors such as histological grade or lymph node status were less successful (61, 78). Since this study, numerous other gene expression signatures have been identified that are associated with poor outcome of cancer patients (77, 121-124). Besides prognosis for survival, molecular signatures have been designed for prediction of specific treatment response (125-127), recurrence rate (128,

129) and development of metastasis (62, 79, 130, 131). Ramaswamy *et al*. were among the first to identify a molecular signature of metastasis that was shared across multiple types of solid primary tumors and suggested the possible existence of a metastatic pathway that is common to different cancers (62). The discovery of several other metastatic signatures across multiple tumor types (79, 130, 131) emphasizes the potential of expression profiling for clinical assessment of metastatic disease.

For head and neck cancer, gene expression profiling has been used for molecular classification of head and neck squamous cell carcinomas (132-136) and to identify gene profiles that are associated with disease progression (137-139). Various studies have started to uncover molecular signatures for development of lymph node metastasis in oral squamous cell carcinoma but so far without validation of the discovered profile on a sufficiently large independent sample set (132, 140-142). Such a thorough validation for reliability and clinical outcome is required to make sure that the profile is not overfitted on the analyzed samples but also works for new independent samples (143, 144).

Before a gene expression signature can become standard clinical practice, precise determination of the clinical relevance and the implications for treatment of cancer patients requires evaluation in a large cohort of individuals, preferably across different institutes (144-146). Although some technical and statistical aspects still need optimizing (147), the potential of cancer transcriptional research is starting to be revealed with the first gene expression signatures becoming available for the clinic (148, 149).

Aim and outline of this thesis

Because of difficulties in accurate detection of lymph node metastasis, a large number patients with head and neck cancer currently receive inadequate or unnecessary surgical treatment. To reduce the number of inappropriately treated patients, either existing clinical diagnostics for lymph node metastatic disease have to be improved or other technologies are needed for accurate assessment. This thesis describes the use of DNA microarray technology to design a gene expression signature that is capable of accurately discriminating HNSCC patients with or without lymph node metastatic disease. Besides the potential for clinical diagnosis, we show that the identified signature likely represents essential molecular processes that are needed for initiation and development of HNSCC metastasis. Furthermore, important aspects concerning proper design of gene expression signatures are unveiled which need to be taken into account for identifying optimal molecular signatures.

Chapter 2 describes the procedural development of the microarray protocols that were used for high-throughput expression profiling of primary tumors. The identification of a gene expression signature for detection of lymph node metastasis in patients with HNSCC is explained in *Chapter 3*. Following a brief Intermezzo concerning the stability of molecular signatures with respect to their gene components, *Chapter 4* demonstrates that the initially identified signature genes are a subset of large set of metastasis associated genes and that

multiple predictive signatures exist for accurate diagnosis of lymph node metastasis. The importance of the identified signature is underlined in *Chapter 5* where we show that the primary tumor metastatic signature is maintained upon lymph node metastasis. The contribution of the tumor cells and the surrounding tumor stroma to the HNSCC metastatic signature is investigated in *Chapter 6* and shows the effect that varying tumor percentage have on the metastatic signature. We also propose methods for improving the prediction of low tumor percentage samples based on developing predictive signatures that are equally based on tumor cell and stromal gene expression. Finally important issues relating to the optimal use of DNA microarray gene expression profiling for cancer research and diagnostics are discussed in *Chapter 7*.

References

1. Bray, F. and B. Moller, Predicting the future burden of cancer. Nat Rev Cancer, 2006. 6(1): p. 63-74.
2. Parkin, D.M., P. Pisani, and J. Ferlay, Estimates of the worldwide incidence of 25 major cancers in 1990. Int J Cancer, 1999. 80(6): p. 827-841.
3. Lopez, A.D., et al., Global and regional burden of disease and risk factors, 2001: systematic analysis of population health data. Lancet, 2006. 367(9524): p. 1747-1757.
4. Genden, E.M., et al., Referral guidelines for suspected cancer of the head and neck. Auris Nasus Larynx, 2005.
5. Reid, B.C., et al., Head and neck in situ carcinoma: incidence, trends, and survival. Oral Oncol, 2000. 36(5): p. 414-420.
6. Visser, O., et al., Incidence of cancer in the Netherlands in 1998, in Tenth report of the Netherlands Cancer Registry. 2002: Utrecht.
7. Pindborg, J.J., Control of oral cancer in developing countries. A WHO meeting. Bull World Health Organ, 1984. 62(6): p. 817-830.
8. Day, G.L., et al., Racial differences in risk of oral and pharyngeal cancer: alcohol, tobacco, and other determinants. J Natl Cancer Inst, 1993. 85(6): p. 465-473.
9. Sankaranarayanan, R., et al., Head and neck cancer: a global perspective on epidemiology and prognosis. Anticancer Res, 1998. 18(6B): p. 4779-4786.
10. Nederlandse Werkgroep Hoofd-Halstumoren, Epidemiologie mondholte- en orofarynxcarcinoom, in Richtlijn Mondholte- en Orofarynxcarcinoom. 2004, Van Zuiden Communications B.V.: Alphen aan den Rijn. p. 15-26.
11. Forastiere, A., et al., Head and neck cancer. N Engl J Med, 2001. 345(26): p. 1890-1900.
12. Decker, J. and J.C. Goldstein, Risk factors in head and neck cancer. N Engl J Med, 1982. 306(19): p. 1151-1155.
13. Andre, K., et al., Role of alcohol and tobacco in the aetiology of head and neck cancer: a case-control study in the Doubs region of France. Eur J Cancer B Oral Oncol, 1995. 31B(5): p. 301-309.
14. Schildt, E.B., et al., Oral snuff, smoking habits and alcohol consumption in relation to oral cancer in a Swedish case-control study. Int J Cancer, 1998. 77(3): p. 341-346.
15. Deleyiannis, F.W., et al., Alcoholism: independent predictor of survival in patients with head and neck cancer. J Natl Cancer Inst, 1996. 88(8): p. 542-549.
16. Macfarlane, G.J., et al., Alcohol, tobacco, diet and the risk of oral cancer: a pooled analysis of three case-control studies. Eur J Cancer B Oral Oncol, 1995. 31B(3): p. 181-187.
17. Jaber, M.A., et al., Risk factors for oral epithelial dysplasia--the role of smoking and alcohol. Oral Oncol, 1999. 35(2): p. 151-156.
18. Franceschi, S., et al., Comparison of the effect of smoking and alcohol drinking between oral and pharyngeal cancer. Int J Cancer, 1999. 83(1): p. 1-4.
19. Blot, W.J., et al., Smoking and drinking in relation to oral and pharyngeal cancer. Cancer Res, 1988. 48(11): p. 3282-3287.
20. Schlecht, N.F., et al., Interaction between tobacco and alcohol consumption and the risk of cancers of the upper aero-digestive tract in Brazil. Am J Epidemiol, 1999. 150(11): p. 1129-1137.
21. Neville, B.W. and T.A. Day, Oral cancer and

precancerous lesions. CA Cancer J Clin, 2002. 52(4): p. 195-215.
22. Franceschi, S., et al., Cessation of alcohol drinking and risk of cancer of the oral cavity and pharynx. Int J Cancer, 2000. 85(6): p. 787-790.
23. Brennan, J.A., et al., Association between cigarette smoking and mutation of the p53 gene in squamous-cell carcinoma of the head and neck. N Engl J Med, 1995. 332(11): p. 712-717.
24. Gillison, M.L., et al., Evidence for a causal association between human papillomavirus and a subset of head and neck cancers. J Natl Cancer Inst, 2000. 92(9): p. 709-720.
25. Foulkes, W.D., et al., Familial risks of squamous cell carcinoma of the head and neck: retrospective case-control study. Bmj, 1996. 313(7059): p. 716-721.
26. Yu, K.K., et al., Familial head and neck cancer: molecular analysis of a new clinical entity. Laryngoscope, 2002. 112(9): p. 1587-1593.
27. Freier, K., et al., Tissue Microarray Analysis Reveals Site-specific Prevalence of Oncogene Amplifications in Head and Neck Squamous Cell Carcinoma. Cancer Res, 2003. 63(6): p. 1179-1182.
28. Huang, Q., et al., Genetic differences detected by comparative genomic hybridization in head and neck squamous cell carcinomas from different tumor sites: construction of oncogenetic trees for tumor progression. Genes Chromosomes Cancer, 2002. 34(2): p. 224-233.
29. Agrama, M.T., et al., Nodal yield in neck dissection and the likelihood of metastases. Otolaryngol Head Neck Surg, 2003. 128(2): p. 185-190.
30. Forastiere, A.A., et al., Concurrent chemotherapy and radiotherapy for organ preservation in advanced laryngeal cancer. N Engl J Med, 2003. 349(22): p. 2091-2098.
31. Cardesa, A. and P.J. Slootweg, Benign and Potentially Malignant Lesions of the Squamous Epithelium and Squamous Cell Carcinoma, in Pathology of the Head and Neck. 2006, Springer-Verlag: Berlin Heidelberg. p. 2-29.
32. O'Sullivan, B. and J. Shah, New TNM staging criteria for head and neck tumors. Semin Surg Oncol, 2003. 21(1): p. 30-42.
33. Hanahan, D. and R.A. Weinberg, The hallmarks of cancer. Cell, 2000. 100(1): p. 57-70.
34. Nagai, M.A., Genetic alterations in head and neck squamous cell carcinomas. Braz J Med Biol Res, 1999. 32(7): p. 897-904.
35. Califano, J., et al., Genetic progression model for head and neck cancer: implications for field cancerization. Cancer Res, 1996. 56(11): p. 2488-2492.
36. Mao, L., et al., Frequent microsatellite alterations at chromosomes 9p21 and 3p14 in oral premalignant lesions and their value in cancer risk assessment. Nat Med, 1996. 2(6): p. 682-685.
37. Hunter, K.D., E.K. Parkinson, and P.R. Harrison, Profiling early head and neck cancer. Nat Rev Cancer, 2005. 5(2): p. 127-135.
38. Izzo, J.G., et al., Cyclin D1 genotype, response to biochemoprevention, and progression rate to upper aerodigestive tract cancer. J Natl Cancer Inst, 2003. 95(3): p. 198-205.
39. Kyomoto, R., et al., Cyclin-D1-gene amplification is a more potent prognostic factor than its protein over-expression in human head-and-neck squamous-cell carcinoma. Int J Cancer, 1997. 74(6): p. 576-581.
40. Mutirangura, A., et al., Telomerase activity in oral leukoplakia and head and neck squamous cell carcinoma. Cancer Res, 1996. 56(15): p. 3530-3533.
41. Quon, H., F.F. Liu, and B.J. Cummings, Potential molecular prognostic markers in head and neck squamous cell carcinomas. Head Neck, 2001. 23(2): p. 147-159.
42. Nigro, J.M., et al., Mutations in the p53 gene occur in diverse human tumour types. Nature, 1989. 342(6250): p. 705-708.
43. Partridge, M., K. Gaballah, and X. Huang, Molecular markers for diagnosis and prognosis. Cancer Metastasis Rev, 2005. 24(1): p. 71-85.
44. Nylander, K., E. Dabelsteen, and P.A. Hall, The p53 molecule and its prognostic role in squamous cell carcinomas of the head and neck. J Oral Pathol Med, 2000. 29(9): p. 413-425.
45. Levine, A.J., J. Momand, and C.A. Finlay, The p53 tumour suppressor gene. Nature, 1991. 351(6326): p. 453-456.
46. Koch, W.M., et al., p53 mutation and locoregional treatment failure in head and neck squamous cell carcinoma. J Natl Cancer Inst, 1996. 88(21): p. 1580-1586.
47. Shin, D.M., et al., Biochemopreventive therapy for patients with premalignant lesions of the head and neck and p53 gene expression. J Natl Cancer Inst, 2000. 92(1): p. 69-73.

48. Patturajan, M., et al., DeltaNp63 induces beta-catenin nuclear accumulation and signaling. Cancer Cell, 2002. 1(4): p. 369-379.
49. Sartor, M., et al., Role of p16/MTS1, cyclin D1 and RB in primary oral cancer and oral cancer cell lines. Br J Cancer, 1999. 80(1-2): p. 79-86.
50. Liggett, W.H., Jr. and D. Sidransky, Role of the p16 tumor suppressor gene in cancer. J Clin Oncol, 1998. 16(3): p. 1197-1206.
51. Wen, Q.H., et al., Prognostic value of EGFR and TGF-alpha in early laryngeal cancer treated with radiotherapy. Laryngoscope, 1996. 106(7): p. 884-888.
52. Slaughter, D.P., H.W. Southwick, and W. Smejkal, Field cancerization in oral stratified squamous epithelium; clinical implications of multicentric origin. Cancer, 1953. 6(5): p. 963-968.
53. Braakhuis, B.J., et al., Second primary tumors and field cancerization in oral and oropharyngeal cancer: molecular techniques provide new insights and definitions. Head Neck, 2002. 24(2): p. 198-206.
54. Bedi, G.C., et al., Multiple head and neck tumors: evidence for a common clonal origin. Cancer Res, 1996. 56(11): p. 2484-2487.
55. Jang, S.J., et al., Multiple oral squamous epithelial lesions: are they genetically related? Oncogene, 2001. 20(18): p. 2235-2242.
56. Pantel, K. and R.H. Brakenhoff, Dissecting the metastatic cascade. Nat Rev Cancer, 2004. 4(6): p. 448-456.
57. Leemans, C.R., et al., Regional lymph node involvement and its significance in the development of distant metastases in head and neck carcinoma. Cancer, 1993. 71(2): p. 452-456.
58. Jones, A.S., et al., The level of cervical lymph node metastases: their prognostic relevance and relationship with head and neck squamous carcinoma primary sites. Clin Otolaryngol, 1994. 19(1): p. 63-69.
59. Fidler, I.J. and M.L. Kripke, Metastasis results from preexisting variant cells within a malignant tumor. Science, 1977. 197(4306): p. 893-895.
60. Talmadge, J.E., S.R. Wolman, and I.J. Fidler, Evidence for the clonal origin of spontaneous metastases. Science, 1982. 217(4557): p. 361-363.
61. van 't Veer, L.J., et al., Gene expression profiling predicts clinical outcome of breast cancer. Nature, 2002. 415(6871): p. 530-536.
62. Ramaswamy, S., et al., A molecular signature of metastasis in primary solid tumors. Nat Genet, 2003. 33(1): p. 49-54.
63. Bernards, R. and R.A. Weinberg, A progression puzzle. Nature, 2002. 418(6900): p. 823.
64. Fidler, I.J., The pathogenesis of cancer metastasis: the 'seed and soil' hypothesis revisited. Nat Rev Cancer, 2003. 3(6): p. 453-458.
65. Balkwill, F., Cancer and the chemokine network. Nat Rev Cancer, 2004. 4(7): p. 540-550.
66. Minn, A.J., et al., Genes that mediate breast cancer metastasis to lung. Nature, 2005. 436(7050): p. 518-524.
67. Bissell, M.J. and D. Radisky, Putting tumours in context. Nat Rev Cancer, 2001. 1(1): p. 46-54.
68. Liotta, L.A. and E.C. Kohn, The microenvironment of the tumour-host interface. Nature, 2001. 411(6835): p. 375-379.
69. Bissell, M.J. and M.A. Labarge, Context, tissue plasticity, and cancer; Are tumor stem cells also regulated by the microenvironment? Cancer Cell, 2005. 7(1): p. 17-23.
70. Pollard, J.W., Tumour-educated macrophages promote tumour progression and metastasis. Nat Rev Cancer, 2004. 4(1): p. 71-78.
71. Mueller, M.M. and N.E. Fusenig, Friends or foes - bipolar effects of the tumour stroma in cancer. Nat Rev Cancer, 2004. 4(11): p. 839-849.
72. Condeelis, J. and J.W. Pollard, Macrophages: obligate partners for tumor cell migration, invasion, and metastasis. Cell, 2006. 124(2): p. 263-266.
73. Christofori, G., New signals from the invasive front. Nature, 2006. 441(7092): p. 444-450.
74. Dvorak, H.F., Tumors: wounds that do not heal. Similarities between tumor stroma generation and wound healing. N Engl J Med, 1986. 315(26): p. 1650-1659.
75. Kalluri, R. and M. Zeisberg, Fibroblasts in cancer. Nat Rev Cancer, 2006. 6(5): p. 392-401.
76. Skobe, M., et al., Halting angiogenesis suppresses carcinoma cell invasion. Nat Med, 1997. 3(11): p. 1222-1227.
77. Huang, E., et al., Gene expression predictors of breast cancer outcomes. Lancet, 2003. 361(9369): p. 1590-1596.
78. van de Vijver, M.J., et al., A gene-expression signature as a predictor of survival in breast cancer. N Engl J Med, 2002. 347(25): p. 1999-

2009.
79. Wang, Y., et al., Gene-expression profiles to predict distant metastasis of lymph-node-negative primary breast cancer. Lancet, 2005. 365(9460): p. 671-679.
80. Braun, S., et al., Cytokeratin-positive cells in the bone marrow and survival of patients with stage I, II, or III breast cancer. N Engl J Med, 2000. 342(8): p. 525-533.
81. Robbins, K.T., et al., Neck dissection classification update: revisions proposed by the American Head and Neck Society and the American Academy of Otolaryngology-Head and Neck Surgery. Arch Otolaryngol Head Neck Surg, 2002. 128(7): p. 751-758.
82. Robbins, K.T., et al., Standardizing neck dissection terminology. Official report of the Academy's Committee for Head and Neck Surgery and Oncology. Arch Otolaryngol Head Neck Surg, 1991. 117(6): p. 601-605.
83. Nederlandse Werkgroep Hoofd-Halstumoren, Beeldvormende diagnostiek van halskliermetastasen, in Richtlijn Mondholte- en Orofarynxcarcinoom. 2004, Van Zuiden Communications B.V.: Alphen aan den Rijn. p. 95-111.
84. Wide, J.M., et al., Magnetic resonance imaging in the assessment of cervical nodal metastasis in oral squamous cell carcinoma. Clin Radiol, 1999. 54(2): p. 90-94.
85. Curtin, H.D., et al., Comparison of CT and MR imaging in staging of neck metastases. Radiology, 1998. 207(1): p. 123-130.
86. Hodder, S.C., et al., Ultrasound and fine needle aspiration cytology in the staging of neck lymph nodes in oral squamous cell carcinoma. Br J Oral Maxillofac Surg, 2000. 38(5): p. 430-436.
87. Don, D.M., et al., Evaluation of cervical lymph node metastases in squamous cell carcinoma of the head and neck. Laryngoscope, 1995. 105(7 Pt 1): p. 669-674.
88. van Wilgen, C.P., et al., Shoulder and neck morbidity in quality of life after surgery for head and neck cancer. Head Neck, 2004. 26(10): p. 839-844.
89. Kuntz, A.L. and E.A. Weymuller, Jr., Impact of neck dissection on quality of life. Laryngoscope, 1999. 109(8): p. 1334-1338.
90. Jones, A.S., et al., Occult node metastases in head and neck squamous carcinoma. Eur Arch Otorhinolaryngol, 1993. 250(8): p. 446-449.
91. Woolgar, J.A., Pathology of the N0 neck. Br J Oral Maxillofac Surg, 1999. 37(3): p. 205-209.
92. Pillsbury, H.C., 3rd and M. Clark, A rationale for therapy of the N0 neck. Laryngoscope, 1997. 107(10): p. 1294-1315.
93. van den Brekel, M.W., et al., Outcome of observing the N0 neck using ultrasonographic-guided cytology for follow-up. Arch Otolaryngol Head Neck Surg, 1999. 125(2): p. 153-156.
94. Nederlandse Werkgroep Hoofd-Halstumoren, Behandeling van het mondholtecarcinoom, in Richtlijn Mondholte- en Orofarynxcarcinoom. 2004, Van Zuiden Communications B.V.: Alphen aan den Rijn. p. 95-111.
95. Weiss, M.H., L.B. Harrison, and R.S. Isaacs, Use of decision analysis in planning a management strategy for the stage N0 neck. Arch Otolaryngol Head Neck Surg, 1994. 120(7): p. 699-702.
96. Medina, J.E. and R.M. Byers, Supraomohyoid neck dissection: rationale, indications, and surgical technique. Head Neck, 1989. 11(2): p. 111-122.
97. Short, S.O., et al., Shoulder pain and function after neck dissection with or without preservation of the spinal accessory nerve. Am J Surg, 1984. 148(4): p. 478-482.
98. van Wilgen, C.P., et al., Shoulder pain and disability in daily life, following supraomohyoid neck dissection: a pilot study. J Craniomaxillofac Surg, 2003. 31(3): p. 183-186.
99. Pitman, K.T., et al., Sentinel lymph node biopsy in head and neck cancer. Oral Oncol, 2003. 39(4): p. 343-349.
100. Nieuwenhuis, E.J., et al., Wait-and-see policy for the N0 neck in early-stage oral and oropharyngeal squamous cell carcinoma using ultrasonography-guided cytology: is there a role for identification of the sentinel node? Head Neck, 2002. 24(3): p. 282-289.
101. van Dongen, G.A., et al., Radioimmunoscintigraphy of head and neck cancer using 99mTc-labeled monoclonal antibody E48 F(ab')2. Cancer Res, 1992. 52(9): p. 2569-2574.
102. Braams, J.W., et al., Nodal spread of squamous cell carcinoma of the oral cavity detected with PET-tyrosine, MRI and CT. J Nucl Med, 1996. 37(6): p. 897-901.
103. Buckley, J.G. and K. MacLennan, Cervical node metastases in laryngeal and hypopharyngeal cancer: a prospective analysis of prevalence and distribution. Head Neck, 2000. 22(4): p.

380-385.
104. Takes, R.P., Staging of the neck in patients with head and neck squamous cell cancer: imaging techniques and biomarkers. Oral Oncol, 2004. 40(7): p. 656-667.
105. McPherson, J.D., et al., A physical map of the human genome. Nature, 2001. 409(6822): p. 934-941.
106. Venter, J.C., et al., The sequence of the human genome. Science, 2001. 291(5507): p. 1304-1351.
107. Collins, F.S., et al., A vision for the future of genomics research. Nature, 2003. 422(6934): p. 835-847.
108. Guttmacher, A.E. and F.S. Collins, Genomic medicine--a primer. N Engl J Med, 2002. 347(19): p. 1512-1520.
109. Lander, E.S., Array of hope. Nat Genet, 1999. 21(1 Suppl): p. 3-4.
110. Slonim, D.K., From patterns to pathways: gene expression data analysis comes of age. Nat Genet, 2002. 32 Suppl 2: p. 502-508.
111. Lockhart, D.J., et al., Expression monitoring by hybridization to high-density oligonucleotide arrays. Nat Biotechnol, 1996. 14(13): p. 1675-1680.
112. Hughes, T.R., et al., Expression profiling using microarrays fabricated by an ink-jet oligonucleotide synthesizer. Nat Biotechnol, 2001. 19(4): p. 342-347.
113. DeRisi, J., et al., Use of a cDNA microarray to analyse gene expression patterns in human cancer. Nat Genet, 1996. 14(4): p. 457-460.
114. Kim, J.H., Bioinformatics and genomic medicine. Genet Med, 2002. 4(6 Suppl): p. 62S-65S.
115. Bassett, D.E., Jr., M.B. Eisen, and M.S. Boguski, Gene expression informatics--it's all in your mine. Nat Genet, 1999. 21(1 Suppl): p. 51-55.
116. Butte, A., The use and analysis of microarray data. Nat Rev Drug Discov, 2002. 1(12): p. 951-960.
117. Alizadeh, A.A., et al., Distinct types of diffuse large B-cell lymphoma identified by gene expression profiling. Nature, 2000. 403(6769): p. 503-511.
118. Chung, C.H., P.S. Bernard, and C.M. Perou, Molecular portraits and the family tree of cancer. Nat Genet, 2002. 32 Suppl 2: p. 533-540.
119. Golub, T.R., et al., Molecular classification of cancer: class discovery and class prediction by gene expression monitoring. Science, 1999. 286(5439): p. 531-537.
120. Perou, C.M., et al., Molecular portraits of human breast tumours. Nature, 2000. 406(6797): p. 747-752.
121. Ahr, A., et al., Identification of high risk breast-cancer patients by gene expression profiling. Lancet, 2002. 359(9301): p. 131-132.
122. Haqq, C., et al., The gene expression signatures of melanoma progression. Proc Natl Acad Sci U S A, 2005. 102(17): p. 6092-6097.
123. Nutt, C.L., et al., Gene expression-based classification of malignant gliomas correlates better with survival than histological classification. Cancer Res, 2003. 63(7): p. 1602-1607.
124. Valk, P.J., et al., Prognostically useful gene-expression profiles in acute myeloid leukemia. N Engl J Med, 2004. 350(16): p. 1617-1628.
125. Ma, X.J., et al., A two-gene expression ratio predicts clinical outcome in breast cancer patients treated with tamoxifen. Cancer Cell, 2004. 5(6): p. 607-616.
126. Chang, J.C., et al., Gene expression profiling for the prediction of therapeutic response to docetaxel in patients with breast cancer. Lancet, 2003. 362(9381): p. 362-369.
127. Jansen, M.P., et al., Molecular classification of tamoxifen-resistant breast carcinomas by gene expression profiling. J Clin Oncol, 2005. 23(4): p. 732-740.
128. Paik, S., et al., A multigene assay to predict recurrence of tamoxifen-treated, node-negative breast cancer. N Engl J Med, 2004. 351(27): p. 2817-2826.
129. Iizuka, N., et al., Oligonucleotide microarray for prediction of early intrahepatic recurrence of hepatocellular carcinoma after curative resection. Lancet, 2003. 361(9361): p. 923-929.
130. Tamoto, E., et al., Gene-expression profile changes correlated with tumor progression and lymph node metastasis in esophageal cancer. Clin Cancer Res, 2004. 10(11): p. 3629-3638.
131. Talbot, S.G., et al., Gene expression profiling allows distinction between primary and metastatic squamous cell carcinomas in the lung. Cancer Res, 2005. 65(8): p. 3063-3071.
132. Chung, C.H., et al., Molecular classification of head and neck squamous cell carcinomas using patterns of gene expression. Cancer Cell, 2004. 5(5): p. 489-500.
133. Belbin, T.J., et al., Molecular classification

of head and neck squamous cell carcinoma using cDNA microarrays. Cancer Res, 2002. 62(4): p. 1184-1190.
134. Choi, P. and C. Chen, Genetic expression profiles and biologic pathway alterations in head and neck squamous cell carcinoma. Cancer, 2005. 104(6): p. 1113-1128.
135. Irie, T., T. Aida, and T. Tachikawa, Gene expression profiling of oral squamous cell carcinoma using laser microdissection and cDNA microarray. Med Electron Microsc, 2004. 37(2): p. 89-96.
136. Mendez, E., et al., Transcriptional expression profiles of oral squamous cell carcinomas. Cancer, 2002. 95(7): p. 1482-1494.
137. Leethanakul, C., et al., Distinct pattern of expression of differentiation and growth-related genes in squamous cell carcinomas of the head and neck revealed by the use of laser capture microdissection and cDNA arrays. Oncogene, 2000. 19(28): p. 3220-3224.
138. Belbin, T.J., et al., Molecular profiling of tumor progression in head and neck cancer. Arch Otolaryngol Head Neck Surg, 2005. 131(1): p. 10-18.
139. Toruner, G.A., et al., Association between gene expression profile and tumor invasion in oral squamous cell carcinoma. Cancer Genet Cytogenet, 2004. 154(1): p. 27-35.
140. Schmalbach, C.E., et al., Molecular profiling and the identification of genes associated with metastatic oral cavity/pharynx squamous cell carcinoma. Arch Otolaryngol Head Neck Surg, 2004. 130(3): p. 295-302.
141. O'Donnell, R.K., et al., Gene expression signature predicts lymphatic metastasis in squamous cell carcinoma of the oral cavity. Oncogene, 2005. 24(7): p. 1244-1251.
142. Nagata, M., et al., Identification of potential biomarkers of lymph node metastasis in oral squamous cell carcinoma by cDNA microarray analysis. Int J Cancer, 2003. 106(5): p. 683-689.
143. Simon, R., et al., Pitfalls in the use of DNA microarray data for diagnostic and prognostic classification. J Natl Cancer Inst, 2003. 95(1): p. 14-18.
144. Ransohoff, D.F., Rules of evidence for cancer molecular-marker discovery and validation. Nat Rev Cancer, 2004. 4(4): p. 309-314.
145. Simon, R., Development and validation of therapeutically relevant multi-gene biomarker classifiers. J Natl Cancer Inst, 2005. 97(12): p. 866-867.
146. Bertucci, F., et al., Gene expression profiling of cancer by use of DNA arrays: how far from the clinic? Lancet Oncol, 2001. 2(11): p. 674-682.
147. Tinker, A.V., A. Boussioutas, and D.D. Bowtell, The challenges of gene expression microarrays for the study of human cancer. Cancer Cell, 2006. 9(5): p. 333-339.
148. Kallioniemi, O., Medicine: profile of a tumour. Nature, 2004. 428(6981): p. 379-382.
149. Garber, K., Genomic medicine. Gene expression tests foretell breast cancer's future. Science, 2004. 303(5665): p. 1754-1755.

2

A pilot study for expression profiling of head and neck squamous cell carcinomas

A pilot study for expression profiling of head and neck squamous cell carcinomas

Paul Roepman, Marian J.A. Groot Koerkamp, Antony J. Miles, Dik van Leenen, Joop van Helvoort and Frank C.P. Holstege

Department of Physiological Chemistry, University Medical Center Utrecht, Universiteitsweg 100, 3584 CG Utrecht, the Netherlands.

Head and neck cancer is the fifth most common malignancy worldwide but despite increased knowledge about this cancer the estimated five-year survival rate has not increased over the last twenty years and remains constant at fifty percent. An important prognostic factor for survival is the presence of regional lymph node metastasis in patients diagnosed with head and neck cancer. However, due to difficulties in detecting the presence of neck lymph node metastasis, a large group of patients receive inappropriate surgical treatment. To improve the diagnosis of metastasis we plan to perform a gene expression profiling study on primary head and neck tumors to identify a gene signature that can discriminate tumors from patients with or without lymph node metastasis. Before starting with this large profiling study, we used a limited number of tumor samples to set up and validate all necessary protocols and procedures. Three prime issues in establishing a workable tumor profiling procedure are reproducibility, the limited amount of individual tumor tissue that is available for this study and the large number of tumors that need to be analyzed. In this pilot study we have minimized the amount of tumor tissue needed by introducing a linear amplification step to generate enough target material for microarray hybridization, optimized labeling and hybridization procedures and tested the procedure for reproducibility and possible cross-hybridization. We have also set up a high-throughput microarray hybridization platform to quickly analyze multiple samples in parallel with a restricted number of manual steps. A proposed reference-based study design with a common reference pool of all experimental samples was also tested for discriminatory power between different tumor samples. The results of these tests and procedures are described. Using the expression profiling procedures set up here we will be able to carry out a large profiling study to identify a molecular expression signature for detection of lymph node metastasis in patients with head and neck cancer.

Introduction

Head and neck cancer consists of a large group of neoplasms that arise in the head and neck region. The majority of these neoplasms (90%) are head and neck squamous cell carcinomas (HNSCC) and arise in the epithelium of the oral cavity, oropharynx, hypopharynx or larynx. HNSCC is the fifth most common malignancy worldwide with over 500,000 new patients each year (1) and is especially frequent in regions where tobacco use and alcohol

consumption is high (2). Despite increased knowledge about this type of cancer, the estimated overall 5-year survival rate for patients diagnosed with head and neck cancer has not changed significantly over the past twenty years and remains constant at fifty percent (3). Treatment strategy for HNSCC largely depends on the progression stage of the disease (4) and relies on the use of prognostic factors. An important prognostic factor is the presence of cervical lymph node metastasis; the survival rate of patients with positive nodes drops by almost 50 percent (5, 6). Therefore, it is of clinical importance to determine whether a patient diagnosed with HNSCC also has developed regional lymph node metastasis. Based on this assessment, the most appropriate neck therapy can be chosen.

Patients diagnosed positively for cervical lymph node metastasis undergo a radical neck dissection, which encompasses uni- or bilateral surgical removal of submental, submandibular, upper, middle and lower cervical as well as supraclavicular nodes (7). Histological examination of such surgically removed lymph nodes reveals that current clinical assessment of positive (N+) status is reasonably accurate, with only 10 percent of cases showing no sign of metastasis. However, current clinical diagnostics of the negative (N0) status is quite inaccurate. After histological examination of electively operated clinically negative (N0) patients, about one-third actually show positive neck nodes. Since the prevalence of clinically false-negative patients is high, our clinic prefers surgery to a "watch and wait" policy and perform a supra-omohyoidal neck dissection (SOHND) for all clinically diagnosed N0 patients. A SOHND includes the removal of the submental, submandibular, upper and middle cervical lymph nodes only, saving the lower cervical and supraclavicular node regions (7, 8). As a consequence of avoiding undertreatment of the falsely diagnosed N0 patients, two-thirds of the N0 patients, with an accurate clinical diagnosis, now receive unnecessary surgery since they do not have metastasis. Although a SOHND is less severe than a radical neck dissection, it still results in disfigurement, long-term discomfort and pain and can lead to further complications such as shoulder disability (9-11). It is therefore highly desirable to improve the diagnosis in order to reduce the number of patients that receive unnecessary neck surgery.

To improve the detection of cervical lymph node metastases pre-operatively, new diagnostic technologies are needed. Current diagnosis of neck metastasis is based on imaging of the neck region by palpation, ultrasound examination, computed tomography (CT), magnetic resonance imaging (MRI), and aspiration cytology (12-14). In principle, an entirely different approach for identification of patients with neck metastasis could be based on the cellular and molecular processes of the metastatic primary tumor. Cancer is caused by an accumulation of genetic and epigenetic changes leading to inappropriate function or regulation of processes such as cell cycle control, cell death and DNA repair, immune response, cell adhesion, and (lymph)angiogenesis (15, 16). Measuring the activity of genes involved in these processes could provide information about the processes involved in tumor formation, progression and metastasis (17, 18). It is unlikely that we can elucidate these processes by studying individual genes. To fully understand complex biological processes, including the development and progression of cancer, a global approach is required such as studying gene expression of thousands of genes (19). Microarray technology makes it

Figure 2.1 | DL23 cell line mRNA amplification and fluorescent label incorporation.
(**A**) Gel electrophoresis of DL23 total RNA, cRNA generated using 500 ng and 1000 ng total RNA and a negative control for mRNA amplification lacking reverse transcriptase. (**B**) Different aa-UTP concentrations show different amplification yield and label incorporation. Yield (bars) and label percentages (lines) are shown for a total uracil (aa-UTP + UTP) concentrations of 12 µM and 23 µM, and for an aa-UTP/UTP ratio of 2.33, 4, and 9. Green and red lines indicates Cy3 and Cy5 label incorporation, respectively. (**C**) CRNA (upper) and cDNA (lower) spectra showing absorbance peaks of nucleic acids (260 nm), Cy3 fluophores (550 nm) and Cy5 fluophores (649 nm) for low, normal and high label incorporation The asterisk indicated the wavelength (600 nm) of the second cy5 peak, which shows a stronger absorbance peak in higher labeled cRNA samples due to quenching of the dye molecules.

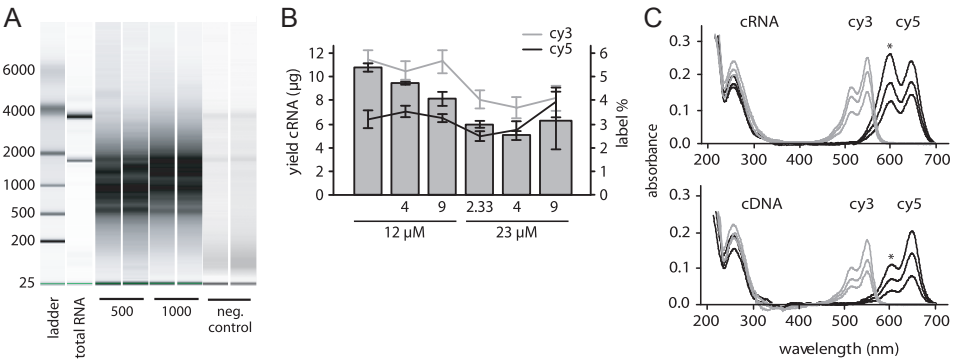

possible to take a genome-wide snapshot of gene expression and, thus, of cellular processes and functions (20). Gene expression profiling has recently been used to investigate tumor (sub)classification (21-25), cancer progression (26-28), clinical outcome (29, 30), and treatment response (31, 32). Several microarray studies have been published for HNSCC (33-36), but so far no clinically relevant expression profile for detection of lymph node metastasis in HNSCC has been found.

Here we present work aimed at developing and validating microarray protocols for high-throughput expression profiling of HNSCC tumors. A number of technical aspects are addressed including RNA isolation, mRNA amplification, high-throughput hybridization, and cross-hybridization of specific RNA targets. Additionally, we validated the reproducibility of the technical procedures and tested the robustness of a reference-design study setup (37), in which all samples are compared against a common reference sample consisting of a pool of all the experimental samples. Together, the resulting procedures form the basis for a large-scale gene expression profiling study to identify a gene expression signature for head and neck lymph node metastasis.

Results

Development of protocols using a carcinoma cell line

Isolated colon carcinoma cell line (DL23) total RNA was used to establish protocols for removal of DNA contaminants and for mRNA amplification and coupling of fluorescent labels (cy-dyes) to the generated cRNA. Two methods for RNA cleanup after DNase digestion were tested: lithium chloride precipitation and a commercial DNAse inactivation with RNA

Table 2.1 | Tumor samples. Total RNA yield (after DNase treatment) are based on isolation using two 20-µm sections. cRNA yields are based on amplification of 1,000 ng total RNA.

Sample	Tumor ID	Section size (mm^2)	Tumor %	Total RNA yield (µg)	cRNA yield (µg)	Label incorporation (%)	
						Cy5	Cy3
T97	T97-01621	9	80	0.6	9.7	2.0–3.5	2.0–3.5
T98	T98-01545	33	70	1.0	10.1	2.0–4.0	3.5–6.0
T99	T99-05003	24	80	1.5	10.4	1.5–3.0	4.0–5.5
T00	T00-08701	10	50	Degraded total RNA			

cleanup reagent (DNA-free kit, Ambion) which resulted in a loss of nucleic acids of 78 ± 3.8 percent and 35 ± 2.5 percent, respectively. Gel electrophoresis confirmed the higher RNA yield using the commercial DNA-free kit (data not shown).

The T7 linear amplification procedure (Methods) generated single stranded complementary RNA (cRNA) with a median length of 1,000 base pairs (bp) and a range of 500 – 2,000 bp (Fig. 2.1 A). Ribosomal RNA bands were clearly visible in total RNA samples but absent in the generated cRNA samples, indicating that only mRNA has been amplified. Starting with 500 and 1,000 ng DNA-free total RNA, the amplification procedure yielded 2.8 ± 0.4 and 10.9 ± 2.3 µg of cRNA, respectively. A two-fold reduction in starting material resulted in a four-fold reduction in cRNA yield.

During the amplification step, aminoallyl-UTP was incorporated into the cRNA. Different ratios of UTP and aminoallyl-UTP resulted in different cRNA yields presumably due to the more difficult enzymatic incorporation of the aminoallyl-UTP. The highest cRNA yield was achieved for an aa-UTP/UTP ratio of 2.33 and a total UTP (aa-UTP and UTP) concentration of 11.7 µM (Fig. 2.1 B). Typical cy-dye incorporation ranged between 2.5 and 4 percent for cy5, and between 4 and 6 percent for cy3 (Fig. 2.1 B). When comparing the cRNA and cDNA spectra we noticed that the absorbance ratio of the two cy5 peaks (600 and 649 nm) increased for labeled cRNA (Fig. 2.1 C). This effect increased for higher cy5 incorporations. The elevated second cy5 absorbance peak at 600 nm is derived from a non-fluorescent form and is caused by quenching of cy5 dye molecules that are in close proximity and is specific for RNA molecules (38, 39).

Tumor sections and RNA isolation

Four tumor samples (T97, T98, T99 and T00) were selected for this pilot study (Table 2.1). After sectioning, RNA isolation and DNase treatment, one tumor sample (T00) showed degraded total RNA and was excluded from further analysis. The other three tumor samples contained high quality total RNA and showed clearly visible ribosomal RNA bands (Fig. 2.2 A). The minimal number of 20-µm sections needed to obtain 1 µg of DNA-free total RNA needed for linear amplification depended on the size of the tumor samples. For the tumor samples larger than 30 mm^2 (T98 and T99) only two sections were needed but if the tumor sample was smaller (T97) more sections were needed (Fig. 2.2 B). The average RNA yield

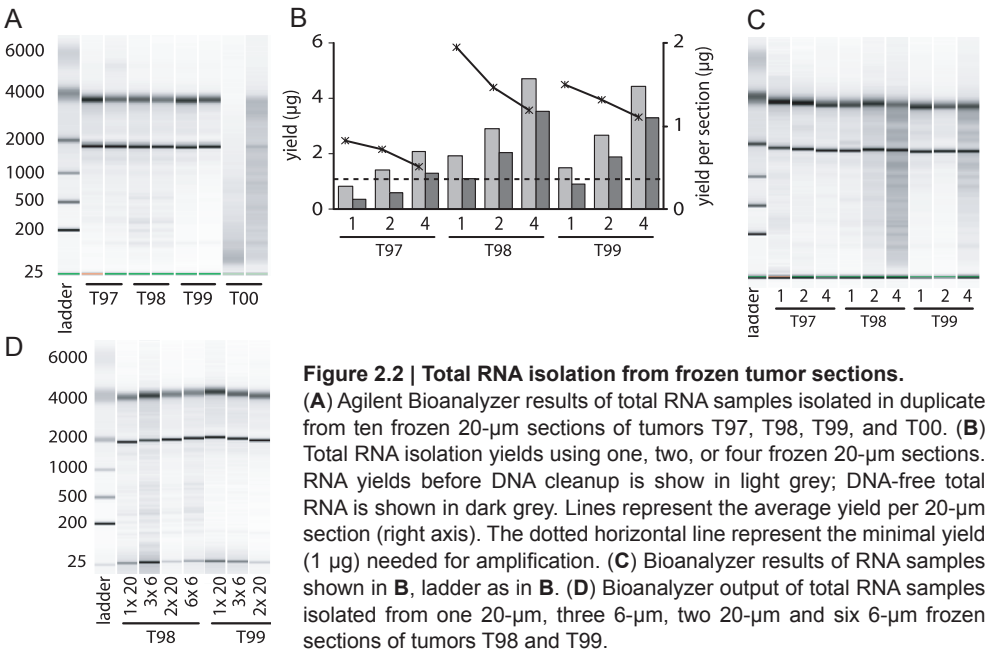

Figure 2.2 | Total RNA isolation from frozen tumor sections. (**A**) Agilent Bioanalyzer results of total RNA samples isolated in duplicate from ten frozen 20-µm sections of tumors T97, T98, T99, and T00. (**B**) Total RNA isolation yields using one, two, or four frozen 20-µm sections. RNA yields before DNA cleanup is show in light grey; DNA-free total RNA is shown in dark grey. Lines represent the average yield per 20-µm section (right axis). The dotted horizontal line represent the minimal yield (1 µg) needed for amplification. (**C**) Bioanalyzer results of RNA samples shown in **B**, ladder as in **B**. (**D**) Bioanalyzer output of total RNA samples isolated from one 20-µm, three 6-µm, two 20-µm and six 6-µm frozen sections of tumors T98 and T99.

per 20-µm section decreased for multiple sections (Fig. 2.2 B, lines). Remarkably, total RNA was partially degraded when more than two sections were used for RNA isolation of larger tumor samples (T98 and T99) (Fig. 2.2 C). This degradation was caused by a reduced RNA stability in cases when multiple large tumor sections were put into an relative small volume of the RNA stabilizing reagent (RNAlater). The protective capability of the RNAlater reagent could be restored by increasing the volume (data not shown). Finally, no differences were found between isolation using 6-µm or 20-µm sections for RNA yield (80.3 ± 16.2 and 80.0 ± 24.5 ng/µm, respectively) and RNA quality (Fig. 2.2 D).

Linear mRNA amplification

A linear amplification procedure was used to amplify the mRNA population of the total RNA samples. Amplification yields were reproducible for all tumor samples and, when started with 1,000 ng total RNA, ranged between 8.9 and 11.3 µg cRNA (Fig. 2.3 A). This cRNA yield is sufficient to perform multiple sample hybridizations and to establish a common reference by pooling half of all cRNA samples (described below). Tumor sample cRNA fragments were of the same length as DL23 cell line with a median length of 1,000 bp (Fig. 2.3 B). No residual ribosomal RNA bands were visible.

To check for possible biases that had been introduced by the amplification procedure, fourteen external control RNAs (ECs) (40) were spiked into the total RNA samples at known amounts and ratios (Fig. 2.3 C). After amplification, labeling and, the EC signals indicated that no biases were introduced during the amplification procedure. Both the nine normal-ECs (EC 1–9, spiked in at a ratio of 1:1) and the five ratio-ECs (EC 10–14, spiked in at differential

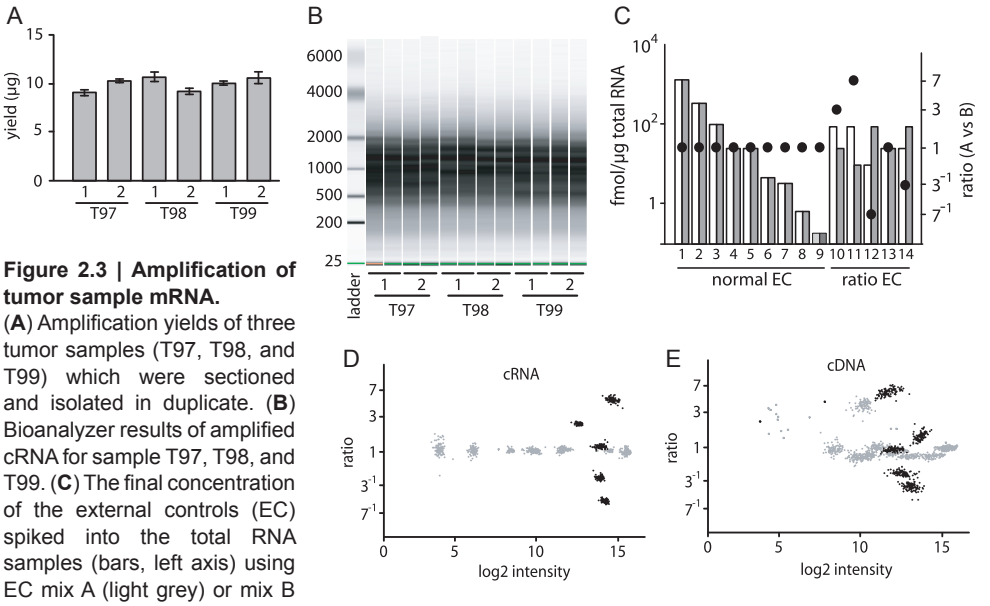

Figure 2.3 | Amplification of tumor sample mRNA.
(**A**) Amplification yields of three tumor samples (T97, T98, and T99) which were sectioned and isolated in duplicate. (**B**) Bioanalyzer results of amplified cRNA for sample T97, T98, and T99. (**C**) The final concentration of the external controls (EC) spiked into the total RNA samples (bars, left axis) using EC mix A (light grey) or mix B (dark grey). When a sample containing mix A is combined and hybridized with a sample containing mix B, the ECs will show specific expression intensities and ratios (circles, right axis). The fourteen ECs can be separated into a group of 'normal-ECs' (1-9) showing a differential ratio of one, and a group of 'ratio-ECs' (10-14) that shows differential ratios of 7, 3, 1, 1/3, and 1/7. (**D-E**) External control signals and ratios from microarray hybridization using amplified cRNA (**D**) or non-amplified cDNA (**E**) as target. ECs signal intensities are plotted on the horizontal axis and ECs ratios on the vertical axis. Black indicates normal-ECs, grey indicates ratio-ECs.

ratios) showed the corresponding ratios in which they had been spiked into the total RNA samples (Fig. 2.3 D). The differential ratios of the ratio-ECs were all slightly diminished. Since hybridizations with non-amplified cDNA samples also showed a similar reduction in ratios (Fig. 2.3 E) this artifact was probably caused by the hybridization procedure and not due to the linear amplification. Hybridization signals of cRNA samples more closely resembled the original spiked-in EC amounts than hybridization using cDNA samples, indicating that the amplification procedure is more accurate and robust in generating labeled targets than the standard cDNA synthesis.

Reproducibility and study setup

Next, the reproducibility of the procedure was tested. Tumor sample T99 was sectioned in duplicate (T99-1 and T99-2), RNA isolation and cRNA synthesis were performed independently, and the duplicates were hybridized against the same reference samples. Of the 21,329 gene features present on the microarray, 11,809 showed a significant expression above the background signal in both duplicate samples. Of these significantly expressed genes, only 49 genes showed a difference in expression ratio larger than two-fold by the two technical replicates (P = 0.004) (Fig. 2.4 A). The high correlation of the T99 duplicate

samples (cosine correlation 0.884) indicated that the sampling and hybridization procedures are adequately reproducible.

The sensitivity and robustness of a proposed 'reference-design' study setup for expression profiling of HNSCC tumors (Fig. 2.4 B) was tested using three tumor samples (T97, T98, and T99) (Fig. 2.4 C). Based on 10,972 significantly expressed genes, two duplicates of each tumor sample grouped together (Euclidian distance, complete hierarchical clustering), demonstrating that the reference design is capable of discriminating the three samples (Fig. 2.4 D). Using a stringent selection criterion, the reference-design identified 182 genes that were differentially expressed ($P < 0.01$, Student's t-test with Bonferroni multiple testing correction) between the three samples while showing identical expression between the duplicates (Fig. 2.4 E). These results indicate that a reference-based study design has enough discriminatory power to identify differences between head and neck tumor samples from different patients, even when using only a limited number of samples.

Figure 2.4 | Reproducibility of procedures and feasibility of 'reference-design' study setup.
(**A**) Reproducibility of the expression profiling procedures. Tumor sample T99 was processed in duplicate (T99-1 and T99-2) and hybridized against the same reference. Expression ratios are plotted for 11,809 significantly expressed genes. The diagonal lines indicate 2-fold differences between the duplicate samples, and the 48 genes that showed a difference larger than 2-fold are plotted in black. (**B**) Study design for expression profiling of a tumor population using a reference design. The tumor samples, derived from both N0 and N+ patients, are analyzed in dye swap against a common reference sample consisting of a pool of all experimental samples. (**C**) In this pilot study three tumor samples (T97, T98, and T99) were processed in duplicate and analyzed based on a reference-design setup. The reference consists of a pool of cRNA from all six duplicates. (**D**) Hierarchical clustering (Euclidian distance, complete clustering) of the six duplicate tumor samples using 10,972 significantly expressed genes. (**E**) Differentially expressed genes (Pearson around zero correlation, centroid clustering) between the three pilot tumors (*P* < 0.01, Student's t-test with Bonferroni multiple testing correction), black indicates upregulation and white indicates downregulation of a gene.

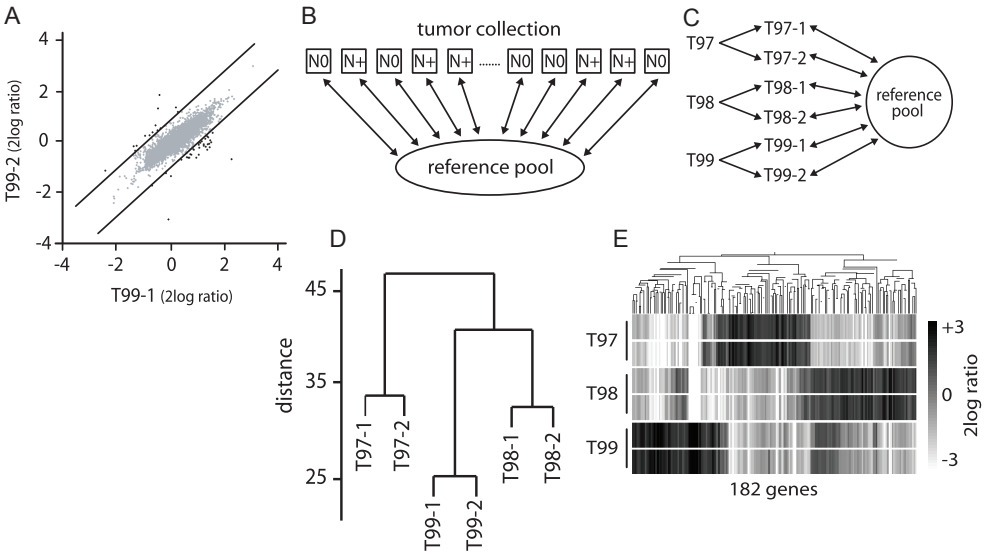

Cross-hybridization of external controls

Within the set of differently expressed genes ($P < 0.05$) across the six analyzed samples, we noticed a subset of genes that showed a remarkable expression pattern: an opposed expression between the corresponding duplicates for all three analyzed tumors (Fig. 2.5 A). These genes seemed downregulated in one sample and appeared upregulated in the matching duplicate, or visa versa. Investigation of the individual sample hybridizations indicated that this expression pattern correlated with the spiked-in external control (EC) mix (Fig. 2.5 B). A probable cause is cross hybridization of the ratio-ECs on the corresponding gene spots on the microarray. When ratio-EC mix A was spiked into a sample, these genes showed a differential expression, which was inverted when the opposed ratio-EC mix B was used. In total 233 genes showed a differential expression on the microarray not due to differential gene expression in the tumor samples but because of cross-hybridization with the external ratio controls (correlation with ratio-EC pattern of at least 0.60). Based on this result, the ratio external controls were omitted from further use in microarray experiments using human RNA samples.

High-throughput hybridization

Expression profiling of a large number of head and neck tumor samples would benefit from a high-throughput hybridization platform for performing multiple parallel array hybridizations. A Ventana Discovery Hybridization station was acquired and set up for high-throughput microarray hybridization. The initially supplied pre-manufactured pre-hybridization/blocking buffer (ChipSpread) and 2x hybridization buffer (Chiphybe) resulted in poor hybridization quality (Fig. 2.6 A, left panels). In consultation with the manufacturer

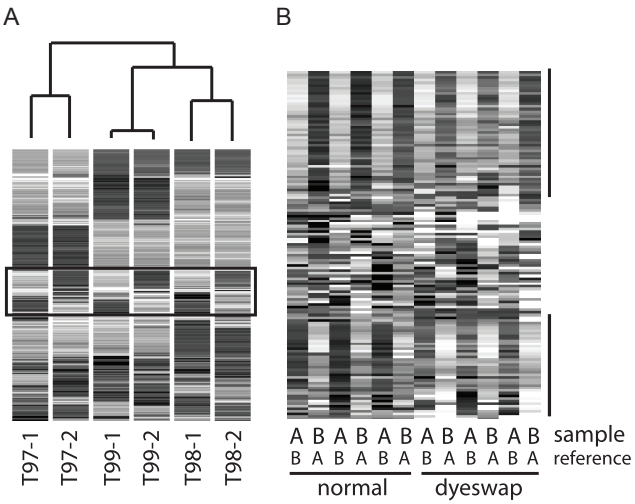

Figure 2.5 | Cross-hybridization of external controls on gene spots. (**A**) The set of differentially expressed genes across the six duplicate samples include a subset of genes (indicated by the box) which expression pattern is inverted between the corresponding tumor sample duplicates. (**B**) Detailed view of individual hybridizations indicating genes showing cross hybridization with ratio external controls (black bars). Differential expression patterns are shown for twelve hybridizations (normal and dyeswap). The tumor sample and reference were respectively spiked in with ratio-EC mixes A and B or with B and A. Black indicates upregulation and white indicates downregulation of a gene.

we discovered that the poor hybridization performance was due to suboptimal formamide concentration of the hybridization buffer, limited shelf-life and wrong formulation of the blocking buffer. The hybridization performance was greatly improved by increasing the formamide concentration in the 2x hybridization buffer to 80 percent (Chiphybe80) (Fig. 2.6 A, upper panels) and by using freshly made filter-sterilized blocking buffer (Fig. 6a, lower panels), following a recipe released by Ventana.

Microarray hybridizations that were performed using the Ventana Hybridization station resulted in lower hybridization signals, mainly for the cy5-channel, compared to manual hybridizations (Fig 2.6 B). Despite the differences in signal intensity, a manual and Ventana hybridization gave similar expression ratios (0.991, cosine correlation) when analyzing the same target samples. Two-channel spotted microarray hybridizations, using both cy3 and cy5 fluorescent dyes, can suffer from auto-fluorescence of spotted oligo nucleotide preparations in the cy3-channel (41). Due to the lower hybridization signals, this cy3-artifact becomes more apparent for Ventana hybridizations (Fig. 2.6 C). Although data normalization is able to correct for this intensity bias on average (42), we introduced an additional treatment with sodium borohydrate to reduce the cy3 auto-fluorescence for all individual spots (41, 43) (Fig.

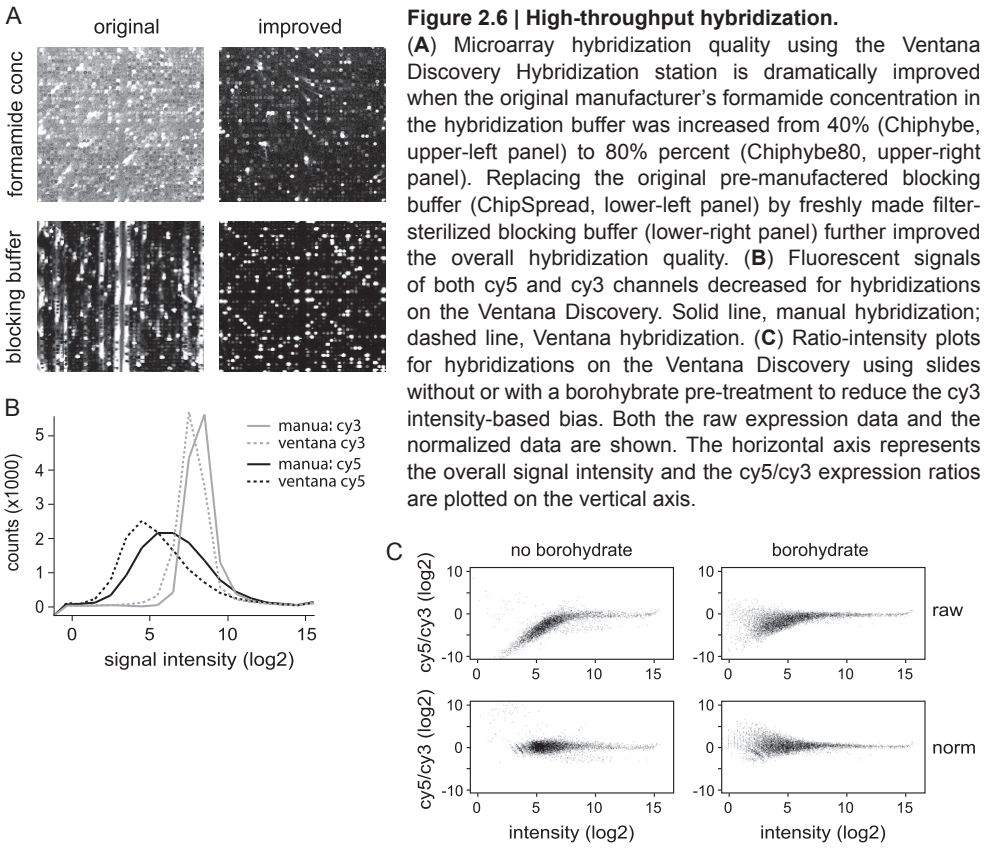

Figure 2.6 | High-throughput hybridization.
(**A**) Microarray hybridization quality using the Ventana Discovery Hybridization station is dramatically improved when the original manufacturer's formamide concentration in the hybridization buffer was increased from 40% (Chiphybe, upper-left panel) to 80% percent (Chiphybe80, upper-right panel). Replacing the original pre-manufactered blocking buffer (ChipSpread, lower-left panel) by freshly made filter-sterilized blocking buffer (lower-right panel) further improved the overall hybridization quality. (**B**) Fluorescent signals of both cy5 and cy3 channels decreased for hybridizations on the Ventana Discovery. Solid line, manual hybridization; dashed line, Ventana hybridization. (**C**) Ratio-intensity plots for hybridizations on the Ventana Discovery using slides without or with a borohybrate pre-treatment to reduce the cy3 intensity-based bias. Both the raw expression data and the normalized data are shown. The horizontal axis represents the overall signal intensity and the cy5/cy3 expression ratios are plotted on the vertical axis.

2.6 C). Inclusion of a manual high-throughput offline washing step allowed us to perform twenty sample hybridizations in parallel, making the system suitable for expression analysis of a larger number of samples in a short time.

Discussion

Using a small set of primary head and neck tumors, we have set up an experimental procedure for high-throughput genome wide expression profiling of HNSCC tumors by means of DNA microarrays. After setup and verification of all the technical procedures, we have validated the value of a 'reference-based' study design (37) which will be used for a large profiling study to identify an expression signature that is capable of discriminating tumors from patients with and without neck lymph node metastasis.

An important aspect for setting up the procedures for a large HNSCC expression profiling study is the limited availability of frozen primary tumor specimen, while the microarray hybridizations require a relative larger amount of high quality target sample. To overcome this shortage of tumor sample we optimized the RNA isolation procedure and introduced an mRNA amplification step to generate large quantities of complementary RNA (cRNA) which can be used as targets for microarray hybridization. The linear mRNA amplification procedure is based on the original protocol published by Eberwine (44), and introduces less biases in the mRNA population than other PCR-based amplification procedures (45-47). Briefly, using a double anchored poly(T) primer modified 5' with a T7 RNA polymerase promoter sequence the mRNAs were transcribed into double stranded cDNA which was subsequently used for in vitro transcription to generate multiple copies of cRNA. We confirmed the linearity of the amplification procedure by using artificially introduced external control (EC) RNAs (40). While the ECs are a useful tool for validating the expression measurements, we noticed significant cross-hybridization of the ratio control RNAs on specific gene features. This is explained by the fact that the external controls were originally designed for the budding yeast genome prior to the availability of all human genome sequences. The cross-hybridization was not seen for yeast microarray hybridizations (40). Consequently, the ratio control RNAs were omitted from use in further microarray experiments concerning human RNA samples.

To carry out a single microarray hybridization, multiple laborious methodological steps need to be completed. Therefore, manual processing of a large set of tumor sample, which requires over two-hundred hybridizations, is time consuming and will undoubtedly lead to an increased variation between the analyzed samples. Therefore, we set up an high-throughput semi-automated analysis platform that requires a limited number of manual steps and by which twenty microarray hybridization can processed in parallel. This technique allows analysis of large numbers of tumor samples in a limited time-span using a less laborious procedure. As a result, the technical variation between the analyzed samples is expected to be reduced and the extracted gene expression measurements will likely be more powerful for identifying specific expression signatures.

Not only is the degree of technical noise in the expression measurements of influence

on the power to deduce statistical differences in gene expression between different tumor types; also the correct study design greatly improves the results and conclusions that can be drawn from a certain set of samples (37, 48). The optimal study design depends on the type of (biological) question that needs answering, but also on the number of samples and slides that are available and whether technical or biological replicates can be included (49, 50). The design of a microarray experiment can range from a simple sample-to-sample comparison to screen for potential targets, to an extensive loop-design with multiple spokes or a reference based design to indirectly compare multiple samples via a common reference (48). All designs have their own flaws and advantages and the optimal study design, therefore, depends on the goal of a particular microarray project.

For the large HNSCC expression profiling study we have decided to use a reference based design. The advantage of the reference design is the relative limited number of microarray hybridization that are needed for analysis of a large number of samples, and the possibility to add samples later without re-analysis of the previous samples. On the other hand, a disadvantage of the reference design is the reduction of discriminative power when comparing samples indirectly via a reference sample (37). Nevertheless, this pilot study shows that the reference design is capable of discriminating different primary tumors, even when using only a limited number of samples. In the pilot study and the planned HNSCC profiling study the common reference consists of a pool of all experimental samples. For dual channel microarray hybridization, this type of reference is preferred over a cancer cell line or healthy head and neck tissue since all transcripts that are present in the experimental samples will also be present in the pooled reference. If a transcript is not present in the reference, due to noise, the calculated expression ratios will suffer from a great deal of inaccuracy.

With this small scale pilot study we have tackled two obstacles in successful expression profiling for tumor tissue: limited starting material and the great numbers of tumor samples. These obstacles were dealt with by introducing an mRNA amplification step and using a high-throughput hybridization platform. Furthermore, a reference based study design was selected to be most useful for this profiling study and was validated using a small number of primary tumors. In conclusion, we have designed a robust expression profiling platform for head and neck primary tumors by which a large scale profiling study can be performed in a limited time using a small amount of tissue material.

Materials and Methods

DL23 cell line and RNA isolation | DL23 cells (51) were grown until 50% confluence in RPMI 1640 medium with 2 mM L-glutamine adjusted to contain 1.5 g/L sodium bicarbonate, 4.5 g/L glucose, 10 mM HEPES (pH 7.5), 1.0 mM sodium pyruvate and 10% fetal bovine serum. The cells were washed once with PBS and a small volume of Trizol was added to the flask and incubated on ice for 15 minutes to lyse the cells. The lysate was removed to a 50ml tube, the flask was rinsed again with a small volume of Trizol and added to the first sample. Aliquots (1 ml) of the Trizol lysate were placed in eppendorf tubes, 0.2 ml chloroform was added, vortexed for 15 seconds and incubated at room temperature for 3 minutes. Next, the sample were centrifuged at 14,000 rpm for 20 minutes at 4°C. The aqueous phase was precipitated with isopropanol, air dried and resuspended in milliQ water. The RNA was further purified using a Qiagen midi column (Qiagen) with DNase treatment on the column according to the manufacturers protocol.

Tumor sectioning and RNA isolation | For this pilot study, four samples were selected from a collection of primary HNSCC tumors. Fresh tumor tissue was taken from the surgical specimen, immediately snap frozen in liquid nitrogen and stored at –80°C. Tumor sample characteristics are presented in Table 1. A haematoxylin and eosin stained section (6 µm) was prepared for tumor percentage assessment. Frozen sections (6-µm and 20-µm) were cut for RNA isolation and immediately transferred to ice-cold RNA stabilizing solution (RNAlater, Ambion). To isolate total RNA, Trizol (Invitrogen) reagent was added, incubated for 5 min at room temperature (RT), and after adding 10 µl pre-heated (37°C) Proteinase K incubated for 30 min at 37°C. Chloroform was added (20 µl per 100 µl Trizol) and mixed vigorously. After centrifugation (4°C, 20 min at 14,000 rpm) the water-phase was transferred to a new microcentrifuge tube. RNeasy columns (Qiagen) were used for further cleanup according to the manufacturers protocol. Yield and quality was analyzed by spectrophotometry and by the 2100 Bioanalyzer (Agilent). Total RNA samples were stored at –80°C or directly used for DNase treatment.

DNase treatment of total RNA | Three µl 10x DNaseI buffer and 1 µl DNase I (2 units) were added to the total RNA samples (26 µl, max 1 µg/µl) and incubated for 30 min at 37°C. Clean up of DNA-free RNA was done using lithium chloride (LiCl) precipitation (DL23 total RNA) or using a commercial DNAse inactivation and RNA cleanup reagent (DNA-free kit, Ambion) (DL23 and tumor sample total RNA). Following LiCl precipitation, milliQ water was added to a final volume of 150 µl. An equal volume of phenol/chloroform/isoamylalcohol (25:24:1) was added, mixed thoroughly and centrifuged 5 min. at 14,000 rpm. Upper water phase was subsequently extracted using an equal volume of chloroform. RNA was precipitated by adding half a volume of LiCl precipitation solution (7.5 M LiCl, 50 mM EDTA) and incubation for at least 30 min at -20°C. After centrifugation (4°C, 5 min at 14,000 rpm) the pellet was washed with 70% ethanol, dried and dissolved in 10 µl milliQ water. Using the DNA-free kit (Ambion), DNase inactivation reagent (3 µl) was added, incubated 2 min at RT, and centrifuged 5 min at 10,000 rcf. The water phase containing DNA-free RNA was extracted, yield was determined by spectrophotometry, and the samples were stored at –80°C.

cDNA synthesis and aminoallyl incorporation | Total RNA was dissolved in 7 µl milliQ water, and 6 µl Oligo $dT_{(12-18)}$ primer (0.25 µg/µl) was added. Sample were incubated 10 min at 70°C and cooled on ice. The labeling mix (3 µl dGAC-mix (1 mM each), 0.9 µl dTTP (1 mM), 2.1 µl aminoallyl-dUTP (1 mM, Sigma), 6.0 µl 5x 1st strand buffer (Invitrogen), and 3 µl DTT (0.1 M, Invitrogen)) was prepared on ice, 15 µl was added to the RNA/primer samples and incubated 2 min at RT. Two µl SuperScript II Reverse Transcriptase (200 U/µl, Invitrogen) was added and the samples were incubated for 60 min at 42°C. After reverse transcription, samples were incubated 2 min at 95°C and cooled on ice. During reverse transcription, aminoallyl-dUTP was incorporated into single stranded cDNA (ratio aa-dUTP/dTTP of 2.33). Ten µl NaOH (1 M) and 10 µl EDTA (0.5 M) were added and incubated for 15 min at 65°C to remove the RNA template. The reaction was neutralized by adding 25 µl HEPES buffer (1 M, pH 7.5). Samples were cleaned using a Microcon-30 column (Ambion). The cDNA samples were eluted by centrifugation for 3 min at 10,000 rcf, and the yield determined using spectrophotometry. Samples were stored at –20°C.

mRNA amplification and aminoallyl incorporation | The mRNA amplification protocol is an adapted 'Eberwine' linear amplification protocol (44). Total RNA (500 – 2,000 ng) was dissolved in 9 µl, 1 µl T7-poly(dT) primer (5'-GG CCAGTGAATTGTAATACGACTCACTATAGGGA $GGCGGT_{(24)}$VN-3') was added and incubated 10 min at 70°C and afterwards kept at 48°C. First strand mix (4 µl 5x 1st strand buffer (Invitrogen), 2 µl DTT (0.1 M, Invitrogen), 1 µl linear acrylamide (0.1 µg/µl), 1 µl dNTPs (20 mM), and 1 µl RNase inhibitor (40 U/µl, Roche)) was preheated to 48°C and added to the RNA sample. After adding 1 µl Superscript II Reverse Transcriptase (200 U/µl, Invitrogen), the samples were incubated for 2 hours at 48°C. Next, second strand mix (106 µl milliQ water, 15 µl 10x 2nd strand buffer (200 mM Tris-HCl pH 6.9, 900 mM KCl, 46 mM Mg Cl_2, 1.5 mM β-NAD^+, 100 mM $(NH_4)_2SO_4$), 3 µl dNTPs (20 mM), 1 µl T4 DNA ligase (20 U/µl, Promega), 4 µl E.Coli DNA polymerase I (9 U/µl, Promega), and 1 µl RNAse H (2 U/µl, Promega)) was added to the reaction products and incubated for 2 hours at 16°C followed by 10 min at 65°C. Double stranded cDNAs were purified using Qiagen PCR clean up columns according to manufacturers protocol. After clean up, samples were concentrated to 8 µl and used for in vitro transcription (IVT) using the

T7 Megascript Kit (Ambion). After IVT for 4 hours, the generated cRNA was purified using RNeasy mini columns (Qiagen). During transcription, 5-(3-aminoallyl)-UTP (aa-UTP) was incorporated into single-stranded cRNA (ratio aaUTP/UTP of 2.33). Yield and quality were quantified using spectrophotometry and the 2100 Bioanalyzer. Samples were stored at –80°C.

Fluorescent labeling of cDNA and cRNA | Cy3 and cy5 fluorphores (Amersham) could be directly coupled to the incorporated aminoallyl groups of the generated cRNAs or cDNAs. Samples (500 ng) were concentrated or diluted to 8 µl and 1 µl sodium bicarbonate buffer (pH 9.0) was added. Cy3 / cy5 fluophores were resuspended in 10 µl dimethyl sulfoxide (DMSO) (Merck) and 1.25 µl aliquots were added to the cRNA or cDNA samples and incubated in the dark at room temperature for 60 minutes. To prevent cross coupling during hybridization, the cy-dyes were quenched by adding 4.5 µl hydroxylamine (4 M, Sigma Aldrich) and incubated for 15 minutes. The remaining uncoupled fluophore molecules were removed using a ChromoSpin-30 column (BD Biosciences). After centrifugation (700 rcf, 5 min) the elute contained the purified labeled cRNA or cDNA. Yield and label incorporation was determined using spectrophotometry (Fig. 2.1 C). Sample were stored in the dark at –20°C or kept on ice until hybridization. For hybridization, cy-labeled tumor sample targets were combined with an equal amount of reverse labeled reference target.

Microarray production | The Human Array-Ready Oligo set (version 2.0) was purchased from Operon and printed on Corning UltraGAPS slides with a MicroGrid II (Biorobotics) using 48-quill pins (Microspot2500; Apogent Discoveries) in 3x SSC at 50% humidity and at 18°C, and were processed by ultraviolet crosslinking (2,400 millijoules, 10 min) with a Stratalinker 2400 (Stratagene). The microarrays contained 70-mer oligo-nucleotides representing 21,329 gene features as well as 3871 additional features for control purposes.

Manual microarray hybridization | Excess unbound DNA was removed by rigorously shaking the microarray slides for 1 minute in buffer containing 2x SSC and 0.05% SDS. Before hybridization, the slides were incubated in preheated (42°C) borohydrate buffer (2x SSC, 0.05% SDS and 0.25% sodium borohydrate (Aldrich)) for 30 minutes at 42°C, washed with milliQ water and dried using pressurized air or by centrifugation at 500 rpm for 2 minutes. Microarray slides were prehybridized in buffer containing 5x SSC, 25% formamide (Merck), 0.1% SDS and 1% bovine serum albumin (BSA, Sigma) at 42°C for 45 minutes. Slides were washed with milliQ water and isopropanol, air-dried and directly used for sample hybridization. Fresh 2x hybridization buffer (50% formamide, 10x SSC and 0.2% SDS) was prepared and filter sterilized using a 0.22 micron filter. Five µl Herring Sperm DNA (10 µg/µl, sheared) and 5 µl tRNA (20 µg/µl) were added to 250 µl preheated (42°C) hybridization buffer and the buffer was preheated to 42°C. Cy5 and cy3 labeled targets were combined (max 40 µl) and 40 µl preheated 2x hybridization buffer was added, heated to 95°C for 5 minutes and centrifuged at 12,000 rpm for 2 minutes. After centrifugation, the hybridization mix was immediately applied to a prepared microarray slide covered with a LifterSlip (Erie Scientific) and placed in a Corning Hybridization Chamber (Corning). The slides were incubated in the dark at 42°C for 16-20 hours. The hybridized slides were subsequently washed for 4 minutes in low-stringent wash buffer (1xSSC and 0.2% SDS), high-stringent wash buffer (0.1x SSC and 0.2% SDS) and 0.1x SSC. Slides were dried using pressurized air or by centrifugation (2 min at 500 rpm) and scanned in the Agilent G2565AA DNA Microarray Scanner (100% laser power, 30% photomultiplier tube (PMT)).

High throughput microarray hybridization | Microarray slides were processed simultaneously in batches of 20 slides. Excess unbound DNA was removed by rigorously stirring (1200 rpm) for 3 minutes using an ArrayIt® High-Throughput Wash Station (Telechem Int.) filled with 500 ml buffer containing 2x SSC and 0.05% SDS. Slides were transferred to another Wash Station containing preheated (42°C) borohydrate buffer (2x SSC, 0.05% SDS and 0.25% sodium borohydrate (Aldrich)) and incubated for 30 minutes at 42°C and 450 rpm. Slides were washed using milliQ water and dried by centrifugation at 500 rpm for 2 minutes. High throughput hybridizations were performed using the Ventana Discovery Hybridization Station in combination with the ChipMap or ChipMap-80 kit (Ventana Europe). The following hybridization program was used: Prehybridization [selected], probe [selected], Denaturation [70°C, 6 min], Hybridization [42°C, 10 hours], Stringency Wash #1 [selected, 37°C, 6 min], ChipClean [selected]. ChipSpread mix was prepared freshly before each run by dissolving 0.3

g bovine BSA in 10 ml milliQ water and adding 3 ml 20x SSC, 300 µl SDS and 15 ml formamide (Merck). The total volume was adjusted to 30 ml with milliQ water and filter sterilized. After prehybridization, the labeled cRNA targets were hybridized at 42°C for 10 hours. Using an ArrayIt® Wash Station, the slides were subsequently washed for 2 minutes in RiboWash (Ventana Europe) and 2 minutes in 0.1x SSC. Slides were briefly dipped in 96% ethanol and dried using centrifugation (2 min at 500 rpm). The Ventana barcode label was removed and the backside of the slides was cleaned with 70% ethanol. Microarray slides were scanned in the Agilent G2565AA DNA Microarray Scanner (100% laser power, 30% PMT).

Preprocessing of expression data | Scanned images were quantified and corrected for background using Imagene 4.0 software (Biodiscovery). Aberrant spots were flagged and not used for further analysis. Quantified expression data was normalized for dye and print-tip biases by a Lowess per print-tip normalization algorithm (42) applied in the statistical package R (52) using the existing packages 'SMA' (http://www.stat.berkeley.edu/users/terry/zarray/Software/smacode.html) and 'com.braju.sma' (http://www.maths.lth.se/help/R/com.braju.sma). Alterations were made for import of Imagene 4.0 data, flagging of spot, Lowess line calculation on subsets of spots and extrapolation to all spots in the subgrid. This has been incorporated into an R package called 'genomics.sma'. The normalization rule applied in this study used gene spots to calculate the fitted Lowess line for each subgrid and applies this line to normalize all spots. Duplicate dye-swap hybridizations were averaged and for each gene a sample-reference ratio was calculated. Further analysis of expression data was performed in the statistical package R (http://www.r-project.org/) and in the software package GeneSpring 5.0 (Silicon Genetics).

References

1. Genden, E.M., et al., Referral guidelines for suspected cancer of the head and neck. Auris Nasus Larynx, 2005.
2. Sankaranarayanan, R., et al., Head and neck cancer: a global perspective on epidemiology and prognosis. Anticancer Res, 1998. 18(6B): p. 4779-4786.
3. Reid, B.C., et al., Head and neck in situ carcinoma: incidence, trends, and survival. Oral Oncol, 2000. 36(5): p. 414-420.
4. Forastiere, A., et al., Head and neck cancer. N Engl J Med, 2001. 345(26): p. 1890-1900.
5. Jones, A.S., et al., The level of cervical lymph node metastases: their prognostic relevance and relationship with head and neck squamous carcinoma primary sites. Clin Otolaryngol, 1994. 19(1): p. 63-69.
6. Hahn, S.S., et al., The prognostic significance of lymph node involvement in pyriform sinus and supraglottic cancers. Int J Radiat Oncol Biol Phys, 1987. 13(8): p. 1143-1147.
7. Robbins, K.T., et al., Neck dissection classification update: revisions proposed by the American Head and Neck Society and the American Academy of Otolaryngology-Head and Neck Surgery. Arch Otolaryngol Head Neck Surg, 2002. 128(7): p. 751-758.
8. Medina, J.E. and R.M. Byers, Supraomohyoid neck dissection: rationale, indications, and surgical technique. Head Neck, 1989. 11(2): p. 111-122.
9. Ewing, M.R. and H. Martin, Disability following radical neck dissection; an assessment based on the postoperative evaluation of 100 patients. Cancer, 1952. 5(5): p. 873-883.
10. Short, S.O., et al., Shoulder pain and function after neck dissection with or without preservation of the spinal accessory nerve. Am J Surg, 1984. 148(4): p. 478-482.
11. van Wilgen, C.P., et al., Shoulder pain and disability in daily life, following supraomohyoid neck dissection: a pilot study. J Craniomaxillofac Surg, 2003. 31(3): p. 183-186.
12. Baatenburg de Jong, R.J., et al., Metastatic neck disease. Palpation vs ultrasound examination. Arch Otolaryngol Head Neck Surg, 1989. 115(6): p. 689-690.
13. van den Brekel, M.W., et al., Modern imaging techniques and ultrasound-guided aspiration cytology for the assessment of neck node metastases: a prospective comparative study. Eur Arch Otorhinolaryngol, 1993. 250(1): p. 11-17.
14. Hillsamer, P.J., et al., Improving diagnostic accuracy of cervical metastases with computed tomography and magnetic resonance imaging. Arch Otolaryngol Head Neck Surg, 1990. 116(11): p. 1297-1301.
15. Hanahan, D. and R.A. Weinberg, The hallmarks of cancer. Cell, 2000. 100(1): p. 57-70.
16. Jefferies, S. and W.D. Foulkes, Genetic

mechanisms in squamous cell carcinoma of the head and neck. Oral Oncol, 2001. 37(2): p. 115-126.
17. Ludwig, J.A. and J.N. Weinstein, Biomarkers in Cancer Staging, Prognosis and Treatment Selection. Nat Rev Cancer, 2005.
18. Sidransky, D., Emerging molecular markers of cancer. Nat Rev Cancer, 2002. 2(3): p. 210-219.
19. Miller, L.D., et al., Optimal gene expression analysis by microarrays. Cancer Cell, 2002. 2(5): p. 353-361.
20. Macgregor, P.F. and J.A. Squire, Application of microarrays to the analysis of gene expression in cancer. Clin Chem, 2002. 48(8): p. 1170-1177.
21. Golub, T.R., et al., Molecular classification of cancer: class discovery and class prediction by gene expression monitoring. Science, 1999. 286(5439): p. 531-537.
22. Alizadeh, A.A., et al., Distinct types of diffuse large B-cell lymphoma identified by gene expression profiling. Nature, 2000. 403(6769): p. 503-511.
23. Tay, S.T., et al., A Combined Comparative Genomic Hybridization and Expression Microarray Analysis of Gastric Cancer Reveals Novel Molecular Subtypes. Cancer Res, 2003. 63(12): p. 3309-3316.
24. Perou, C.M., et al., Molecular portraits of human breast tumours. Nature, 2000. 406(6797): p. 747-752.
25. Valk, P.J., et al., Prognostically useful gene-expression profiles in acute myeloid leukemia. N Engl J Med, 2004. 350(16): p. 1617-1628.
26. Wang, Y., et al., Gene-expression profiles to predict distant metastasis of lymph-node-negative primary breast cancer. Lancet, 2005. 365(9460): p. 671-679.
27. Huang, E., et al., Gene expression predictors of breast cancer outcomes. Lancet, 2003. 361(9369): p. 1590-1596.
28. Ahr, A., et al., Identification of high risk breast-cancer patients by gene expression profiling. Lancet, 2002. 359(9301): p. 131-132.
29. van 't Veer, L.J., et al., Gene expression profiling predicts clinical outcome of breast cancer. Nature, 2002. 415(6871): p. 530-536.
30. van de Vijver, M.J., et al., A gene-expression signature as a predictor of survival in breast cancer. N Engl J Med, 2002. 347(25): p. 1999-2009.
31. Ma, X.J., et al., A two-gene expression ratio predicts clinical outcome in breast cancer patients treated with tamoxifen. Cancer Cell, 2004. 5(6): p. 607-616.
32. Jansen, M.P., et al., Molecular classification of tamoxifen-resistant breast carcinomas by gene expression profiling. J Clin Oncol, 2005. 23(4): p. 732-740.
33. Belbin, T.J., et al., Molecular classification of head and neck squamous cell carcinoma using cDNA microarrays. Cancer Res, 2002. 62(4): p. 1184-1190.
34. Leethanakul, C., et al., Distinct pattern of expression of differentiation and growth-related genes in squamous cell carcinomas of the head and neck revealed by the use of laser capture microdissection and cDNA arrays. Oncogene, 2000. 19(28): p. 3220-3224.
35. Chung, C.H., et al., Molecular classification of head and neck squamous cell carcinomas using patterns of gene expression. Cancer Cell, 2004. 5(5): p. 489-500.
36. Mendez, E., et al., Transcriptional expression profiles of oral squamous cell carcinomas. Cancer, 2002. 95(7): p. 1482-1494.
37. Yang, Y.H. and T. Speed, Design issues for cDNA microarray experiments. Nat Rev Genet, 2002. 3(8): p. 579-588.
38. Gruber, H.J., et al., Anomalous fluorescence enhancement of Cy3 and cy3.5 versus anomalous fluorescence loss of Cy5 and Cy7 upon covalent linking to IgG and noncovalent binding to avidin. Bioconjug Chem, 2000. 11(5): p. 696-704.
39. t Hoen, P.A., et al., Fluorescent labelling of cRNA for microarray applications. Nucleic Acids Res, 2003. 31(5): p. e20.
40. van de Peppel, J., et al., Monitoring global messenger RNA changes in externally controlled microarray experiments. EMBO Rep, 2003. 4(4): p. 387-393.
41. Martinez, M.J., et al., Identification and removal of contaminating fluorescence from commercial and in-house printed DNA microarrays. Nucleic Acids Res, 2003. 31(4): p. e18.
42. Yang, Y.H., et al., Normalization for cDNA microarray data: a robust composite method addressing single and multiple slide systematic variation. Nucleic Acids Res, 2002. 30(4): p. e15.
43. Raghavachari, N., et al., Reduction of autofluorescence on DNA microarrays and slide surfaces by treatment with sodium borohydride. Anal Biochem, 2003. 312(2): p.

101-105.
44. Phillips, J. and J.H. Eberwine, Antisense RNA Amplification: A Linear Amplification Method for Analyzing the mRNA Population from Single Living Cells. Methods, 1996. 10(3): p. 283-288.
45. Wadenback, J., et al., Comparison of standard exponential and linear techniques to amplify small cDNA samples for microarrays. BMC Genomics, 2005. 6(1): p. 61.
46. Wang, E., et al., High-fidelity mRNA amplification for gene profiling. Nat Biotechnol, 2000. 18(4): p. 457-459.
47. Puskas, L.G., et al., RNA amplification results in reproducible microarray data with slight ratio bias. Biotechniques, 2002. 32(6): p. 1330-1334, 1336, 1338, 1340.
48. Churchill, G.A., Fundamentals of experimental design for cDNA microarrays. Nat Genet, 2002. 32 Suppl 2: p. 490-495.
49. Tumor Analysis Best Practices Working Group, T., Expression profiling-best practices for data generation and interpretation in clinical trials. Nat Rev Genet, 2004. 5(3): p. 229-237.
50. Ransohoff, D.F., Rules of evidence for cancer molecular-marker discovery and validation. Nat Rev Cancer, 2004. 4(4): p. 309-314.
51. Kops, G.J., et al., Control of cell cycle exit and entry by protein kinase B-regulated forkhead transcription factors. Mol Cell Biol, 2002. 22(7): p. 2025-2036.
52. Ihaka, R. and R. Gentleman, R: a language for data analysis and graphics. J Comp Graph Statist, 1996. 5: p. 299–314.

3

An expression profile for diagnosis of lymph node metastases from primary head and neck squamous cell carcinomas

Nature Genetics. 2005 Feb; 37 (2): 182-186

An expression profile for diagnosis of lymph node metastases from primary head and neck squamous cell carcinomas

Paul Roepman[1], Lodewyk F.A. Wessels[5,6], Nienke Kettelarij[1], Patrick Kemmeren[1], Antony J. Miles[1], Philip Lijnzaad[1], Marcel G.J. Tilanus[2], Ronald Koole[3], Gert-Jan Hordijk[4], Peter C. van der Vliet[1], Marcel J.T. Reinders[5], Piet J. Slootweg[2], Frank C.P. Holstege[1]

[1]Department of Physiological Chemistry, [2]Department of Pathology, [3]Department of Oral and maxillofacial surgery, [4]Department of Otorhinolaryngology, University Medical Center Utrecht, Universiteitsweg 100, 3584 CG Utrecht, the Netherlands. [5]Faculty of Electrical Engineering, Mathematics and Computer Science, Delft University of Technology, Mekelweg 4, 2628 CD Delft, the Netherlands. [6]Department of Pathology, The Netherlands Cancer Institute, Plesmanlaan 121, 1066 CX Amsterdam, the Netherlands.

Nature Genetics. 2005 Feb; 37 (2): 182-186

Metastasis is the process by which cancers spread to distinct sites in the body. It is the principal cause of death in individuals suffering from cancer. For some types of cancer, early detection of metastasis at lymph nodes close to the site of the primary tumor is pivotal for appropriate treatment. Because it can be difficult to detect lymph node metastases reliably, many individuals currently receive inappropriate treatment. We show here that DNA microarray gene expression profiling can detect lymph node metastases for primary head and neck squamous cell carcinomas that arise in the oral cavity and oropharynx. The predictor, established with an 82-tumor training set, outperforms current clinical diagnosis when independently validated. The 102 predictor genes offer unique insights into the processes underlying metastasis. The results show that the metastatic state can be deciphered from the primary tumor gene-expression pattern and that treatment can be substantially improved.

Introduction

Head and neck squamous cell carcinomas (HNSCCs) are a heterogeneous group of tumors that arise from the epithelium of the upper aerodigestive tract. HNSCC is the fifth most common malignancy in humans and is associated with high alcohol and tobacco use (1). As with most forms of cancer, treatment depends largely on progression stage (2). Detection of local lymph node metastasis is pivotal for choosing appropriate treatment, especially for individuals diagnosed with HNSCC in the oral cavity or oropharynx (3). Most of these individuals have the primary tumor removed. Treatment of individuals clinically diagnosed with lymph node metastasis (N+ status) involves the additional surgical removal of a substantial portion of the neck, including all five local lymph node levels (radical neck dissection, RND) (4). Upon histological examination of removed tissue, 10–20% of clinically diagnosed N+ individuals turn out to be metastasis-free (N0) (5). Clinical diagnosis of N0 status is even less accurate. Postoperative histological examination shows that approximately one-third of

clinically diagnosed N0 individuals have metastasis-positive lymph nodes in the neck (6). Different strategies exist for treating diagnosed N0 individuals (7). In the 'watch and wait' strategy, diagnosed N0 individuals do not undergo any neck dissection; this risks fatality by allowing overlooked metastases to spread further. Because the false-negative rate is very high, most clinics carry out neck surgery for all diagnosed N0 individuals. In these cases, a supraomohyoidal neck dissection (SOHND) is done, which removes the three upper lymph node levels (4). SOHND is less appropriate than RND for N+ individuals falsely diagnosed as N0 and, moreover, is completely unnecessary for individuals correctly diagnosed as N0. Although SOHND is less rigorous than RND, the treatment causes disfigurement, long-term discomfort and pain and can lead to additional complications such as shoulder disability (8, 9). Both strategies result in inappropriate treatment because of limitations in detecting lymph node metastasis reliably.

DNA microarray gene-expression profiling is useful for cancer classification (10-13) and prognosis-based treatment (14). Genes differentially regulated in metastases have been identified (15, 16) and a 17-gene expression signature that is common to both primary tumors and metastases has been found (17). Primary tumors may therefore carry expression patterns capable of predicting the presence of or potential for lymph node metastases. Such expression signatures are starting to be uncovered (18), but so far without independent validation for reliability and clinical outcome. Here we determine whether a gene expression signature exists for detecting the presence of HNSCC lymph node metastasis and whether this could improve current diagnosis and treatment.

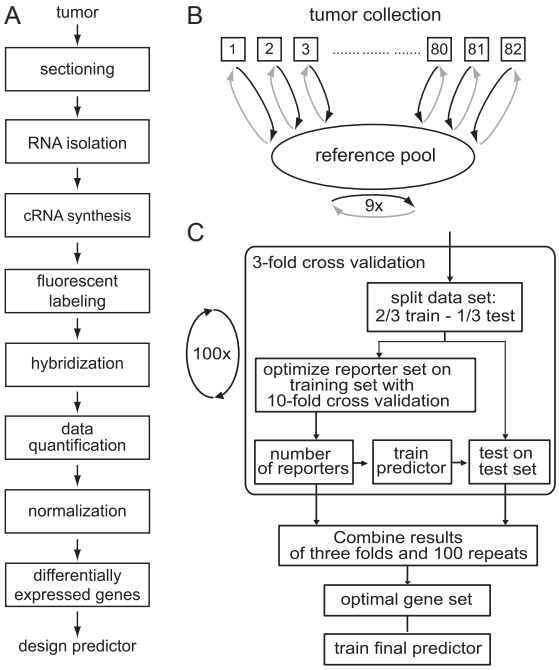

Figure 3.1 | Study design and procedure overview. (**A**) RNA was isolated from 2–3 tumor sections, followed by mRNA amplification and fluorescent labeling. After hybridization, scanned images were quantified and the data was normalized. Duplicates of each tumor were averaged and a predictor was designed using the differentially expressed genes. Quality control monitoring occurred after total RNA isolation, cRNA synthesis, labeling, scanning and normalization. (**B**) The training experiment involved 82 primary HNSCC tumors, compared in duplicate dyeswap against a common reference pool containing equal amount of cRNA from all 82 tumors. Nine reference pool self-self comparisons were generated in parallel, to establish an error-model for technical variation. (**C**) The predictor was designed using a double training-validation procedure. See methods section for details.

Results

To identify a predictive gene expression signature, we analyzed 82 primary tumors located in the oropharynx or oral cavity regions, including 45 tumors derived from individuals who were found to be N+ postoperatively (n = 44) or who subsequently developed metastasis in the lymph nodes in the neck (n = 1) and 37 tumors from individuals who were found to be N0 postoperatively and who remained metastasis-free. Selection criteria included the presence of at least 50% tumor cells in tumor sections and RNA passing the quality control criteria proposed by the Tumor Analysis Best Practices Working Group (19) (see Methods for selection criteria and Appendix Table 3.1 and 3.2 for individual characteristics). For each sample, we generated two expression profiles in dyeswap experiments against a common

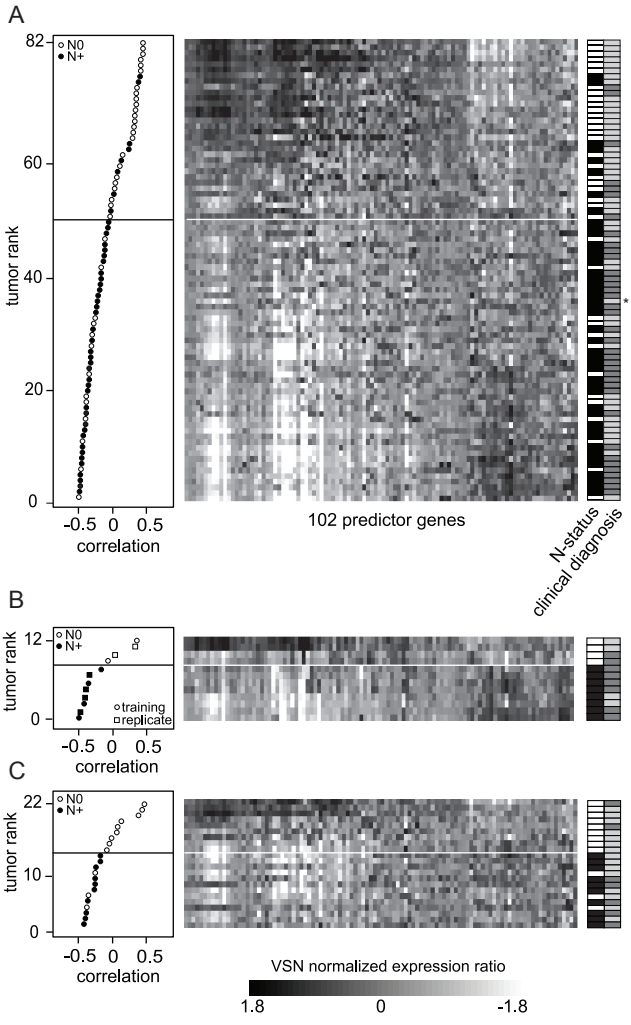

Figure 3.2 | A predictor for HNSCC lymph node metastasis. (**A**) Expression profiles of the 102 predictor genes on the 82 primary tumor training set (middle). The predictor genes are clustered based on their similarities across the 82 tumors (Pearson around zero correlation, centroid clustering). Tumors are rank-ordered according to their correlation with the average N0 expression profile (left). The solid line represents the threshold for optimal overall accuracy. Tumors above the threshold show an expression profile that indicates that the individual is free of lymph node metastasis. In the right panel, each individual's histological N status, including the 3-year follow-up period, and the clinical diagnosis are shown (black indicates postoperative histological N+; white indicates postoperative histological N0; dark gray indicates clinical N+; and light gray indicates clinical N0). The asterisk indicates an individual who developed lymph node metastasis after treatment. (**B**) Expression profiles and tumor correlations from six training tumors samples (circles) and their technical replicates (squares). (**C**) Expression profiles of the 102 predictor genes on an independent validation set of 22 primary HNSCC tumors. The threshold is set according to the optimal threshold established with the latter half of the training set (Fig. 3.3 D). VSN, variance stabilization normalization

reference pool. We selected genes that were expressed differentially in at least 30 samples (1,986 genes) and used them to build a predictor (Fig. 3.1 and Methods).

To identify genes capable of discriminating between N+ and N0 individuals, we applied a supervised classification approach that is related to those used previously (14). This approach involves repeatedly splitting the data into training (two-thirds) and test subsets (one-third) and assessing performance on the iteratively generated test sets, which is well suited to establishing a classifier without bias towards the training set (20). We reached optimal prediction with a set of 102 genes (Table 3.1 and Appendix Table 3.3).

The predictor correctly determined the neck metastasis status for 61 of 82 individuals in the training set (Fig. 3.2 A). Because this improvement is only incremental compared with current clinical diagnosis, we next determined whether any individual or sample parameter was associated with predictive performance. We found that performance increased gradually as more recent samples were analyzed (Fig. 3.3). This result indicates that long-term storage of tumor tissue has an adverse effect on its predictive value. The N0 predictive accuracy for the most recent tumors was >90%. Although one possible explanation for loss of predictive accuracy over time could be degradation of tumor material (21), we found no evidence for RNA degradation in our samples. The total RNA and cRNA samples all passed quality control (19), and no significant association could be established between total RNA yield, cRNA yield, cRNA fragment length and tumor storage time. The high predictive accuracy for the most recent tumors (Fig. 3.3) is compatible with the goal of analyzing fresh biopsies, and so we tested the predictor further.

We first determined technical reproducibility for six of the training set tumors, starting from frozen tissue (Fig. 3.2 B). The technical replicates showed a high correlation with the training outcome ($R^2 = 0.92$) and identical ranking and prediction in each case. The most appropriate test of predictive accuracy is validation on independent tumors (14). We generated expression profiles for an additional 22 samples, which were surgically removed in 2000 or

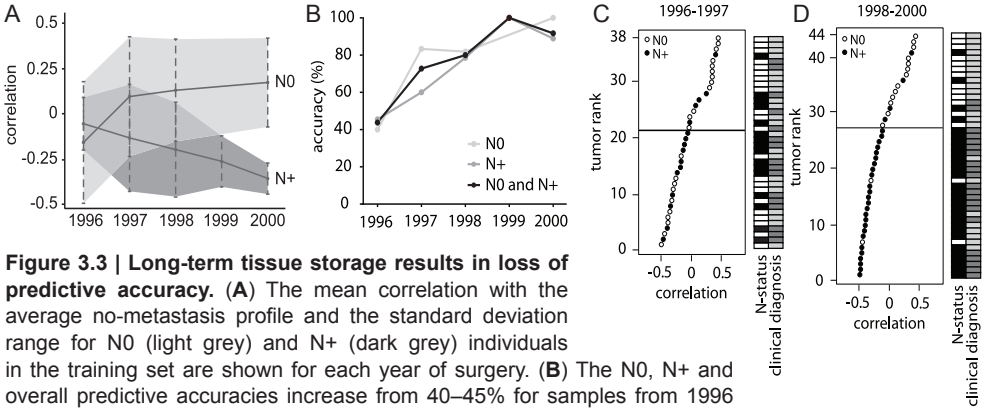

Figure 3.3 | Long-term tissue storage results in loss of predictive accuracy. (**A**) The mean correlation with the average no-metastasis profile and the standard deviation range for N0 (light grey) and N+ (dark grey) individuals in the training set are shown for each year of surgery. (**B**) The N0, N+ and overall predictive accuracies increase from 40–45% for samples from 1996 to 89–100% for samples from 2000. (**C,D**) Correlation data from tumors with longer (**C**; samples from 1996–1997) or shorter (**D**; samples from 1998–2000) storage time. The predictor correctly predicts 22 of 38 and 38 of 44 samples, respectively.

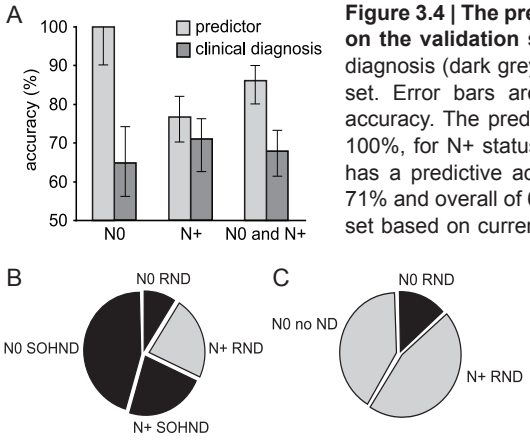

Figure 3.4 | The predictor outperforms current clinical diagnosis on the validation set. (**A**) Predictive accuracies of current clinical diagnosis (dark grey) and the predictor (light grey) on the validation set. Error bars are based on the standard error for predictive accuracy. The predictor has a predictive accuracy for N0 status of 100%, for N+ status of 77% and overall of 86%. Clinical diagnosis has a predictive accuracy for N0 status of 67%, for N+ status of 71% and overall of 68%. (**B,C**) Treatment accuracy for the validation set based on current clinical diagnosis (**B**) or on predictor outcome (**C**). Completely appropriate treatment is shown in grey and under- or overtreatment in black. Current diagnosis resulted in 23% of individuals receiving appropriate treatment (50% of N+ individuals receiving an RND). Predictor-based treatment would result in 86% of individuals receiving appropriate treatment (75% of N0 individuals no longer receiving any neck dissection and 100% of N+ individuals receiving an RND).

2001. The predictive signature performed well on the validation set, correctly predicting 19 of 22 tumors (Fig. 3.2 C). No false negative predictions were made, which is most important for the goal of achieving clinical relevance. The predictor performed better than current clinical diagnosis on this small group of individuals, particularly for N0 individuals (Fig. 3.4 A). The predictor has an overall accuracy of 86% compared with 68% for clinical diagnosis. The chance of randomly achieving the overall accuracy of the predictor was 0.0004, compared with P = 0.10 for the result of the clinical diagnosis (hypergeometric test). The odds ratios were at least 30 for the predictor (P = 0.006) and 5 for clinical diagnosis (P = 0.10).

The validation set represents more recent tumors in the collection, and its robust performance compared with that of the training set is consistent with the idea that increased storage leads to loss of predictor performance (Fig. 3.3). The three false-positive predictions (Fig. 3.2 C) might be correct; these three individuals were clinically diagnosed as N0 and underwent SOHND. Metastases in the remaining lymph nodes may have gone undetected during long-term monitoring owing to the postoperative radiation therapy that these individuals received. Regardless of this possibility and the effect of long-term tissue storage, the conclusion from the validation set is that the predictor can detect local lymph node metastases using material from primary HNSCCs, with better performance than current clinical diagnosis.

Because of the restricted size of the validation set, precise determination of the clinical relevance and implications for treatment awaits evaluation in a larger cohort of individuals whose biopsies are starting to be analyzed by expression profiling in parallel with standard diagnosis and treatment. Until these individuals have been monitored for sufficiently long periods of time, we can only extrapolate from the validation set. Substantially improved treatment is projected from the independent validation set. Only 23% of these individuals received completely appropriate treatment (Fig. 3.4 B). Applying the predictor would have raised the treatment accuracy to 86% (Fig. 3.4 C). This includes relieving all N0-diagnosed individuals (54%) from the superfluous neck surgery that they presently undergo as well as ensuring the most appropriate treatment for N+ individuals.

Discussion

Despite metastasis being the principal cause of death in individuals suffering from cancer, the events leading to it are poorly understood (22). In addition to providing a basis for improved diagnosis and treatment, this study is also a screen for metastasis associated genes. Many of the predictor genes have previously been implicated in metastasis (Table 3.1 and Appendix Table 3.3), but more than half of the predictor genes have not been directly associated with tumorigenesis or metastasis before and provide starting points for further investigations. In addition to expected epithelial marker genes, categories of potential interest include genes (putatively) encoding extracellular matrix components; genes involved in cell adhesion, including three members of the plakin family of cytolinkers and the enzyme transglutaminase 3, which have a crucial role in maintaining tissue integrity; cell death genes; cell growth and maintenance genes; and genes encoding hydrolyzing activities, including proteins involved in degradation of the extracellular matrix (*PLAU* and *SERPINE1*) and a metalloproteinase. Another feature of the HNSCC metastasis signature is that more downregulation (two-thirds) than upregulation is associated with metastasis. This indicates that loss of various activities has a dominant role in the acquisition of the metastatic signature. As previously proposed, this process probably involves stromal and immuneregulatory components (23, 24). Many of the predictor genes belong to these categories, strengthening the argument for profiling bulk tumor tissue (17) rather than laser-dissected regions densely populated with tumor cells.

The results presented here may also have other implications for future studies. The storage time–dependent decrease in predictive performance (Fig. 3.3) suggests that such studies should be carried out prospectively, with expression profiles generated immediately upon removal of tumor tissue and then analyzed retrospectively. Other factors that may

Table 3.1 | Selection of predictor genes previously found to be involved with metastasis.
See Appendix Table 3.3 for a list of all 102 predictor genes. N+ corr, correlation with average N+ profile.

Gene	*Description (metastasis related)*	*Genbank ID*	*N+ corr*
COL5A1	collagen genes are upregulated in primary tumors with metastatic potential	NM_000093	0.63
NCOR2	upregulated in malignant endometrium	NM_006312	0.62
PLAU	essential role in the degradation of the extracelluar matrix	NM_002658	0.54
COL5A3	collagen genes are upregulated in primary tumors with metastatic potential	NM_015719	0.52
SPOCK	involved in metastasis of esophageal squamous cell carcinoma	NM_004598	0.50
SERPINE1	high levels correlate with poor prognosis in breast patients	NM_000602	0.44
EPPK1	plakin family of cytolinkers: maintaining tissue integrity	AB107036	-0.57
S100A7	may be associated with nodal metastasis and poor prognosis	NM_002963	-0.58
ECM1	implicated with cell proliferation, angiogenesis, differentiation	NM_022664	-0.61
TGM3	Involved in crosslinking/anchoring plakin members	NM_003245	-0.63
RAD17	expression correlates with lymph node metastasis from NSCLC	NM_133344	-0.63
PPL	plakin family of cytolinkers: maintaining tissue integrity	NM_002705	-0.67
DSG3	role in the adhesion of carcinoma cells during metastasis	NM_001944	-0.71
LAGY	reduced in lung SCC with increasing grade and stage	NM_032495	-0.79
IVL	diminished in tumors in proportion to the malignancy	NM_005547	-0.80
TNFRSF5	correlation of expression and metastatic spread of lung tumors	NM_001250	-0.80

have contributed to finding a reliable predictive signature include the number of tumors analyzed, the experimental design and focusing on a specific location (i.e., the oral cavity and oropharynx). We chose to focus on a specific location because the large heterogeneity of HNSCCs suggested that tumor location might result in distinct tumor development and that different initial mutations might contribute to diverse primary tumor locations (25, 26).

The HNSCC predictive profile is the first example to our knowledge of an independently validated primary tumor expression signature that can reliably detect the presence of metastases in local lymph nodes. The profile is capable of distinguishing metastasizing from nonmetastasizing tumors, a fundamental biological characteristic strongly associated with disease outcome (27, 28) and pivotal for treatment planning. It is highly plausible that expression profiling will, in future, improve diagnosis and treatment of oral cavity and oropharynx squamous cell carcinomas, particularly by reducing adverse side effects related to overtreatment, but also by reducing the severe risk of fatalities due to overlooked metastases in the case of 'watch and wait' strategies. Reducing the number of unnecessary surgical procedures will also substantially lower the costs for healthcare and the degree of postoperative care presently required. The outcome of this study suggests that treatment of other forms of cancer, similarly dependent on knowing the metastatic state, may also be improved.

Methods

Data accessibility | MIAME (29) compliant data in MAGE-ML (30) format as well as complete descriptions of protocols, microarrays and clinical parameters have been submitted to the public microarray database ArrayExpress (http://www.ebi.ac.uk/arrayexpress/) with the following accession numbers: Microarray layout, A-UMCU-3; HNSCC tumor data, E-UMCU-11; Protocols for sectioning of tumor material, P-UMCU-18; RNA isolation, P-UMCU-19; DNase treatment, P-UMCU-20; mRNA amplification, P-UMCU-21; generating reference pool, P-UMCU-26; cRNA labeling, P-UMCU-22; hybridization and washing of slides, P-UMCU-23 and P-UMCU-24; scanning of slides, P-UMCU-25; Image analysis, P-UMCU-11

Tumor samples | For the training set, 92 samples were randomly taken from a collection of primary tumors surgically removed between 1996 and 2000 and that fulfilled the following criteria: biopsy-proven HNSCC in the oropharynx and oral cavity; no previous malignancies in the head and neck region; tumor sections contained more than 50% tumor cells. Of these 92 tumors, 82 passed total RNA and cRNA quality control (QC) and were included in this study. For the validation set, 27 tumors were randomly taken from the same collection of tumors, surgically removed between 2000 and March 2001, and that fulfilled the same selection criteria. Of these, 22 passed total RNA and cRNA QC and were included in this study. The diagnostic procedures for clinical staging of cervical lymph nodes was performed according to the Netherlands national guidelines for oral cavity and oropharynx carcinomas, by clinical examination (palpation) of the neck region, followed by bilateral ultrasound examination, computed tomography (CT) and/or magnetic resonance imaging (MRI). Suspected nodes were subjected to aspiration cytology. In this way, patients were pre-operatively classified as either N0 or N+, the latter in the case of aspirates yielding metastatic tumor cells. Only in the case of obvious neck involvement, as shown by huge swelling, were the patients classified as N+ without additional efforts to prove the presence of metastasis.

Surgery was aimed at complete tumor removal. With regard to the neck, in the case of clinical N0 only a SOHND was performed (4). In cases clinically classified as N+ a RND was performed including all five lymph node levels (4). Postoperative irradiation was administered in accordance with current practice and depending on margin status, tumor growth features, number of positive nodes and extracapsular growth. In practice, 36 out of 60 clinically assessed N0 patients and 38 out of 43 clinically assessed N+ patients received radiation

therapy. This treatment as well as additional clinical information is presented in Appendix Table 3.1 and 3.2. After surgery, patients were periodically checked for development of neck metastasis, and patients initially classified as N0 but showing positive nodes in their surgical specimen or developing neck nodes within a time span of 3 years after surgery without having another head and neck cancer that could be responsible for this metastasis, were retrospectively added to the N+ patient group. Less than 5% of patients with HNSCC in the oral cavity or oropharynx subsequently develop metastasis after treatment (31, 32). Here, for the training and validation cohorts, one patient subsequently developed positive neck nodes after surgery.
Fresh tumor tissue was taken from the surgical specimen, snap-frozen in liquid nitrogen immediately after surgical removal and stored at –80°C. Frozen sections were cut for RNA isolation and immediately transferred to a RNAlater solution (Ambion). A haematoxylin and eosin stained section was prepared for tumor percentage assessment. Only samples with at least 50 percent tumor cells were used. For a small number of samples the tumor percentage was increased by removing areas with no tumor cells.

RNA isolation | Total RNA was isolated from 2 to 3 sections (20 µm) with TRIzol reagent (Invitrogen), followed by a purification using the RNeasy mini-kit (Qiagen) and a DNase treatment using the Qiagen DNA-free kit. The yield and quality of total RNA was checked by spectrophotometry and by the Agilent 2100 Bioanalyser (Agilent). Total RNA quality control criteria were in accordance with the Tumor Analysis Best Practices Working Group (19), discarding samples with no clear 18S and 28S ribosomal bands. We also removed samples that had a yield lower than 500 ng total RNA or showed mycoplasma contamination.

cRNA synthesis and labeling | mRNA was amplified by in vitro transcription using T7 RNA polymerase on 1 µg of total RNA. First a double stranded cDNA template was generated including the T7 promoter. Next, this template was used for in vitro transcription with the T7 megascript kit (Ambion) to generate cRNA. During the in vitro transcription, 5-(3-aminoallyl)-UTP (Ambion) was incorporated into the single-stranded cRNA. The yield and quality of the cRNA was analyzed by spectrophotometry and by the Agilent 2100 Bioanalyser. Samples with a yield less than 5000 ng or with small cRNA fragments (median less than 500 bp) were not used.
Cy3 or cy5 fluorophores (Amersham) were coupled to 500 ng of cRNA. After coupling, free dye molecules were removed using Clontech ChromoSpin-30 columns (Clontech). The yield and label incorporation (5-7%) of the cy-labeled cRNA was checked using spectrophotometry. Before hybridization, 300 ng of cy-labeled cRNA from one tumor was mixed with an equal amount of reverse color cy-labeled material from the reference sample.

Microarray production | The Human Array-Ready Oligo set (version 2.0) was purchased from Qiagen and printed on Corning UltraGAPS slides as described elsewhere (33). The microarrays contained 70-mer oligo-nucleotides representing 21,329 genes as well as 3871 additional features for control purposes.

Microarray hybridization | Before use, the microarray slides were treated with sodium-borohydrate solution to reduce auto-fluorescence in the cy3-channel. The labeled cRNA targets were hybridized on the microarray for 10 hours at 42°C using the Ventana Discovery Hybridization Station in combination with the ChipMap-80 Kit (Ventana Europe). After hybridization the slides were manually washed and scanned in the Agilent G2565AA DNA Microarray Scanner (100% laser power, 30% PMT).

Preprocessing of expression data | The scanned images were quantified and background corrected using Imagene 4.0 software (Biodiscovery). The expression data was normalized for dye and print-tip biases using a Lowess per print-tip normalization algorithm (34) applied in the statistical package R (35). Following normalization, variance stabilization (VSN) (36) was applied to stabilize variance in the intensity data. Both duplicate dye-swap hybridizations of each tumor were averaged and for each gene a tumor-reference ratio was calculated. Reference versus reference hybridizations were used to build a gene error model for technical variation. Nine reference self-self comparisons were performed in dye-swap (18 hybridizations), resulting in nine reference ratios for each gene on the microarray. These nine reference ratios yield an estimate of the technical variation for each gene. To test whether a gene in a tumor samples shows differential expression, a Student's t-test was applied on the tumor ratio and the corresponding nine reference ratios (technical

variation). The calculated p-values for differential expression were used to select those genes that show differential expression in the tumor samples.

Supervised classification | A classifier was constructed to distinguish between N0 and N+ patients. Of the 21,329 genes on the microarray, 6221 were excluded based on aberrant signal and spot morphology in one of the 164 hybridizations. From these remaining 15,108 genes, only genes that were significantly different from the reference in at least 31 tumors were selected based on the error model for technical variation ($P < 0.01$). This resulted in a set of 1,986 genes. For these genes the signal-to-noise-ratio (SNR) (10) was computed and employed to rank the genes (top ranked genes being genes that are best suited to distinguish the outcome classes). The optimal gene set to employ in the classifier (a nearest mean classifier similar to the classifier employed in (14)), was determined by gradually expanding the gene set starting from the highest ranked gene. At each expansion round the nearest mean classifier (14) was trained on a training set and tested on a test set. The performance on the test set served as a quality measure of the gene set. The performance was measured as the average of the false positive (N0 classified as N+) and false negative (N+ classified as N0) rates of the test samples. Initially the performance increases as the set is expanded. The expansion of the gene set is terminated when the performance deteriorates, i.e. when the optimal performance is reached. The steps of ranking the genes and training and testing the classifier are performed in a 10-fold cross-validation procedure. The output of this procedure is an optimal number of top-ranked genes and a trained classifier. To ensure independent validation, this process of optimizing the set of genes and training the classifier is wrapped in a second 3-fold cross-validation loop. This entails that the optimization of the gene set and the training of the classifier is performed on 2/3 of the data, while the classifier is validated on 1/3 of the data. Since this 1/3 of the data is never involved in any of the gene selection and training steps, this ensures completely independent validation of the classifier, which avoids selection bias (20, 37) and therefore results in a reliable performance estimate. This double-loop procedure determined 102 genes to form the final diagnostic classifier. This classifier was trained on the complete set of 82 samples by recalculating the signal-to-noise ratio for all genes and subsequently selecting the top 102 genes. The predictor was trained using the 102 selected genes and the 82 training samples. A decision threshold for this classifier was fixed such that the highest overall predictive accuracy for both N0 and N+ tumors was reached.

Statistics | Odds ratios (OR) were calculated by fitting a logistic regression model on the prediction outcome of the validation set. The predictor had an infinitive OR since no false negative prediction was made. To get an estimate of the OR for the predictor, one false negative was artificially introduced resulting in a predictor OR of 30 ($P = 0.006$) and a clinical OR of 4.2 ($P = 0.15$). The standard error for predictive accuracy (Fig. 3.4 A) includes the predictions made on the latter half of the training set.

References

1. Sankaranarayanan, R., et al., Head and neck cancer: a global perspective on epidemiology and prognosis. Anticancer Res, 1998. 18(6B): p. 4779-4786.
2. Forastiere, A., et al., Head and neck cancer. N Engl J Med, 2001. 345(26): p. 1890-1900.
3. Pantel, K. and R.H. Brakenhoff, Dissecting the metastatic cascade. Nat Rev Cancer, 2004. 4(6): p. 448-456.
4. Robbins, K.T., et al., Neck dissection classification update: revisions proposed by the American Head and Neck Society and the American Academy of Otolaryngology-Head and Neck Surgery. Arch Otolaryngol Head Neck Surg, 2002. 128(7): p. 751-758.
5. Woolgar, J.A., Pathology of the N0 neck. Br J Oral Maxillofac Surg, 1999. 37(3): p. 205-209.
6. Jones, A.S., et al., Occult node metastases in head and neck squamous carcinoma. Eur Arch Otorhinolaryngol, 1993. 250(8): p. 446-449.
7. Pillsbury, H.C., 3rd and M. Clark, A rationale for therapy of the N0 neck. Laryngoscope, 1997. 107(10): p. 1294-1315.
8. Short, S.O., et al., Shoulder pain and function after neck dissection with or without preservation of the spinal accessory nerve. Am J Surg, 1984. 148(4): p. 478-482.
9. van Wilgen, C.P., et al., Shoulder pain and disability in daily life, following supraomohyoid neck dissection: a pilot study. J Craniomaxillofac Surg, 2003. 31(3): p. 183-186.
10. Golub, T.R., et al., Molecular classification of cancer: class discovery and class prediction by gene expression monitoring. Science, 1999.

286(5439): p. 531-537.
11. Alizadeh, A.A., et al., Distinct types of diffuse large B-cell lymphoma identified by gene expression profiling. Nature, 2000. 403(6769): p. 503-511.
12. Perou, C.M., et al., Molecular portraits of human breast tumours. Nature, 2000. 406(6797): p. 747-752.
13. Valk, P.J., et al., Prognostically useful gene-expression profiles in acute myeloid leukemia. N Engl J Med, 2004. 350(16): p. 1617-1628.
14. van 't Veer, L.J., et al., Gene expression profiling predicts clinical outcome of breast cancer. Nature, 2002. 415(6871): p. 530-536.
15. Clark, E.A., et al., Genomic analysis of metastasis reveals an essential role for RhoC. Nature, 2000. 406(6795): p. 532-535.
16. Saha, S., et al., A phosphatase associated with metastasis of colorectal cancer. Science, 2001. 294(5545): p. 1343-1346.
17. Ramaswamy, S., et al., A molecular signature of metastasis in primary solid tumors. Nat Genet, 2003. 33(1): p. 49-54.
18. Chung, C.H., et al., Molecular classification of head and neck squamous cell carcinomas using patterns of gene expression. Cancer Cell, 2004. 5(5): p. 489-500.
19. Tumor Analysis Best Practices Working Group, T., Expression profiling-best practices for data generation and interpretation in clinical trials. Nat Rev Genet, 2004. 5(3): p. 229-237.
20. Simon, R., et al., Pitfalls in the use of DNA microarray data for diagnostic and prognostic classification. J Natl Cancer Inst, 2003. 95(1): p. 14-18.
21. Matsuo, S., et al., Preservation of pathological tissue specimens by freeze-drying for immunohistochemical staining and various molecular biological analyses. Pathol Int, 1999. 49(5): p. 383-390.
22. Fidler, I.J., The pathogenesis of cancer metastasis: the 'seed and soil' hypothesis revisited. Nat Rev Cancer, 2003. 3(6): p. 453-458.
23. Pollard, J.W., Tumour-educated macrophages promote tumour progression and metastasis. Nat Rev Cancer, 2004. 4(1): p. 71-78.
24. Chambers, A.F., A.C. Groom, and I.C. MacDonald, Dissemination and growth of cancer cells in metastatic sites. Nat Rev Cancer, 2002. 2(8): p. 563-572.
25. Huang, Q., et al., Genetic differences detected by comparative genomic hybridization in head and neck squamous cell carcinomas from different tumor sites: construction of oncogenetic trees for tumor progression. Genes Chromosomes Cancer, 2002. 34(2): p. 224-233.
26. Freier, K., et al., Tissue Microarray Analysis Reveals Site-specific Prevalence of Oncogene Amplifications in Head and Neck Squamous Cell Carcinoma. Cancer Res, 2003. 63(6): p. 1179-1182.
27. Jones, A.S., et al., The level of cervical lymph node metastases: their prognostic relevance and relationship with head and neck squamous carcinoma primary sites. Clin Otolaryngol, 1994. 19(1): p. 63-69.
28. Hahn, S.S., et al., The prognostic significance of lymph node involvement in pyriform sinus and supraglottic cancers. Int J Radiat Oncol Biol Phys, 1987. 13(8): p. 1143-1147.
29. Brazma, A., et al., Minimum information about a microarray experiment (MIAME)-toward standards for microarray data. Nat Genet, 2001. 29(4): p. 365-371.
30. Spellman, P.T., et al., Design and implementation of microarray gene expression markup language (MAGE-ML). Genome Biol, 2002. 3(9): p. RESEARCH0046.
31. Carvalho, A.L., et al., Ipsilateral neck cancer recurrences after elective supraomohyoid neck dissection. Arch Otolaryngol Head Neck Surg, 2000. 126(3): p. 410-412.
32. Ridge, J.A., Squamous cancer of the head and neck: surgical treatment of local and regional recurrence. Semin Oncol, 1993. 20(5): p. 419-429.
33. van de Peppel, J., et al., Monitoring global messenger RNA changes in externally controlled microarray experiments. EMBO Rep, 2003. 4(4): p. 387-393.
34. Yang, Y.H., et al., Normalization for cDNA microarray data: a robust composite method addressing single and multiple slide systematic variation. Nucleic Acids Res, 2002. 30(4): p. e15.
35. Ihaka, R. and R. Gentleman, R: a language for data analysis and graphics. J Comp Graph Statist, 1996. 5: p. 299–314.
36. Huber, W., et al., Variance stabilization applied to microarray data calibration and to the quantification of differential expression. Bioinformatics, 2002. 18 Suppl 1: p. S96-104.
37. Ambroise, C. and G.J. McLachlan, Selection bias in gene extraction on the basis of microarray gene-expression data. Proc Natl Acad Sci U S A, 2002. 99(10): p. 6562-6566.

Intermezzo

Tumor Profiling Turmoil

Cell Cycle. 2005 May; 4 (5): 659-660

Tumor Profiling Turmoil

Paul Roepman, Frank C.P. Holstege

Department of Physiological Chemistry, University Medical Center Utrecht, Universiteitsweg 100, 3584 CG Utrecht, the Netherlands.

Cell Cycle. 2005 May; 4 (5): 659-660

Tumor profiling aims to determine gene expression signatures that can discriminate between different sub-types of tumors. We have recently discovered a signature that can reliably detect which primary head-neck tumors have metastasized to local lymph nodes. This signature has great potential for clinical application and also offers unique insights into how metastasis occurs. Despite these obvious advances, discussed here alongside several other findings, such tumor profiling studies are currently receiving harsh criticism. We make clear that such evaluations can themselves also be critically evaluated. The separation between the two factions actually shows that it is too early to either dismiss or exalt tumor profiling studies. Final judgment requires waiting for the results of larger prospective studies carried out in parallel with current clinical practice.

DNA microarrays are frequently used to study cancer. Besides analyzing cancerous tissue or models of cancer development, such global measurements are also used for tumor profiling. Profiling studies identify sets of genes that are able to discriminate between groups of tumors or patients. To date, most profiles can be divided into two types; classifiers which group tumors into previously known or newly discovered subtypes (1) and predictors that deliver a prognosis, usually patient survival rates or response to treatment (2). We have recently described an example of a third type of profile, detectors. Detectors are capable of identifying a basic biological property of tumors, which in this case is the presence of lymph node metastasis (3). Great efforts are being made to discover clinically relevant profiles, but such studies have recently received significant criticism. A recent comparison of tumor profiling studies concluded that the composition of microarray gene expression signatures is highly unstable and dependent on the selection of patients used for determining the signature (4). Furthermore, due to insufficient sample numbers and improper validation, the authors conclude that the results of such studies are overoptimistic. Scientific rigor is required for all studies, including tumor profiling. However in this case the severe and sweeping nature of the conclusions runs the risk of throwing out the baby with the bathwater and the analysis by Michiels and colleagues should also be critically evaluated. Here we place such criticism into perspective and discuss several interesting implications of the newly discovered lymph node metastasis profile (3).

That some early as well as current profiling studies are overoptimistic due to small sample size, overfitting of data and lack of independent validation is actually old news (5, 6). The studies evaluated in the Michiels paper were published mostly in 2002 and were therefore performed even earlier. It would have been much more fair, as well as more useful, if recent studies had been evaluated that were performed and published after such issues had become common knowledge and guidelines were proposed.

Staleness also applies to another general critique expressed in the Michiels article, which is that tumor profiles are not stable with regard to the genes composing the signature. Different sets of training samples within the same study result in predictive profiles composed of quite different sets of genes. This too has been reported before (7). While providing no interpretation for this instability, the insinuation of Michiels et al is that this is a bad property of profiling studies, which they seemingly report here for the first time. In fact the earlier report already provided plausible biological interpretation of this phenomenon. This interpretation is not at all unfavorable for profiling studies. Many genes are simply interchangeable without affecting predictive accuracy because many predictive genes have similar, if not identical expression patterns across tumor samples (7). Genes with related function showing similar expression patterns was one of the first general findings to come out of microarray studies (8). Surprise at discovering this phenomenon again for tumor profiling studies (4) demonstrates lack of biological insight as well as disregard for previously published work. Because predictive genes with similar expression patterns are interchangeable, this leads to different compositions of predictive profiles depending on the composition of the training set and marginal differences in expression values determined by microarrays. This interpretation could at least have been discussed in the Michiels evaluation, especially since it has been proposed before. According to Michiels et al., five of the seven evaluated studies do not result in profiles that perform better than chance (4). Advocating more stringent training approaches which are less-biased towards the training set is certainly an important point, but again one which has been made before (9). Furthermore, the Michiels evaluation applies very stringent criteria for determining whether performance is better than random. This is formally correct and should be used to evaluate the extent to which such studies can claim better performance. However, realistic evaluation of such studies should also take into account the requirement of first performing initial studies (such as the ones under evaluation), before determining whether larger scale studies with sufficient numbers of patients are worth pursuing. Finally, Michiels et al., evaluated overall performance, whereas in some cases correctly predicting only one specific clinical outcome is more important than overall performance.

Although it is admirable to critically evaluate tumor profiling studies, the Michiels evaluation is unjustly harsh, lacks biological interpretation and is based on issues which had already been described but after the evaluated studies were published. The evaluation study is itself as much to blame for bias in its conclusions as some of the studies that were evaluated. Tumor profiling is still in its early stages and can certainly be improved, but such uncompromising evaluations are too negative and run the risk of having its conclusions generalized to all profiling studies, including those with clinical potential.

One example of a profile with clinical potential is a recently identified expression signature for primary head and neck tumors which can discriminate between patients with and without lymph node metastasis (3). Because of difficulties in detecting these metastases reliably using present diagnostics, many patients currently receive inappropriate treatment. Besides detecting a fundamental property of primary tumors, comparison with current diagnosis indicates that the profile will significantly improve treatment, especially in the case of determining which patients do not need to be treated for lymph node metastasis. Although this claim now warrants further testing of the profile, for example by prospectively studying a large cohort of patients, we note that this study does pass the criteria applied in the Michiels paper.

Microarray profiling of head-neck squamous cell carcinomas has been described many times previously. The reasons why the lymph node metastasis project was successful are probably related to the experimental design, a sufficient number of samples, inclusion of a validation set and perhaps most importantly, the focus on only two closely related subsites within the head and neck region; the oral cavity and oropharynx. This reduction in sample scope was chosen because of evidence that different head and neck subsites can give rise to different types of tumors, for example with different clinical outcome (10). It is also important to note that this tumor type lends itself to finding a profile associated with lymph node metastasis because distant metastases that arise from the head-neck locations studied here, nearly always metastasize through the lymph node (11). Besides emphasizing the importance of considering tumor heterogeneity, the head-neck study reports another finding which may have implications for future studies. It was found that the predictive profile was much less accurate for tumors that had been stored for longer periods of time. If this is also confirmed in other projects, the implication is that future studies should perhaps be performed prospectively, with analysis in retrospect.

The head and neck lymph node metastasis profile supports a model in which the development of metastasis is not due to changes in a small subset of cells but a characteristic of the entire primary tumor, including both tumor cells and surrounding tissue (12). The metastatic profile was identified using bulk tumor sections, which included both cancer and stromal cells, and therefore unlikely originated from a small subset of metastatic cells within the primary tumor. Instead, most cells in the primary tumor show the "metastatic" phenotype, indicating that the complete tumor microenvironment plays an important role in development of metastases. This hypothesis challenges the traditional model by which metastatic cells are rare and arise in later stages of tumor development (13). Besides identifying a signature correlating with nodal status, this study is also a screen, rich in genes involved in development of metastasis. The role of stromal cells is further indicated by examination of the functional categories of genes that compose the metastatic signature. These include genes for extracellular matrix components, cell adhesion, maintenance of tissue integrity, extracellular matrix degrading activities as well as immune regulatory genes. More downregulation than upregulation of signature genes are associated with metastatic primary tumors. Together this indicates that

loss of function in both tumor and stromal cells plays a dominant role in acquiring metastatic potential.

Tumor expression profiling is a relatively new discipline. Besides gaining insight into oncogenesis and the genes involved, expression signatures have great potential for improvement of diagnosis and (personalized) treatment. Both pro- and antagonistic reports need to be evaluated carefully. For a definitive conclusion only the outcome of large multi-center prospective studies, performed in parallel to existing diagnosis, will determine which faction is correct. It is therefore much too early to condemn tumor profiling studies in general.

References

1. Golub, T.R., et al., Molecular classification of cancer: class discovery and class prediction by gene expression monitoring. Science, 1999. 286(5439): p. 531-537.
2. van 't Veer, L.J., et al., Gene expression profiling predicts clinical outcome of breast cancer. Nature, 2002. 415(6871): p. 530-536.
3. Roepman, P., et al., An expression profile for diagnosis of lymph node metastases from primary head and neck squamous cell carcinomas. Nat Genet, 2005. 37(2): p. 182-186.
4. Michiels, S., S. Koscielny, and C. Hill, Prediction of cancer outcome with microarrays: a multiple random validation strategy. Lancet, 2005. 365(9458): p. 488-492.
5. Simon, R., et al., Pitfalls in the use of DNA microarray data for diagnostic and prognostic classification. J Natl Cancer Inst, 2003. 95(1): p. 14-18.
6. Ransohoff, D.F., Rules of evidence for cancer molecular-marker discovery and validation. Nat Rev Cancer, 2004. 4(4): p. 309-314.
7. Ein-Dor, L., et al., Outcome signature genes in breast cancer: is there a unique set? Bioinformatics, 2005. 21(2): p. 171-178.
8. Eisen, M.B., et al., Cluster analysis and display of genome-wide expression patterns. Proc Natl Acad Sci U S A, 1998. 95(25): p. 14863-14868.
9. Ambroise, C. and G.J. McLachlan, Selection bias in gene extraction on the basis of microarray gene-expression data. Proc Natl Acad Sci U S A, 2002. 99(10): p. 6562-6566.
10. Huang, Q., et al., Genetic differences detected by comparative genomic hybridization in head and neck squamous cell carcinomas from different tumor sites: construction of oncogenetic trees for tumor progression. Genes Chromosomes Cancer, 2002. 34(2): p. 224-233.
11. Pantel, K. and R.H. Brakenhoff, Dissecting the metastatic cascade. Nat Rev Cancer, 2004. 4(6): p. 448-456.
12. Bernards, R. and R.A. Weinberg, A progression puzzle. Nature, 2002. 418(6900): p. 823.
13. Fidler, I.J. and M.L. Kripke, Metastasis results from preexisting variant cells within a malignant tumor. Science, 1977. 197(4306): p. 893-895.

4

Multiple robust signatures for detecting lymph node metastasis in head and neck cancer

Cancer Research. 2006 Feb; 66 (4): 2361-2366

Multiple robust signatures for detecting lymph node metastasis in head and neck cancer

Paul Roepman[1], Patrick Kemmeren[1], Lodewyk F.A. Wessels[2,3], Piet J. Slootweg[4], Frank C.P. Holstege[1]

[1]Department of Physiological Chemistry, University Medical Center Utrecht, Universiteitsweg 100, 3584 CG Utrecht, the Netherlands. [2]Faculty of Electrical Engineering, Mathematics and Computer Science, Delft University of Technology, Mekelweg 4, 2628 CD Delft, the Netherlands. [3]Department of Pathology, The Netherlands Cancer Institute, Plesmanlaan 121, 1066 CX Amsterdam, the Netherlands. [4]Department of Pathology, Radboud University Medical Center, Nijmegen, the Netherlands

Cancer Research. 2006 Feb; 66 (4): 2361-2366

Genome-wide mRNA expression measurements can identify molecular signatures of cancer and are anticipated to improve patient management. Such expression profiles are currently being critically evaluated based on an apparent instability in gene composition and the limited overlap between signatures from different studies. We have recently identified a primary tumor signature for detection of lymph node metastasis in head and neck squamous cell carcinomas. Before starting a large multicenter prospective validation, we have thoroughly evaluated the composition of this signature. A multiple training approach was used for validating the original set of predictive genes. Based on different combinations of training samples, multiple signatures were assessed for predictive accuracy and gene composition. The initial set of predictive genes is a subset of a larger group of 825 genes with predictive power. Many of the predictive genes are interchangeable because of a similar expression pattern across the tumor samples. The head and neck metastasis signature has a more stable gene composition than previous predictors. Exclusion of the strongest predictive genes could be compensated by raising the number of genes included in the signature. Multiple accurate predictive signatures can be designed using various subsets of predictive genes. The absence of genes with strong predictive power can be compensated by including more genes with lower predictive power. Lack of overlap between predictive signatures from different studies with the same goal may be explained by the fact that there are more predictive genes than required to design an accurate predictor.

Introduction

Microarray analysis has the potential to change the diagnosis and treatment of cancer (1, 2). Genome-wide gene expression measurements have been used to identify expression signatures capable of estimating a patient's survival rate and treatment response (3, 4) and to predict the metastatic potential of primary tumors (5). Such expression profiles or signatures are expected to improve treatment strategies by providing a more personalized therapy, based for example on disease severity (6). As yet, the majority of signatures are still

in a developmental stage. Prospective validation of the first profiles has been launched at institutes in Europe and the United States (2). These clinical trials are done on a large number of patients, require a great investment, and can only be carried out for profiles showing strong potential.

Despite the possible benefits, genome-wide studies for improvement of cancer diagnostics are currently being critically evaluated (7-10). Several microarray studies have identified gene sets capable of predicting a similar prognostic outcome, such as survival rate of breast cancer patients (3, 5, 11, 12). Interestingly, the overlap between the predictive gene sets from these different studies is limited to only a few genes. A recent analysis of microarray signatures found that the gene composition of expression signatures depends on the samples that were used for building the signature (7). Although the instability in gene composition is not necessarily a negative property of signatures, it does not simplify the task of choosing which genes are the best candidates for designing a diagnostic predictor.

Recently, we have identified a signature for detection of lymph node metastasis in patients with head and neck cancer based on gene expression measurements in the primary tumor (13). The potential clinical relevance of this signature resides in the difficulties for currently diagnosing the absence of lymph node metastasis in patients with head and neck cancer. Many patients receive inappropriate treatment due to difficulties in detection of metastases in the cervical lymph nodes (14, 15). The identified expression signature has the potential to improve diagnosis and treatment of head and neck cancer, particularly by reducing the number of patients given unnecessary neck surgery. The molecular signature has been validated on an independent set of tumor samples to make sure that the signature was not overfitted on the training samples and also works on new samples (13), as has been previously advocated (16). Independent validation of this signature showed an accuracy of 100% for metastasis-free predictions with an overall accuracy of 86% for all samples. Importantly, no false-negative predictions were made. Current clinical diagnosis of these patients showed an overall accuracy of 68% and included five false-negative predictions. The results of the validation set show the clinical potential of the signature. A large multicenter prospective validation study is required to confirm this potential before the signature can be applied in patient management.

Figure 4.1 | Limited overlap between signatures due to interchangeable genes. (**A**) Overlap of 49 predictive genes between the signatures designed using samples from 1996 to 2000 (102 genes) and using samples from 1998 to 2001 (202 genes). (**B**) Genes showing similar expression patterns across samples as the initially identified predictor genes. Bottom, a set of collagen related genes with similar expression patterns. Original predictor genes are indicated with a black square. Black, upregulation of a gene; white, down-regulation of a gene.

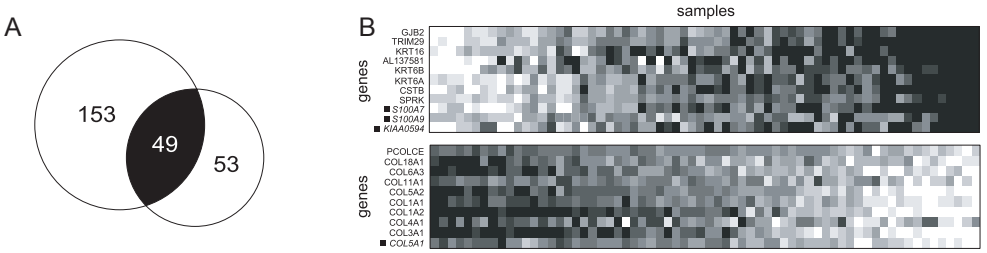

Before starting such a large validation study, we decided to thoroughly evaluate the optimal gene composition of the signature (7, 17), also because the signature showed higher accuracy on samples collected later, possibly due to prolonged sample storage time (13). We report here that the initial set of predictive genes for lymph node metastasis in patients with head and neck cancer is a subset of a larger group of 825 genes with significant predictive power. This is in agreement with earlier observations (7), and for the head and neck metastasis profile, we conclude that this is because there are many genes with a similar expression pattern across the sample collection. In contrast to other profiling studies, the predictive head and neck metastasis signature has a more stable gene composition, with a larger number of genes used in all tested predictors. Strikingly, exclusion of the most frequently occurring predictor genes could be compensated by increasing the number of genes included in the signature. Together, these analyses reveal the most comprehensive set of predictive genes that can be included in further development of a diagnostic tool for lymph node metastasis.

Results

The recently reported signature for detection of lymph node metastasis in patients with head and neck cancer showed a strong predictive performance with an independent validation set. The accuracy for the oldest samples in the training set was lower, perhaps due to prolonged storage of these samples (13). To investigate the influence of the older samples on the composition and performance of the signature, we left out the oldest samples and rebuilt the signature using 66 samples from 1998 to 2001 (44 from the initial training set and 22 from the validation set). This signature was designed in exactly the same way as the previous published signature (Methods). Importantly, the predictive outcome of the signature on the newer samples is similar to the original (85% accuracy), indicating that the previous presence of older samples did not interfere with the performance on the newer samples. Interestingly, the overlap in predictive genes found in both predictors is limited to 49 genes (Fig. 4.1 A). Cursory examination of the signature genes indicated that the incomplete overlap is due to the presence of a large number of genes with similar patterns of expression across the samples (e.g. Fig. 4.1 B). This indicates that many predictive genes can be interchanged without influencing the predictive outcome and suggests that multiple, different gene sets can be made that are useful for accurate prediction. Because the goal of this work is to detect the

Figure 4.2 | The predictive outcome of different signatures is stable. Predictive correlation outcome of 66 tumors samples using a multiple training approach. A thousand different molecular signatures of 50 (**A**), 100 (**B**), or 200 (**C**) genes were used to predict each sample approximately 100 times. light grey, samples from patients without metastasis; dark grey, samples from patients with lymph node metastasis. Shaded area, 95% confidence interval for the sample predictions.

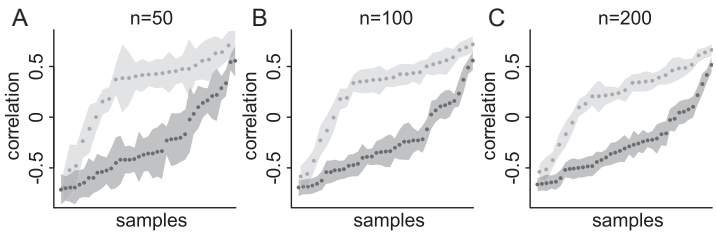

most useful set of predictive genes for head and neck metastasis prediction, we decided to investigate this further.

To study whether different gene sets show similar predictive outcome, we used a multiple training approach similar to the one Michiels et al. used for validating prognostic significance of previously published microarray signatures (7). Samples were randomly divided into training and test sets using a 10-fold cross-validation procedure. The 50, 100, or 200 most predictive genes were selected and used to classify the metastasis status of the test samples. Repeating this procedure generated 3,000 different predictive gene sets consisting of 50, 100, or 200 genes. Although the sets had a different gene composition, the power to discriminate between histologically determined metastasis (N+) and metastasis-free (N0) tumors remained similar. The predictive outcome on individual tumor samples was generally similar, with decreased variance for larger gene sets (100 and 200 genes; Fig. 4.2 A-C).

The similar predictive outcome of the multiple gene sets is not caused by a fixed set of genes present in all signatures. In the multiple signatures consisting of 50, 100, or 200 genes, 10, 27, or 49 genes were always selected respectively, and 41, 88, and 180 genes were selected in at least half of each of the thousand signatures (Fig. 4.3 A-B). These frequently selected genes account for only 5% of the total of 825 predictive genes selected at least once during the multiple sampling approach (Appendix Table 4.1). This degree of stability is higher than for the two most stable signatures previously analyzed by Michiels et al. (7). The hepatocellular carcinoma predictive signature of Iizuka et al. (18) showed 13 genes selected in at least half of the signatures with none of these genes selected always (Fig. 4.3 C). The breast cancer data set of van't Veer et al. (3) showed 24 genes selected in at least 50% of the signature with one gene selected always (Fig. 4.3 D).

Genes commonly used in the multiple training signatures show a strong overlap with the

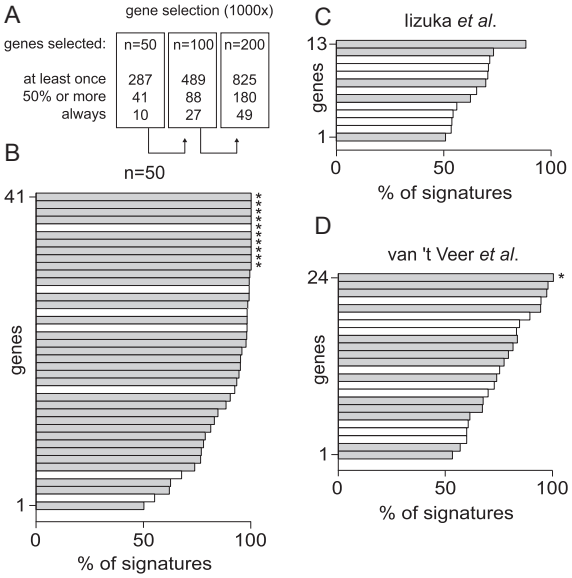

Figure 4.3 | Stability of signature composition. (**A**) Table containing the number of predictive genes selected using the multiple training approach. Numbers are shown for genes selected always, at least 50% and at least once in the predictive lists of 50, 100, and 200 genes, respectively. In total, 287 genes were used to design all various 50-gene signatures, 489 genes for the 100-gene signatures, and 825 genes for the 200-gene signatures. (**B-D**) Genes selected in at least 50% of the predictive lists of 50 genes in the head and neck data set (**B**), the signature of Iizuka *et al*. (**C**), and the predictive signature of van't Veer *et al* (**D**).Genes selected in all signatures are indicated by an asterisk. Gray columns, genes that are also present in the originally identified signatures.

Figure 4.4 | Genes selected most frequently are not essential for prediction.
(**A**) The pool of 825 predictive genes are ranked according to their selection percentage and divided in subsequent sets of 50 genes with a moving windows of 25 genes. Bottom, gray dotted line, selection percentage. The first two sets included genes that were used in all signatures; the last sets included genes selected only once. Predictive accuracy of the subsequent sets gradually decreases from 88% to 74%. Top, gray lines, accuracy of original predictor (86%) and of current clinical diagnosis (75%). (**B**) Same as (**A**) for subsequent sets that increase in size for lower-ranked genes. Gene set size increases stepwise from the 50 highest ranking genes to the 425 lowest ranking genes (bottom). Predictive accuracy remains stable around 86%.

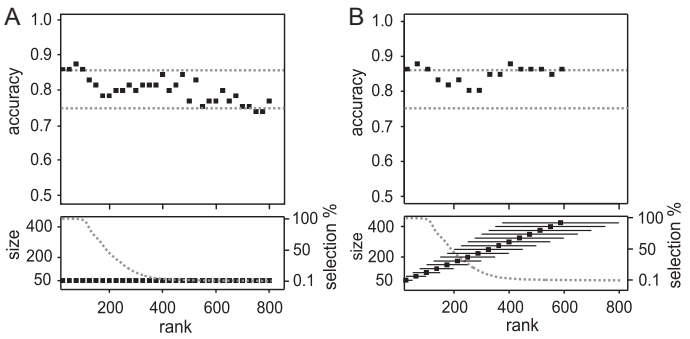

predictive genes identified using the initial two-step supervised classification approach on the same 66 samples. Eighty-three percent of the genes present in the majority of the multiple signatures were also identified using the two-step supervised classification method (Fig. 4.3 B, gray columns). In comparison, the overlap in gene selection between the multiple training approach and the originally published signature was 58% in the van't Veer study and 38% in the Iizuka data set (Fig. 4.3 C-D, gray columns), which represent the studies with the highest stability as analyzed by Michiels et al. (7).

Finding genes that are used in the majority of accurate signatures indicates that these genes are important to include in any signature for head and neck metastasis. To test whether these

Figure 4.5 | Random sets of the 825 predictive genes result in accurate predictions.
(**A**) Random sets of 50, 100, or 200 of the 825 predictive genes show a predictive accuracy between 80% and 90% with slightly higher accuracy for larger gene sets. (**B-D**) The stability in predictive outcome of each tumor samples increases with gene set size. Predictive outcomes of individual N0 tumor samples (grey) and N+ samples (black) based on different random gene sets. The stability between the different predictive outcomes based on different gene sets increases from R^2 = 0.72 for the 50-gene sets (**B**) to R^2 = 0.83 for the 100-gene sets (**C**) and R^2 = 0.92 for the 200-gene sets (**D**). Random genes that are not part of the 825 gene set do not show an accuracy different from random (**A**) and are unstable in their predictive outcome (R^2 = 0.29; **E**).

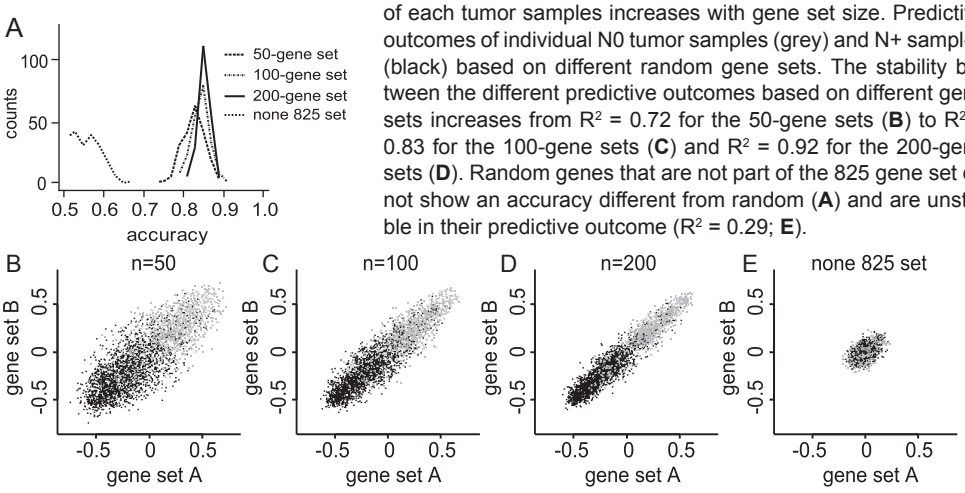

frequently selected genes were pivotal for accurate prediction, the 825 predictive genes that were selected at least once during the repeated sampling procedure were ordered according to the frequency of selection and divided into subsequent sets of 50 genes by applying a moving window with steps of 25 genes (i.e., 1-50, 25-76, 51-100, etc.; Fig. 4.4 A, bottom). These subsequent sets were used for classification of the tumor samples. The predictive accuracy decreases for sets containing less frequently selected genes but does not drop considerably below the current clinical accuracy of 75% (Fig. 4.4). Signatures without the frequently selected genes still show predictive power. This indicates that the frequently selected genes are not essential for prediction, but that they do contribute more towards improved accuracy. Strikingly, the observed decrease in predictive accuracy can be completely compensated by increasing the number of genes used in a signature (Fig. 4.4 B). For enlarged signatures of less frequently selected genes, the accuracy remains around 86%, similar to the accuracy of the original predictor. In other words, increasing the quantity of the predictive genes can compensate for reduced quality. Signatures built from large random sets of 100 to 200 predictive genes resulted in a stable predictive outcome with an accuracy of 80% to 90% (Fig. 4.5 A-E). In conclusion, this indicates that numerous combinations of predictive genes can be used for accurate prediction. In total, we have identified a large set of 825 predictive genes from which multiple accurate predictive signatures can be derived (Fig. 4.6).

Discussion

We report here that our initially identified set of predictive genes for detection of lymph node metastasis in patients with head and neck cancer (13) is a subset of a larger group of predictive genes. Using a resampling approach, we have identified a large set of 825 genes that can be used for prediction of metastasis. Based on this group of genes, multiple predictive signatures can be made with high predictive accuracy. The phenomenon that different sets of genes can be used for accurate prediction is not exclusive for this study but is becoming apparent in other cancer profiling studies (7, 17). Due to minor differences in gene expression, different genes are selected for optimal prediction when the signature is built using different samples, especially when comparing studies that have been done in different institutes (3, 12). This instability in gene composition of different predictive signatures is not detrimental as long as the predictive outcome and accuracy remain similar. Different gene sets can give comparable results because individual genes that show equal expression patterns can be interchanged without affecting the signature profile and the predictive outcome.

Although the predictive signature for lymph node metastasis shows instability in gene composition, it is more stable than other molecular profiles analyzed similarly by Michiels et al. (7). A possible explanation for this higher stability is the reduction of biological variation by analyzing tumors from only two locations within the head and neck region: oropharynx and oral cavity. Another possible explanation of the increased stability is related to the complexity of the different disease characteristics considered in the different studies. The head and neck signature predicts the presence of metastasis in lymph nodes that are close to the site of the primary tumor. Predicting a more complex or long-term patient trait, such as survival rate and

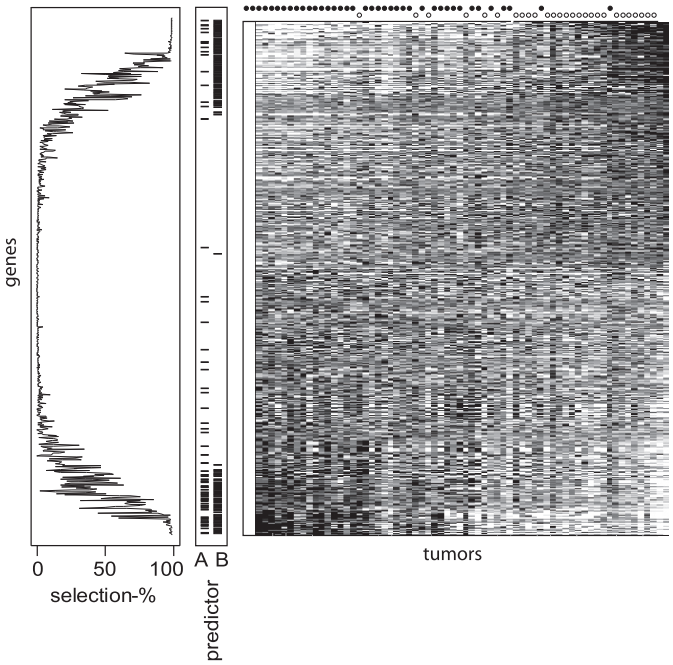

Figure 4.6 | Eight hundred twenty-five predictive genes for lymph node metastasis. Right, expression pattern of the 825 predictive genes across 66 tumor samples. Tumor samples are ordered according to their prediction based on all 825 genes. Dashed line, threshold with optimal predictive accuracy, correctly predicting 58 of 66 samples. Solid circle, tumors from patients with lymph node metastasis; open circle, those of patients without metastasis. Genes are ordered according to their correlation with predictive outcome. Black, up-regulation of a gene; white, down-regulation of a gene. Middle, genes identified using the original supervised classification approach on samples from 1996 to 2001 (A) or from 1998 to 2001 (B). Left, selection percentages for the predictive genes.

development of distant metastasis (3, 12), likely depends on more factors and developmental pathways (19). Therefore, prediction of more complex characteristics over time is probably susceptible to more variation, perhaps resulting in a less stable predictive signature.

Predictive signatures lacking the most frequently selected genes remains reasonably accurate, a phenomenon that was also found by Ein-dor et al. (17) when reanalyzing the breast cancer profile by van't Veer. In addition, here, we show that the reduction in predictive power can be fully compensated by increasing the number of genes used in the signatures. This implies that for expression signatures both the quality and the quantity of the genes are important for predictive accuracy. Selection of the most frequently selected genes is nevertheless helpful for reducing the number of genes in a signature.

Due to the interchangeability of predictive genes, there is no single set of genes with optimal predictive accuracy. Various signatures can be identified by different institutes or simply by using different samples, and the identified gene sets with optimal predictive accuracy will differ due to minor differences in the analyzed samples. This does not mean that the different signatures are based on random noise in the data sets, as Michiels et al. concluded (7). Although the genes identified as most predictive can differ between different studies, the overall predictive profiles can be similar, resulting in an identical predictive outcome.

Now that we know that none of the head and neck lymph node metastasis predictive genes is essential for accurate prediction, is it wise to try to make a predictive list as small as possible? A molecular signature that is based on more genes is likely to be less prone to biases towards specific samples. When certain genes within a larger signature show lower

predictive power for new samples, other predictive genes in the signature may compensate this effect. Ma et al. recently identified a set of only two genes that could accurately predict tamoxifen treatment outcome in breast cancer patients (4). When Reid et al. tried to validate this two-gene signature on independent samples, they we unable to show predictive power of these two genes (8). This example clearly illustrates the risk of reducing a signature to a small number of genes without a thorough validation on independent samples.

The set of lymph node metastasis predictive genes reported here also sheds light on the development of metastasis. Two interesting overrepresented functional categories within the set of predictive genes are binding to the extracellular matrix and protease activity for degradation of the extracellular matrix (Fig. 4.7). Both categories are up-regulated in tumors that metastasize to the lymph nodes. These two categories seem contradictory; however, they support the theory that tumor cells gain mobility by an interplay between anchoring to the extracellular matrix and degradation of this matrix (20). In this way, groups of tumor cells can move through the surrounding tissue by degrading the extracellular matrix while retaining cell to cell and cell to extracellular matrix contact. The invasion in the surrounding tissue is not solely caused by the tumor cells and the extracellular matrix but also includes nontumor cells in the tumor microenvironment, such as stromal fibroblasts, lymphocytes, and macrophages (reviewed in refs. (21, 22). Designing new diagnostics to identify tumors with metastatic potential should therefore not exclusively focus on processes in the tumor cells but also include the tumor microenvironment (23). Targeting both the tumor and nontumor cells may therefore offer a more efficient way to diagnose and treat cancer.

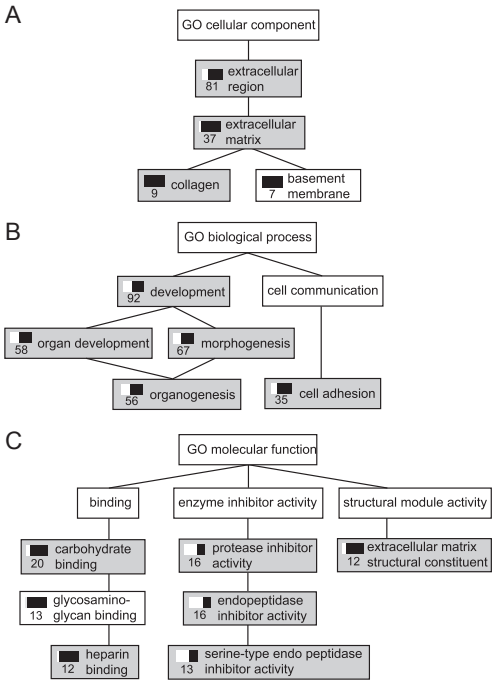

Figure 4.7 | Functional category analysis of the predictive genes.
To identify functional categories within the set of predictive genes we applied a gene ontology (GO) analysis on the predictive genes using the online Expression Profiler software (28, 29). The used GO version was downloaded from http://www.geneontology.org on 10 June 2005. Overrepresented functional classes were determined for the three GO categories: cellular component (**A**), biological process (**B**) and molecular function (**C**). Of the 825 predictive genes, 483 were annotated in the GO database, versus 1634 of the 3064 significantly regulated genes across the tumor samples. P-values for overrepresented GO categories in the group of predictive genes are corrected for multiple testing using a stringent simulation correction (30). Significantly ($P<0.05$) overrepresented categories are colored in grey. The colored bars denote the proportion of upregulation (black) and down-regulation (white).

Methods

Tumor samples and data accessibility | Head and neck squamous cell carcinoma (HNSCC) samples were processed and analyzed as described elsewhere (13). MIAME (24) compliant microarray data in microarray gene expression markup language (MAGE-ML; ref. (25) have been deposited in ArrayExpress (http://www.ebi.ac.uk/arrayexpress/) with the following accession numbers: microarray layout, A-UMCU-3; tumor data, E-UMCU-11. The analysis in the study was done using 66 primary head and neck tumors that were surgically removed from the patients between 1998 and 2001. The tumor samples fulfilled the following criteria: biopsy-proven HNSCC in the oropharynx or oral cavity with no previous malignancy in the head and neck region and tumor sections containing at least 50% tumor cells. Clinical staging of the cervical lymph nodes was done according to the Netherlands national consensus guidelines for oral cavity and oropharynx, by palpation of the neck region, followed by bilateral sound examination, computed tomography, and/or magnetic resonance imaging. Suspected nodes were subjected to aspiration cytology. Based on the clinical staging of the neck, 38 patients were classified as N0 (metastasis-free) and 28 as N+ (presence of metastasis in lymph nodes). Patients assessed to be N0 underwent selective dissection (levels I-III, supra-omohyoidal neck dissection), and patients assessed to be N+ underwent comprehensive dissection (levels I-V, radical neck dissection; ref. (14). In agreement with previous studies (26, 27), there was a high prevalence of smoking within the patient cohort. The samples from the three nonsmokers did not behave discordantly with regard to clinical assessment, microarray prediction, or histologic determination of N status, although we note that this group size is too small to result in statistically meaningful analyses.

Supervised classification | To remove the possible negative influence of the older tumor samples that were surgically removed in 1996 and 1997, we built a new molecular signature for prediction of lymph node metastasis. The supervised classification procedure was identical to the one used previously (13). We left out the 38 tumor samples from 1996 and 1997 and combined the initial training and test sets into a new training set containing 66 tumor samples from 1998 to 2001. After preprocessing the expression data of the 21,329 genes on the microarray, 3,064 were found to be differentially expressed ($P < 0.01$) in at least 15 of the 66 tumor samples. These 3,064 genes were used for designing the predictor with the highest overall accuracy as described previously (13). Briefly, the set of samples were iteratively divided into training (two thirds) and test (one third) sets. On the training set, using a 10-fold cross-validation procedure, the optimal set of genes to employ in the classifier was determined based on the signal-to-noise ratio and classification performance. Performance of this optimal set of genes was validated on the one-third test set. This 3-fold cross-validation loop was repeated 100 times to select the final list of predictive genes used within the molecular signature.

Multiple training approach | A multiple training approach similar to the one used by Michiels et al. was used to study the stability of the identified signature based on the 66 tumor samples from 1998 to 2001. The tumor samples were randomly divided into a training set and test set using a 10-fold cross-validation procedure. Based on the training set, Ps were calculated for all 3,064 differentially expressed genes based on the difference in expression between N+ and N0 tumor samples (Student's t test). The set of genes with the lowest Ps (i.e., most predictive) was used for prediction of the test samples by calculating the correlation with the average N+ and average N0 training profile and, based on these correlations, classifying the test samples as N0 or N+. Repeating this resampling procedure a thousand times resulted in multiple predictions for each tumor sample, based on the different predictive gene sets.

Signature composition analysis | The multiple training approach was done for sets of 50, 100, and 200 genes, which were used for building predictive signatures. Investigation of the stability in signature gene composition was done by scoring each gene for the number of times it was included in a predictive signature. The selection ranged from 0% (used in none of the signatures) to 100% (used in all thousand generated signatures). The complete set of predictive genes was defined as those genes that were selected at least once during the repeated sampling of the multiple training approach, whereby either 50, 100, or 200 genes were selected. The predictive set of 825 genes are found upon repeated sampling of signatures constructed of 200 genes.

References

1. Garber, K., Genomic medicine. Gene expression tests foretell breast cancer's future. Science, 2004. 303(5665): p. 1754-1755.
2. Kallioniemi, O., Medicine: profile of a tumour. Nature, 2004. 428(6981): p. 379-382.
3. van 't Veer, L.J., et al., Gene expression profiling predicts clinical outcome of breast cancer. Nature, 2002. 415(6871): p. 530-536.
4. Ma, X.J., et al., A two-gene expression ratio predicts clinical outcome in breast cancer patients treated with tamoxifen. Cancer Cell, 2004. 5(6): p. 607-616.
5. Ramaswamy, S., et al., A molecular signature of metastasis in primary solid tumors. Nat Genet, 2003. 33(1): p. 49-54.
6. Caldas, C. and S.A. Aparicio, The molecular outlook. Nature, 2002. 415(6871): p. 484-485.
7. Michiels, S., S. Koscielny, and C. Hill, Prediction of cancer outcome with microarrays: a multiple random validation strategy. Lancet, 2005. 365(9458): p. 488-492.
8. Reid, J.F., et al., Limits of predictive models using microarray data for breast cancer clinical treatment outcome. J Natl Cancer Inst, 2005. 97(12): p. 927-930.
9. Ransohoff, D.F., Rules of evidence for cancer molecular-marker discovery and validation. Nat Rev Cancer, 2004. 4(4): p. 309-314.
10. Miklos, G.L. and R. Maleszka, Microarray reality checks in the context of a complex disease. Nat Biotechnol, 2004. 22(5): p. 615-621.
11. Sorlie, T., et al., Gene expression patterns of breast carcinomas distinguish tumor subclasses with clinical implications. Proc Natl Acad Sci U S A, 2001. 98(19): p. 10869-10874.
12. Wang, Y., et al., Gene-expression profiles to predict distant metastasis of lymph-node-negative primary breast cancer. Lancet, 2005. 365(9460): p. 671-679.
13. Roepman, P., et al., An expression profile for diagnosis of lymph node metastases from primary head and neck squamous cell carcinomas. Nat Genet, 2005. 37(2): p. 182-186.
14. Robbins, K.T., et al., Neck dissection classification update: revisions proposed by the American Head and Neck Society and the American Academy of Otolaryngology-Head and Neck Surgery. Arch Otolaryngol Head Neck Surg, 2002. 128(7): p. 751-758.
15. Woolgar, J.A., Pathology of the N0 neck. Br J Oral Maxillofac Surg, 1999. 37(3): p. 205-209.
16. Simon, R., et al., Pitfalls in the use of DNA microarray data for diagnostic and prognostic classification. J Natl Cancer Inst, 2003. 95(1): p. 14-18.
17. Ein-Dor, L., et al., Outcome signature genes in breast cancer: is there a unique set? Bioinformatics, 2005. 21(2): p. 171-178.
18. Iizuka, N., et al., Oligonucleotide microarray for prediction of early intrahepatic recurrence of hepatocellular carcinoma after curative resection. Lancet, 2003. 361(9361): p. 923-929.
19. Pantel, K. and R.H. Brakenhoff, Dissecting the metastatic cascade. Nat Rev Cancer, 2004. 4(6): p. 448-456.
20. Sahai, E., Mechanisms of cancer cell invasion. Curr Opin Genet Dev, 2005. 15(1): p. 87-96.
21. Bissell, M.J. and D. Radisky, Putting tumours in context. Nat Rev Cancer, 2001. 1(1): p. 46-54.
22. Mueller, M.M. and N.E. Fusenig, Friends or foes - bipolar effects of the tumour stroma in cancer. Nat Rev Cancer, 2004. 4(11): p. 839-849.
23. Joyce, J.A., Therapeutic targeting of the tumor microenvironment. Cancer Cell, 2005. 7(6): p. 513-520.
24. Brazma, A., et al., Minimum information about a microarray experiment (MIAME)-toward standards for microarray data. Nat Genet, 2001. 29(4): p. 365-371.
25. Spellman, P.T., et al., Design and implementation of microarray gene expression markup language (MAGE-ML). Genome Biol, 2002. 3(9): p. RESEARCH0046.
26. Kabat, G.C., C.J. Chang, and E.L. Wynder, The role of tobacco, alcohol use, and body mass index in oral and pharyngeal cancer. Int J Epidemiol, 1994. 23(6): p. 1137-1144.
27. Schlecht, N.F., et al., Effect of smoking cessation and tobacco type on the risk of cancers of the upper aero-digestive tract in Brazil. Epidemiology, 1999. 10(4): p. 412-418.
28. Ashburner, M., et al., Gene ontology: tool for the unification of biology. The Gene Ontology Consortium. Nat Genet, 2000. 25(1): p. 25-29.
29. Kapushesky, M., et al., Expression Profiler: next generation--an online platform for analysis of microarray data. Nucleic Acids Res, 2004. 32(Web Server issue): p. W465-470.
30. Boyle, E.I., et al., GO::TermFinder--open source software for accessing Gene Ontology information and finding significantly enriched Gene Ontology terms associated with a list of genes. Bioinformatics, 2004. 20(18): p. 3710-3715.

5

Maintenance of head and neck tumor gene expression profiles upon lymph node metastasis

Cancer Research, *in press*

Maintenance of head and neck tumor gene expression profiles upon lymph node metastasis

Paul Roepman[1], Alike de Jager[1], Marian J.A. Groot Koerkamp[1], J. Alain Kummer[2], Piet J. Slootweg[3] , Frank C.P. Holstege[1]

[1]Department of Physiological Chemistry, [2]Department of Pathology, University Medical Center Utrecht, Universiteitsweg 100, 3584 CG Utrecht, the Netherlands. [3]Department of Pathology, Radboud University Medical Center, Nijmegen, the Netherlands.

Cancer Research, *in press*

Spread of cancer and development of solid metastases at distant sites is the main cause of cancer-related deaths. To understand and treat metastases it is important to determine at which stages the most pivotal steps for development of metastases occur. In head and neck squamous cell carcinoma (HNSCC), metastasis nearly always occurs in local lymph nodes first, before distant metastasis develops. Here we have investigated gene expression patterns in HNSCC lymph node metastases using DNA microarrays. Several types of analyses demonstrate that the gene expression patterns in lymph node metastases are most similar to the corresponding primary tumors from which they arose, as long as samples contain sufficient proportions of tumor cells. Strikingly, gene expression patterns of metastatic primary HNSCC are largely maintained upon spread to the lymph node. Only a single gene, Metastasis-associated gene 1 (*MTA1*), was found to show consistently changed expression between a large number of matched primary tumor-lymph node metastasis pairs. The maintained expression pattern includes the predictive signature for HNSCC lymph node metastasis. These results underscore the importance of the primary tumor gene expression profile for development and treatment of metastasis. The findings also agree with the concept that disseminated cancer cells alter the surrounding tissue into a metastatic environment that resembles the primary tumor microenvironment.

Introduction

Metastasis is the process whereby primary tumor cells spread to distant sites in the body. After spread and development into solid tumors, metastases are the leading cause of cancer-related deaths. In the conventional metastasis model, metastatic potential is acquired late during tumorigenesis as a result of sequential selective steps, with only small subpopulations of tumor cells gaining metastatic capacity and disseminating to other organs (1). Lately, this long-established model has been challenged by the results of gene expression profiling studies aimed at determining metastatic phenotypes (2-4). Use of complete tumor sections in such studies indicates that within primary tumors that have metastasized, most tumor cells

exhibit a metastatic profile. This implies that metastatic potential has been acquired early and sustained throughout multistep tumor development (5).

In line with this new model, metastases too may be similar to the primary tumor from which they originate. An important characteristic of such similarity is exhibition of a similar gene expression pattern. Maintenance of gene expression patterns during development of distant metastasis has indeed recently been shown for haematogenous spread of breast cancer (6). Metastases originating from breast tumors in lymph node negative patients show expression signatures that are highly similar to the corresponding primary tumors (7) and the 70-gene prognostic signature (4) is also preserved throughout the entire metastatic cascade (6). Such findings have important implications for our understanding of how metastasis develops and for cancer treatment. It is therefore imperative to determine whether maintenance of primary gene expression patterns during metastasis is a general property or whether this is restricted to certain types of cancer.

Recently, primary tumor gene expression signature have been discovered that are predictive for the presence of lymph node metastasis for for head and neck squamous cell carcinoma (HNSCC) (3, 8, 9). In contrast to breast cancer, head and neck cancer spreads almost exclusively via a lymphatic route in which the cervical lymph nodes are the first location (10). One explanation for this is that in the lymphatic metastatic cascade exhibited by HNSCC, additional alterations take place in the lymph nodes that enable cancer cells to spread further to distant sites via the blood (11).

Here we have investigated whether HNSCC primary tumor gene expression patterns are preserved during their distinctive lymphatic spread. Strikingly, we find that gene expression profiles of primary metastatic tumors are maintained in their corresponding lymph node metastases. Besides playing a role during initiation of metastasis, the gene expression pattern present in the primary tumor therefore likely also plays an important role in survival and proliferation of metastatic tumor cells in lymph nodes. The results also shed light on development of distant metastases through the lymphatic route.

Results

Treatment of head and neck cancer patients with lymph node metastatic disease involves removal of the primary tumor and of cervical lymph node tissue that contains the metastatic lesions. To investigate the relationship between primary tumors and lymph node metastases, we first selected 14 pairs of primary head and neck squamous cell carcinomas (HNSCC) and their matching cervical lymph node metastases (Table 5.1). The primary tumors originated in the oral cavity or oropharynx and consisted of at least 50 percent tumor cells. The 14 corresponding lymph node metastases samples had a tumor percentage of at least 25 percent.

Gene expression profiles were generated using DNA microarrays that contained 70-mer oligonucleotides representing over 21,000 genes (3). After normalization and statistical analyses, 2135 genes were identified as differentially expressed in at least half of the samples. Unsupervised hierarchical clustering based on similarity measurements across the

patient	gender	age	primary tumor				lymph node metastasis			
			location	size (cm)	tumor %		tumor %			
					>75	50-75	>75	50-75	25-50	<10
1	M	55	oral cavity	3,0	+			+		
2	F	62	oral cavity	4,2	+		+			
3	M	67	oropharynx	7,3		+	+			
4	M	52	oral cavity	2,3	+			+		
5 *	F	38	oral cavity	4,0		+			+	
7	M	51	oral cavity	3,0	+			+		
9 *	M	61	oropharynx	3,5	+				+	
10 *	M	42	oropharynx	5,5		+			+	
11 *	F	55	oral cavity	6,0	+				+	
13	M	82	oral cavity	2,5	+		+			
14	F	52	oropharynx	7,0	+		+			
17	M	61	oral cavity	2,9	+			+		
18 *	M	50	oral cavity	3,0	+				+	
19 *	M	66	oral cavity	5,0	+				+	
6 **	M	50	oral cavity	4,0		+				+
8 **	M	58	oropharynx	3,0		+				+
12 **	F	38	oropharynx	4,0	+					+
15 **	F	63	oropharynx	5,0		+				+
16 **	M	46	oral cavity	5,2	+					+

Table 5.1 | Patient and sample characteristics. Primary tumors and lymph node metastasis samples are grouped according to their tumor percentage. Patients of whom the analyzed metastasis sample contained less than 50 percent tumor cells are marked *. The bottom part comprises five sample pairs for which the lymph node metastases samples contain less than 10 percent tumor cells, are marked ** and are referred to as 'low tumor percentage pairs'. *Age*, age at diagnosis; *size*, diameter of tumor in cm.

2135 differentially expressed genes grouped together 8 of the 14 primary tumor-lymph node metastasis pairs (Fig. 5.1 A). For these 8 clustered pairs, the metastasis sample was most similar to its matching primary tumor. For 5 of the 6 pairs that did not cluster together as a pair, the lymph node metastasis sample contained less than 50 percent tumor cells (Fig. 5.1 A, Table 5.1), indicating that a lower tumor percentage within the lymph node samples was responsible for reduced pairing of samples. In agreement with this, lymph node samples that did not cluster pair-wise with their corresponding primary tumor, did themselves cluster together (Fig. 5.1 A, right hand side).

The idea that lower lymph node tumor percentage is responsible for reduced pairing of samples was further investigated by including 5 pairs for which the metastasis sample contained less than 10 percent tumor cells (Table 5.1), hereafter called 'low tumor percentage

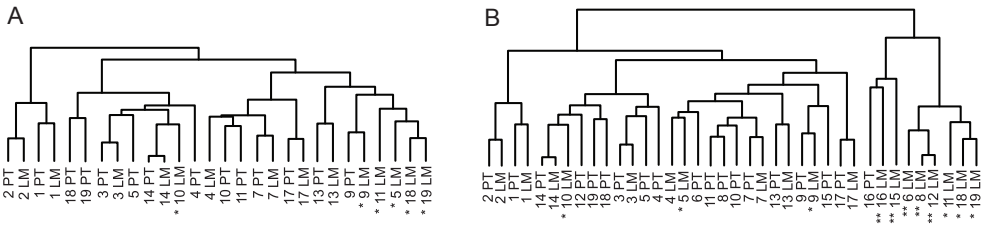

Figure 5.1 | Clustering of lymph node metastases (LM) and primary HNSCC tumors from which they originated (PT). (**A**) Hierarchical clustering of 14 sample pairs of which the metastasis samples contained at least 25 percent tumor cells. (**B**) As **A** including five pairs of which the LM sample contained no or very little tumor cells. Numbers and markings according to the patient information given in Table 5.1.

Figure 5.2 | Within-pair-between-pair-scatter-ratios (WPBPSR) of matched individual pairs of primary tumors and lymph node metastases (**A**) grouped according to the tumor cell percentage of the lymph node metastasis samples (**B**). Pair labels as in Fig. 5.1. Pairs with a metastasis sample containing >50, 25-50 or <10 percent tumor cells are colored dark grey, light grey and white, respectively. Error bars in (**B**) indicate standard error of WPBPSR. *LM*, lymph node metastasis sample (**C**) Permutation test of the overall WPBPSR outcome. The histogram displays the WPBPSR distribution for 10,000 random pairing of the studied samples (1.000 ± 0.058). Solid line, WPBPSR of the 14 samples with at least 25 percent tumor cells in the metastasis sample (0.74; $P < 0.0001$). Dashed line, WPBPSR of all 19 pairs including the five low tumor percentage pairs (0.83; $P = 0.0004$).

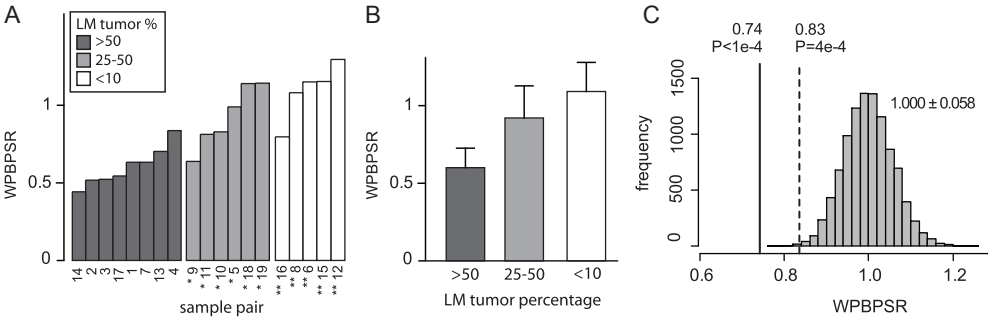

pairs'. The five additional lymph node metastasis samples clustered within the separate lymph node sample group and showed no direct clustering with their corresponding primary tumor samples (Fig. 5.1 B). In summary, eight of the nine sample pairs that contained more than 50% tumor cells co-clustered as a pair. This analysis shows that gene expression profiles of lymph node metastases are most similar to the primary tumor from which they originate, provided that both samples contain enough tumor cells.

The significance of similarities between matched lymph node metastases and primary tumors was further analyzed by calculating a within-pair-between-pair-scatter-ratio (WPBPSR, (7)). A low WPBPSR (<1.0) represents a high similarity between matched samples. Thirteen of the 15 pairs with a metastasis sample that contained at least 25 percent tumor cells had a WPBPSR below one, indicating that these paired samples were more similar to each other than to the other samples (Fig. 5.2 A). The higher WPBPSR for pairs with lower tumor percentage in the metastasis sample demonstrates the importance of tumor cell percentage for the similarity in expression profiles (Fig. 5.2 B). The average WPBPSR for matched metastases and primary tumors was 0.74 (P<0.0001) when excluding, or 0.83 (P=0.004) when including the low tumor percentage pairs (Fig. 5.2 C), demonstrating that the observed WPBPSRs were not the result of random chance. Instead, the lymph node metastases expression patterns are more similar to the primary tumor from which they originated.

Although the overall gene expression patterns of lymph node metastases are similar to that of their corresponding primary tumors, this does not exclude the possibility of a small subset of genes with systematically changed expression upon spread to the lymph nodes. We therefore further investigated the similarity in gene expression upon lymph node metastasis by searching for genes that exhibited consistent changes in expression between a large number

of primary tumors and their corresponding lymph node metastases. At a false discovery rate of 5 percent, only one differentially expressed gene could be identified. Metastasis-associated gene 1 *(MTA1)* shows reduced expression in all 13 metastasis samples compared to the matched primary tumors with a statistically significant downregulation ($P < 0.05$) in six samples. *MTA1* is a component of the Mi-2/nucleosome remodeling and deacetylase (NuRD) complex and has previously been demonstrated to be a regulator of metastatic potential by controlling the epithelial-to-mesenchymal transition (12). Increased expression of *MTA1* is associated with progression to the metastatic state in various primary tumor types (13, 14). Here we find reduced expression of this gene in the lymph node metastases compared to the primary tumors, suggesting that *MTA1* is only needed at the site of primary tumor. That only one gene is found to be differentially expressed by this as well as other statistical analyses suggests that across the samples analyzed here, no specific pathway is consistently affected during subsequent development of lymph node metastasis after detachment and spread of cancer cells from the primary HNSCC tumor.

Preservation of general gene expression patterns upon spread of HNSCC primary tumors suggests that the previously identified metastatic signature (3) is also maintained upon metastasis to the lymph node. Analysis of expression of the 102 signature genes reveals that the metastatic signature profile within lymph node metastases is highly similar to the profile of the corresponding primary tumors (Fig. 5.3 A). Consequently, the metastatic signature outcome based on the 102-gene profile was almost identical for the matched primary tumor and lymph node metastasis samples ($P<0.01$) and opposite to the outcome for non-metastatic (N0) primary tumors (Fig. 5.3 B). Metastatic signature outcome based on the gene profile of an extended set of 825 signature genes (15) also showed a similar outcome for the lymph node metastases compared to the primary tumors ($P<0.01$, Fig. 5.3 C). In one case the metastasis

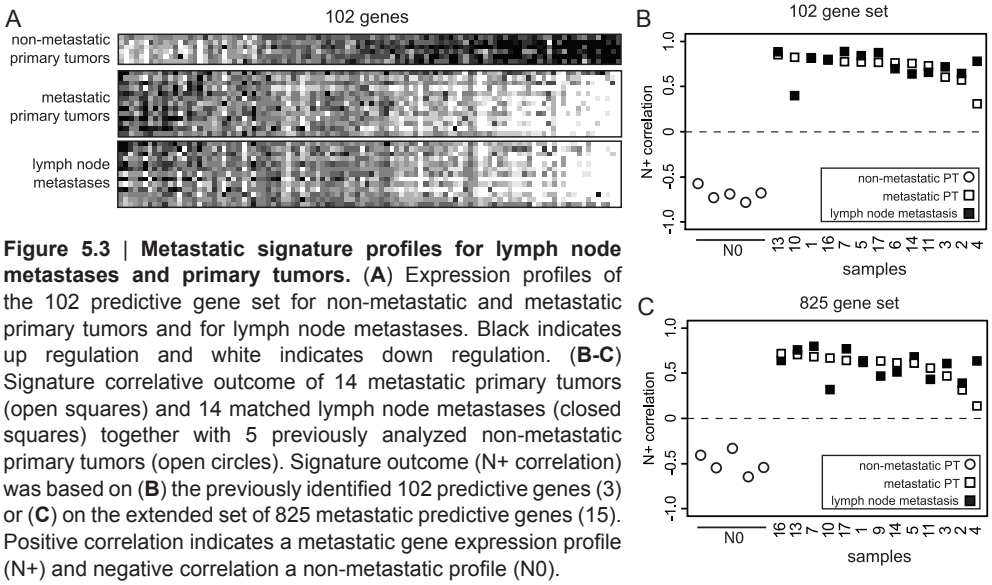

Figure 5.3 | Metastatic signature profiles for lymph node metastases and primary tumors. (**A**) Expression profiles of the 102 predictive gene set for non-metastatic and metastatic primary tumors and for lymph node metastases. Black indicates up regulation and white indicates down regulation. (**B-C**) Signature correlative outcome of 14 metastatic primary tumors (open squares) and 14 matched lymph node metastases (closed squares) together with 5 previously analyzed non-metastatic primary tumors (open circles). Signature outcome (N+ correlation) was based on (**B**) the previously identified 102 predictive genes (3) or (**C**) on the extended set of 825 metastatic predictive genes (15). Positive correlation indicates a metastatic gene expression profile (N+) and negative correlation a non-metastatic profile (N0).

sample showed a stronger metastatic profile than its primary tumor (Fig. 5.3 B-C, nr. 4) and in one case a reduction in metastatic profile for the lymph node sample was observed, which could be explained by the reduced tumor percentage in this sample (nr. 10). As is discussed below, strong preservation of the primary tumor metastatic gene profile during metastases development (Fig. 5.3 C) underlines the importance of the identified signature genes, not only for their association with metastatic potential at the site of the primary tumor but also for further development and treatment of lymph node metastases.

Discussion

Genome-wide expression profiling has made it possible to identify molecular signatures in primary tumors that are predictive for disease outcome and prognosis (2-4). Recently, we have identified a metastatic signature for primary oral cavity and oropharynx squamous cell carcinomas that is capable of identifying which tumors have metastasized to the cervical lymph nodes (3). Here we demonstrate that lymph node metastases reflect both the general and the metastatic gene expression patterns of primary oral cavity and oropharynx tumors from which they originate. Apparently, the different environment does not effect the overall gene expression to such a degree that the metastases are markedly different from the primary tumor. As the expression profile contains both tumorous as well as stromal genes, this finding indicates that the disseminated cancer cells alter their adjacent stroma into a ‘metastatic’ microenvironment that is similar to the primary tumor microenvironment in which they can survive and proliferate (16, 17).

For breast cancer it has previously been shown that primary tumor gene expression patterns are maintained upon metastasis (7). For development of HNSCC lymph node metastasis, we show here that the primary tumor gene expression patterns are also maintained. These findings indicate that disseminated primary tumor cells do not need to undergo additional developmental changes to survive and proliferate in metastatic sites and supports the theory that metastatic properties are acquired early during tumorigenesis and sustained through cancer progression (5). Also, the observed stability in gene expression patterns are in line with the proposal that metastasic gene expression signatures are based on genetic background and influenced too a lesser degree by specific tumorigenic processes (18).

Primary breast tumor cells are directly suitable for distant spread via the haematogenous route without involvement of regional lymph nodes (11). Head and neck cancer, however, nearly always spreads to distant sites via the lymph nodes as an intermediate stage before further haematogenous spread (10). It has therefore previously been postulated that distant dissemination of head and neck cancer depends on the presence of lymph node metastasis, presumably due to additional developmental changes in the solid lymph node metastases that are required for haematogenous distant spread (10, 11). It is therefore striking that the lymph node metastases samples analyzed here show no obvious alterations in gene expression compared to their primary tumors. Apparently, the local lymph nodes provide a fertile environment for development of metastasis. Our results indicate that once the primary tumor has gained the metastatic phenotype, few further alterations in gene expression within the

metastatic tumor cells are required for tumor establishment in the lymph nodes.

Although this study indicates that no additional developmental changes take place upon spread of primary HNSCC tumors to the regional lymph nodes, we cannot completely rule out the possibility that extra alterations are needed for subsequent spread of cancer cells from the established lymph node metastases to distant sites via the blood. Alterations in a small subpopulation of tumor cells within the solid lymph node metastasis could lead to subsequent haematogenous spread and survival at distant sites (1). Alternatively, these changes might not occur in the solid lymph node metastases but afterwards when individual cancer cell circulate through the lymph fluid before entering the blood vessels (19). To be certain whether additional alterations are needed for subsequent distant spread of HNSCC, distant metastases need to be analyzed and compared to corresponding primary tumor and lymph node metastases. However, for the head and neck cancer patients studied here, no distant metastases were available for gene expression analysis.

The maintenance of general primary tumor gene expression patterns upon dissemination of breast cancer (7) and of HNSCC, as shown in this study, indicates that metastatic primary tumors cells already harbor properties for survival and proliferation in foreign sites. Finding two such cases of primary tumor expression-profile maintenance makes it more likely that it is a general property of cancer progression. The previously identified HNSCC metastatic gene expression profile is present in the primary tumor during initiation of metastasis and within developing lymph node metastases, indicating a role during initiation of metastasis and for survival and proliferation in the lymph nodes. Because this signature is present only in metastasizing primary head and neck tumors (3) and is retained in the lymph node metastases (this study), therapeutic targeting of its components forms a rational approach towards preventing or impeding lymph node metastasis, especially when targeting the stable metastatic microenvironment which enables cancer cells to survive and proliferate at remote sites (16, 20).

Materials and Methods

Detailed patient information and primary tumor selection criteria have been described previously (3). Samples taken from surgically removed cervical lymph node tissue were scored for the presence of metastases and, if positive, included for analysis of gene expression. Tissue scoring and sectioning, RNA isolation, mRNA amplification, cRNA labeling, hybridization, scanning and preprocessing of expression data were performed as previously described (3). Microarray layout, expression data and protocols have been deposited in the public microarray database ArrayExpress with accession numbers A-UMCU-3 and E-TABM-114, respectively.

Nineteen pairs of matched oral cavity/oropharynx primary tumor and lymph node metastases were expression profiled in dye-swap duplicate against a previously used reference pool of primary HNSCC samples (3). Following scanning, quantification and data preprocessing, 2135 genes were identified as differentially expressed in at least half of the analyzed samples ($P<0.01$). The samples were hierarchically clustered based on their euclidian distance measurement across the 2135 differentially expressed genes. The 'within-pair-between-pair-scatter-ratio' (WPBPSR, (7)) was determined by calculating the ratio of the within-pair similarity of a matched metastasis and primary tumor samples versus the average similarity of random samples (between-pair similarity). A low WPBPSR (< 1.0) indicates a high similarity between the matched primary tumor and metastasis. The statistical significance of the similarity measurement was determined by a permutation test in which the WPBPSR was calculated for 10,000 random pairings (7).

Identification of changes in gene expression between the primary tumors and the lymph node metastases was done using SAM (http://www-stat.stanford.edu/~tibs/SAM/). With a false discovery rate of 5 percent, only one gene (*MTA1*, q=0) was identified as differentially expressed between primary tumor and lymph node metastases. Metastatic signature outcome of the analyzed samples was determined as described previously (3, 15). Based on the expression pattern of the signature genes, a correlation was calculated with the average HNSCC metastatic profile. Positive correlation indicates a metastatic expression profile (N+) and negative correlation indicates a non-metastatic profile (N0).

References

1. Fidler, I.J. and M.L. Kripke, Metastasis results from preexisting variant cells within a malignant tumor. Science, 1977. 197(4306): p. 893-895.
2. Ramaswamy, S., et al., A molecular signature of metastasis in primary solid tumors. Nat Genet, 2003. 33(1): p. 49-54.
3. Roepman, P., et al., An expression profile for diagnosis of lymph node metastases from primary head and neck squamous cell carcinomas. Nat Genet, 2005. 37(2): p. 182-186.
4. van 't Veer, L.J., et al., Gene expression profiling predicts clinical outcome of breast cancer. Nature, 2002. 415(6871): p. 530-536.
5. Bernards, R. and R.A. Weinberg, A progression puzzle. Nature, 2002. 418(6900): p. 823.
6. Weigelt, B., et al., Molecular portraits and 70-gene prognosis signature are preserved throughout the metastatic process of breast cancer. Cancer Res, 2005. 65(20): p. 9155-9158.
7. Weigelt, B., et al., Gene expression profiles of primary breast tumors maintained in distant metastases. Proc Natl Acad Sci U S A, 2003. 100(26): p. 15901-15905.
8. Chung, C.H., et al., Molecular classification of head and neck squamous cell carcinomas using patterns of gene expression. Cancer Cell, 2004. 5(5): p. 489-500.
9. Schmalbach, C.E., et al., Molecular profiling and the identification of genes associated with metastatic oral cavity/pharynx squamous cell carcinoma. Arch Otolaryngol Head Neck Surg, 2004. 130(3): p. 295-302.
10. Leemans, C.R., et al., Regional lymph node involvement and its significance in the development of distant metastases in head and neck carcinoma. Cancer, 1993. 71(2): p. 452-456.
11. Pantel, K. and R.H. Brakenhoff, Dissecting the metastatic cascade. Nat Rev Cancer, 2004. 4(6): p. 448-456.
12. Zhang, X.Y., et al., Metastasis-associated protein 1 (MTA1) is an essential downstream effector of the c-MYC oncoprotein. Proc Natl Acad Sci U S A, 2005. 102(39): p. 13968-13973.
13. Zhang, H., L.C. Stephens, and R. Kumar, Metastasis tumor antigen family proteins during breast cancer progression and metastasis in a reliable mouse model for human breast cancer. Clin Cancer Res, 2006. 12(5): p. 1479-1486.
14. Gururaj, A.E., et al., MTA1, a transcriptional activator of breast cancer amplified sequence 3. Proc Natl Acad Sci U S A, 2006. 103(17): p. 6670-6675.
15. Roepman, P., et al., Multiple robust signatures for detecting lymph node metastasis in head and neck cancer. Cancer Res, 2006. 66(4): p. 2361-2366.
16. Mueller, M.M. and N.E. Fusenig, Friends or foes - bipolar effects of the tumour stroma in cancer. Nat Rev Cancer, 2004. 4(11): p. 839-849.
17. de Visser, K.E., A. Eichten, and L.M. Coussens, Paradoxical roles of the immune system during cancer development. Nat Rev Cancer, 2006. 6(1): p. 24-37.
18. Hunter, K., Host genetics influence tumour metastasis. Nat Rev Cancer, 2006. 6(2): p. 141-146.
19. Chambers, A.F., A.C. Groom, and I.C. MacDonald, Dissemination and growth of cancer cells in metastatic sites. Nat Rev Cancer, 2002. 2(8): p. 563-572.
20. Joyce, J.A., Therapeutic targeting of the tumor microenvironment. Cancer Cell, 2005. 7(6): p. 513-520.

6

Dissection of a metastasis expression signature into stromal and tumor cell components for improved predictive accuracy and sample scope

Manuscript submitted

Dissection of a metastasis expression signature into stromal and tumor cell components for improved predictive accuracy and sample scope

Paul Roepman[1], Erica de Koning[2], Dik van Leenen[1], J. Alain Kummer[2], Roel A. de Weger[2], Piet J. Slootweg[3] and Frank C.P. Holstege[1]

[1]Department of Physiological Chemistry, [2]Department of Pathology, University Medical Center Utrecht, Universiteitsweg 100, 3584 CG Utrecht, the Netherlands. [3]Department of Pathology, Radboud University Medical Center, Nijmegen, the Netherlands.

Manuscript submitted

Cancer gene expression profiling studies usually analyze complete tumor sections consisting of tumor cells and the surrounding stromal tissue. Although stroma likely plays an important role in tumor invasion and metastasis, tumor samples containing less than 50% tumor cells are generally excluded from such studies, reducing the number patients that can possibly benefit from clinically relevant signatures. To investigate the influence of tumor percentage on predictive gene expresssion signatures, we have dissected a head and neck squamous cell carcinoma (HNSCC) lymph node metastasis signature into six distinct components based on tumor versus stroma expression and association with the metastatic phenotype. A strikingly skewed distribution of metastasis predictor genes is revealed that agrees with poor predictive performance on samples than contain less than 50% tumor cells. Metastasis of HNSCC primary tumors is predominantly characterized by down-regulation of tumor cell specific genes and a concomitant exclusive upregulation of stromal cell specific genes. The results have important implications for design of expression signatures. Methods for reducing tumor composition predictive bias are presented which should lead to an increase in samples which can be included in such analyses. The skewed distribution of metastasis associated genes across the different signature components also increases our understanding of the processes underlying metastasis.

Introduction

DNA microarray technology has advanced our understanding of cancer by providing genome-wide mRNA expression measurements of different tumor types (1-3). Such studies have been used to identify new subtypes of cancer (4-7) and specific gene expression signatures have been found that can predict treatment response (8), metastatic disease (9, 10), recurrence rate (11) and that are associated with poorer outcome in cancer patients (12, 13). Despite the fact that some technical and statistical aspects of signature discovery studies still need optimizing (14-16), the potential of cancer genomics is already starting to be realized, with the first signatures becoming available for use in the clinic or in their final prospective validation phase (17).

Although in a few cases laser capture microdissection (LCM) has been applied (18, 19), expression profiling studies of solid tumors generally employ whole tumor sections consisting of tumor cells and the surrounding tissue microenvironment. This includes extracellular matrix components and stromal cells, such as fibroblasts and immune response cells (20). Because gene expression patterns are thus derived from both tumor cells and stroma, it is important to consider the degree to which inclusion of stromal cells influences the outcome of tumor profiling studies. This general question is particularly interesting when considering signatures for prediction of metastasis. Metastasis is the process whereby cancer cells spread to other sites in the body and is the principal cause of cancer-related deaths. To choose appropriate treatment strategies, it is of great importance to assess the presence of metastasis in cancer patients (21). It has recently become clear that stromal cells play an active role in tumor cell dissemination. This is caused by tumor-host interactions in which the microenvironment surrounding the tumor cells is an active partner during invasion and metastatic spread of cancerous cells (20, 22-24). Indeed, functional analysis of metastasis predictive signatures has indicated that these signatures likely also contain many genes that are specifically expressed in tumor stroma (9, 10, 25).

Although stroma plays an important role in tumor invasion and metastasis, traditionally cancer research has focused mostly on processes within tumor cells. Microarray studies generally only include tumor sections with a high percentage of tumor cells, thereby excluding a significant number of samples from signature analysis. To increase overall predictive accuracy and to increase the number of patients that may benefit from newly developed diagnostic signatures, it is worthwhile to consider ways of designing signatures that also take into account tumor samples with low tumor cell percentages. Increased focus on stroma components will also likely improve our understanding of the mechanisms underlying tumorigenesis.

Head and neck squamous cell carcinomas (HNSCC) arise in the upper aero-digestive tract and are the fifth most common malignancy in western populations, occurring with a rising frequency world-wide due to increased general life-expectancy and an increase in alcohol and tobacco consumption (26, 27). As with other tumor types, appropriate treatment depends on assessment of disease progression and in particular on assessment of the presence of metastases in regional lymph nodes close to the site of the primary tumor. However, due to difficulties in detecting such (micro-) metastases reliably, a large number of patients do not currently receive the most optimal treatment (28-30). Several expression signatures have recently been reported for HNSCC that can discriminate between metastasizing and benign tumors (25, 31-33). Although large-scale multi-center validation is still underway, assessment of a small collection of independent samples indicates that implementation in clinical practice may improve treatment for up to 65% of patients currently diagnosed with HNSCC in the oral cavity and oropharynx (25).

As with other solid-tumor profiling studies, one of the criteria for inclusion of samples in the latter study was the presence of a higher than 50% proportion of tumor cells in tumor sections (25). Here we investigate the influence of stroma/tumor cell percentage and show that

the metastatic state of samples with lower tumor cell percentage is less accurately predicted, despite the presence of stroma expressed genes in metastasis associated signatures. Using LCM to generate 35 related samples that have artificially altered proportions of stroma versus tumor cells, the loss of predictive accuracy is investigated further. The expression patterns of over 600 metastasis associated genes are determined, leading to dissection of the metastatic signature genes into several components based on expression in tumor versus stroma and association with a metastatic or non-metastatic phenotype. Loss of predictive accuracy for lower percentage tumor cell sections is shown to be the result of a skewed distribution of the different signature components and we evaluate several methods for adjusting and redesigning diagnostic signatures with improved accuracy for samples with low proportions of tumor cells. The skewed distribution of genes over the six distinct signature components determined here also forms a starting point for better understanding of the processes underlying metastasis.

Results

HNSCC lymph node metastasis signatures have previously been identified using complete primary tumor sections that contain both tumor cells and stroma (25) Samples containing less than 50% tumor cells were excluded from this previous study, which resulted in identification of over 800 metastasis associated genes useful for prediction in a variety of signature compositions (34). Within the samples included in these previous studies, a trend towards lower predictive accuracy for lower tumor percentage samples is indicated (Fig. 6.1 A, grey bars). This trend is even more apparent upon analysis of new samples with lower than 50% tumor cells (Fig. 6.1 A, white bar). Starting from the optimum tumor percentage of 60% – 70% (Fig. 6.1 C), the discriminatory power of the predictor is clearly reduced for samples

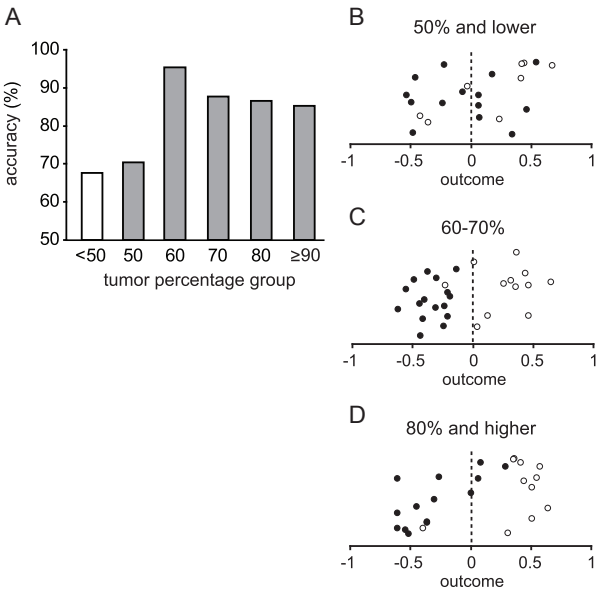

Figure 6.1 | Predictive accuracy of HNSCC signature decreases for samples with low tumor percentage. (**A**) Predictive accuracy of metastatic HNSCC signature per tumor percentage group. Grey bars indicate the accuracies of the previously analyzed 66 tumor samples (25), grouped according to their tumor percentages, whereas the white bar represents the results of 11 additionally analyzed samples with a tumor percentage of less than 50% (**B**) Signature outcome for samples with a tumor percentage of 50% or less, (**C**) between 60 and 70% and (**D**) with 80% or more. A signature outcome less than zero indicates a metastatic (N+) profile, and an outcome above zero indicates a non-metastatic (N0) outcome. Solid circles indicates tumor sample from patients with metastasis, open circles indicate tumor samples from patients without metastasis.

containing less than 50% tumor cells (Fig. 6.1 B), which is in agreement with the loss in predictive accuracy (Fig. 6.1 A). Interestingly, samples with the highest tumor percentage also show slight loss in discriminatory power (Fig. 6.1 D), indicating that there may be an optimal composition of tumor sample sections for accurate prediction of the metastatic state. These results indicate a loss in predictive accuracy that is related to an increased portion of stromal cells in tumor sections, despite the fact that the metastatic signatures carry a considerable number of genes that are expressed in the stroma (9, 34).

Analysis of the influence of section composition is confounded by the availability of sufficient samples representing a wide range of section compositions and within each range of compositions, the availability of enough samples representing possible predictive outcomes, that is either with metastasis (N+) or without metastasis (N0). To circumvent this problem we applied laser capture microdissection (LCM) to generate from complete primary tumor sections, multiple synthetic samples that differ only in tumor percentage (see Fig. 6.2 and methods for details). The samples chosen for this analysis represent a range of predictive accuracies for both the N0 and N+ outcome, including samples which are only marginally well predicted (Fig. 6.3 A, first column). A total of 35 artificial samples were generated by varying the proportion of tumor cells from between 0% and 100%. The advantage of this approach is that any difference in signature profile between multiple synthetic samples derived from a single tumor are entirely due to the different tumor percentages rather than individual sample heterogeneity. To determine whether this approach is valid we first tested whether LCM samples that retained the original tumor percentage (Fig. 6.2 H) show the same signature

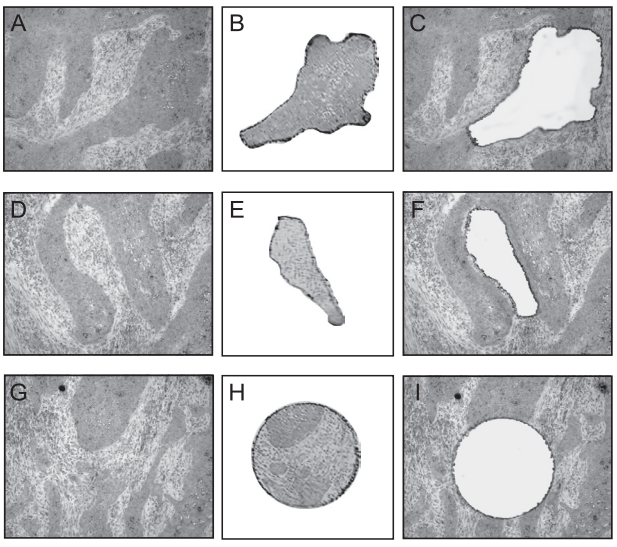

Figure 6.2 | Isolation of tumor cells and tumor stroma from complete primary tumor sections. Laser capture microdissection was used to isolate tumor and stromal areas that were used to generate synthetic samples from complete primary tumor sections. From primary tumor sections (**A, D, G**) areas comprising mainly of tumor cells (**B**) or tumor stroma (**E**), or random circles (**H**) were isolated using LCM. Samples with different tumor percentages were made by combining multiple tumor cell areas (**B**) and multiple tumor stroma areas (**E**) at varying ratios. LCM sample in which the original tumor-stroma proportion was retained were made by isolation of multiple circled areas randomly distributed across the tumor section (**H**). See **methods** section for more details. (**C, F, I**) depict primary tumor section after LCM of desired areas. Tissue sections shown here were colored using hematoxylin-eosin staining.

outcome as compared to the original complete tumor sections. The results of this analysis (Fig. 6.3 A, third column versus second column) confirms that generating artificial samples with LCM and implementation of the required additional RNA amplification procedures does itself not spoil the predictive outcome (Fig. 6.3 A).

From each of seven primary HNSCC tumor samples (3 N0 and 4 N+), five artificial samples were created by combining isolated tumor (Fig. 6.2 B) and stromal areas (Fig. 6.2 E) in different proportions, thereby generating a total of 35 samples consisting of 0%, 25%, 50%, 75% or 100% tumor cells. Dye-swap replicate DNA microarray analysis was performed for these 35 samples and the HNSCC predictive signature outcome was tested using a predictor comprised of 685 genes. These were selected from the total of 825 metastasis associated genes (34) by removing genes that showed any bias in the double amplification procedure required for analysis of the small amounts of material available by LCM. Intriguingly, the predictive outcome was considerably influenced by tumor percentage (Fig. 6.3 B). This is especially true for samples with a low tumor content and agrees with the trend observed on the low tumor percentage sections (Fig. 6.1 A). Although differences between N0 and N+ tumors still remain, all seven analyzed tumors show a bias towards a metastatic (N+) profile upon increase of the stroma percentage and a bias towards a non-metastasis (N0) profile upon increase in tumor cell percentage. Since this counterintuitive tumor percentage predisposition is likely caused by tumor cell or stroma cell specific gene expression, we decided to divide the signature genes into different categories and determine how the different components of the signature influenced the predictive outcome in a tumor percentage dependent manner.

The first criteria for subdividing the metastasis associated genes was based on whether genes are expressed predominantly in stroma, in tumor cells or in both (Fig. 6.3 C). This subdivision into three subsets of genes is based on correlation of gene expression with the different tumor percentages in the entire set of 35 artificial samples, with genes ordered from left to right as stroma expressed and tumor expressed respectively. To verify this subdivision, 100% tumor cell LCM samples were compared to 100% stroma LCM samples directly on 12 additional microarrays (dye-swap replicate for each of six samples for which there was still sufficient LCM material). The ratios of this direct comparison (Fig. 6.3 C, stromal expression depicted as green, tumor expression as red) confirmed the subdivision based on correlation with all the different tumor percentages. Interestingly, the results show that 12% of genes in the predictive signature are predominantly stroma expressed, 25% are more tumor cell specific, with the bulk equally expressed in tumor and stroma.

These three groups were then further subdivided into two categories each, based on whether upregulation is associated with the presence or absence of metastasis (Fig. 6.3 D). Two striking observations become apparent upon subdividing the signature genes in this way. The first is the skewed distribution of genes over the six different categories. While there are a significant number of stroma-expressed genes whereby upregulation is associated with the presence of metastasis, there are virtually no stroma-expressed genes whereby upregulation is associated with the absence of metastasis (Fig. 6.3 D, left-hand side). In other words the presence of metastasis is almost exclusively associated with upregulation of specific stromal expressed genes. For the tumor cell expressed genes within the signature, an oppositely

Figure 6.3 | The HNSCC metastasis predictive signature outcome changes for different tumor percentages due to an imbalance in tumor and stromal metastasis associated signature genes. (**A**) Metastatic signature profiles of seven analyzed primary HNSCC based on complete tumor sections and the originally identified 102-signature genes (25) (*original*), using complete sections and the 685 metastasis-associated predictive genes (*complete*), and based on the 685-gene set and LCM samples in which the original tumor-stroma proportion was retained *(lcm*). White indicates a non-metastatic (N0) profile, black indicates a metastatic (N+) profile. (**B**) Metastatic signature profiles of synthetic samples from 7 primary tumors that retained the original tumor percentage (*lcm*) or contained 0, 25, 50, 75 or 100% tumor cells, respectively. Profiles are based on the predictive 685-gene set. Colors as in **A**. (**C**) The set of 685 predictive genes are ordered according to the correlation of their expression level with analyzed tumor percentages. Colors are based on direct microarray comparison of tumor cells and tumor stroma, which confirmed that negatively correlated (< -0.50) genes are mainly expressed in the stroma and positively correlated gene (>0.50) are tumor cell associated. Uncorrelated genes indeed show equal expression between tumor cells and stroma. *Black* indicates higher expression in tumor stroma compared to tumor cells and *white* indicates higher expression in tumor cells than in tumor stroma. (**D**) Tumor percentage correlation and signature association (N0 or N+) of the predictive genes. Tumor percentage correlative groups as shown in **C**. *Light gray* indicates genes that are upregulated in non-metastatic (N0) tumors, dark gray indicates genes that are upregulated in metastatic (N+) tumors. (**E**) As **B**, for the tumor and stromal specific predictive genes (259 genes). (**F**) As **B**, for the non-specific predictive genes that are equally expressed between tumor cells and tumor stroma (tumor percentage correlation between -0.50 and 0.50).

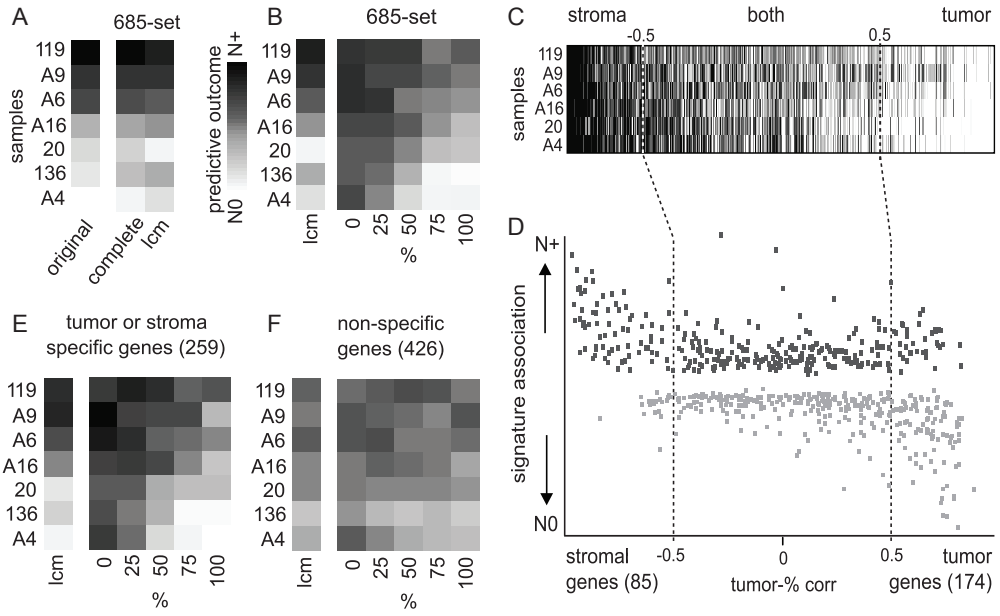

skewed distribution is also evident although to a somewhat lower degree (Fig. 6.3 D, right-hand side). There are a significant number of tumor cell expressed genes whereby increased expression is associated with the absence of a metastasis, but a much lower number of tumor cell expressed genes whereby upregulation is associated with presence of metastasis. Taken together, for HNSCC in the oral cavity or oropharynx, the metastasizing primary tumor is characterized by upregulation of stroma specific genes and inactivation of tumor cell specific

genes.

Besides providing important insights into the metastatic process itself (see discussion), this skewed distribution likely accounts for the predisposition of the complete set of signature genes for falsely predicting the presence of a metastasis on samples with reduced tumor percentage (Fig. 6.3 B). Because metastasis is associated with increased expression of a subset of stroma specific genes, with little to no down-regulation of stroma specific genes, an increased proportion of stroma in whole tumor sections will result in a bias towards an N+ prediction, even for primary tumors that are in fact N0. The other skew in the distribution, more down- than upregulation of tumor cell specific genes in an N+ tumor, works in the same way and adds to the predisposition towards an N+ prediction in low tumor cell percentage samples. To test the idea that the skewed distribution underlies the bias towards predicting an N+ phenotype in samples with reduced tumor cell percentage, N0/N+ predictions were repeated on the 35 artificially composed LCM samples, using only those signature genes specifically expressed in either tumor cells or stroma. As expected, this signature is even more skewed towards predicting the N+ phenotype than the complete set of signature genes (Fig. 6.3 E versus Fig. 6.3 B).

A second important observation that is apparent upon subdividing the signature genes into different categories can be made for genes which are expressed in both stroma and tumor (Fig. 6.3 D, middle group). Whereas hardly any skewed N0/N+ distribution is seen for this group, the predictive power to discriminate between N0 and N+ tumors is markedly reduced compared to the tumor cell and stroma specific genes. This is apparent from the lower degree of association with either an N+ or an N0 phenotype (Fig. 6.3 D). Using only signature genes that are equivalently expressed in both stroma and tumor cells would be an ideal way in which to circumvent tumor cell percentage biases in signatures. Unfortunately in this case, because of their weaker association with either an N0 or N+ phenotype, a signature based exclusively on genes expressed in both tumor cells and stroma has insufficient predictive power to strongly discriminate between N0 and N+ primary tumors, either for the artificially generated samples (Fig. 6.3 F), or as tested on the entire original set of 66 primary tumor samples used to generate Fig. 6.1 (overall accuracy is reduced from 86% to 76%).

Based on the results described above, the previously identified predictive HNSCC signature can be separated into one part that contains genes that are equally expressed between tumor and stroma but with limited predictive power, and a second part with tumor and stromal specific genes that have strong discriminatory power but a skewed N0/N+ distribution. A model for this and the ensuing bias in predictions shows the presence of four unequally distributed components (Fig. 6.4 A), alongside the actual distribution of such stroma and tumor cell specific genes (Fig. 6.4 B). The two large components contain N0 associated tumor genes (tumor N0) and N+ associated stromal genes (stroma N+). The two smaller components contain some tumor N+ genes and hardly any stroma N0 genes (Fig. 6.4 B). As is depicted (Fig. 6.4 A, B), the skewed sizes of these four components results in a signature that is unstable in its predictive outcome with regard to different tumor percentages (Fig. 6.3 E).

If this model is accurate, adjustments to correct for overrepresentation should result in a predictive sigature with reduced bias for different tumor percentages as is indicated in the model shown in Fig. 6.4 C. Accordingly, from the initial comprehensive set of metastasis associated genes, a set of 119 predictive genes were selected that showed the greatest balance for the different signature components (Fig. 6.4 D). As expected, the balanced HNSCC metastasis signature indeed shows a great reduction in tumor cell percentage bias for its predictive outcome when tested on the artificially composed LCM samples (Fig. 6.4 E). Using the balanced signature, the synthetic tumor samples with a tumor percentage ranging from 25% to 100% now show a predictive outcome largely independent of tumor percentage and a strong reduction in the N+ predisposition for N0 samples containing no tumor cells (Fig. 6.4 E).

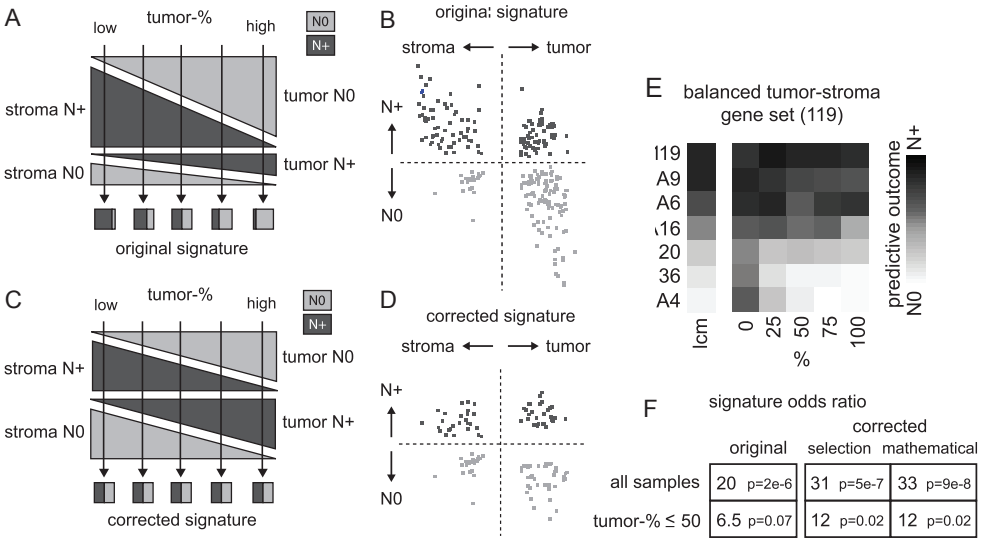

Figure 6.4 | Correction of the tumor and stromal HNSCC signature components result in a more robust and accurate predictive profile. (**A**) Model for the observed tumor percentage related bias of the HNSCC signature. The contributions of the four identified signature components: stroma specific genes associated with a metastatic and non-metastatic profile (*stroma N+* and *stroma N0*, respectively) and tumor cell specific gene associated with a metastatic and non-metastatic profile (tumor N+ and tumor N0, respectively), are shown for analysis across varying tumor percentages. Combining the four components into one predictive outcome (indicated by *arrows*) results in the tumor percentage signature bias as observed in Fig. 6.3 E. Low tumor percentage samples (left hand side) show a more N+ profile (*dark grey*), whereas samples with a very high tumor percentage (right hand side) exhibit a bias towards a more N0 profile (*light grey*). (**B**) Signature components as shown in **A** for the originally identified HNSCC signature. Light grey indicates N0 associated genes, dark grey indicates N+ associated genes. (**C**) As **A**, for a corrected signature composition that does not exhibited a bias towards the predictive outcome of low and high tumor percentage samples. (**D**) Selection of a set of 119 HNSCC signature genes that are equally distributed across the four different components, plotted similar as in **B**. (**E**) Predictive outcomes based on the corrected signature that consists of the 119 genes shown in **D**. The corrected signature shows a strong reduction in predictive bias for samples with a low or very high tumor percentage. Colors as in Fig. 6.3 E. (**F**) Odd ratios for the signature outcome for prediction of metastasis based on the original signature and corrected using a gene selection procedure or via a mathematical correction.

To test whether predictive bias correction using a balanced signature does not exclusively work on the LCM composed samples, the performance of the balanced signature was determined on the set of 77 complete primary tumor sections (Fig. 6.1), including the additional samples with less than 50% tumor cell percentage. Here too, the balanced HNSCC metastasis signature outperforms the original signatures (34), especially for samples with a lower degree of tumor cells (Fig. 6.4 F). The reported odds ratio (OR) expresses the chance that the performance is based on random occurrence and the overall predictive accuracy for samples with 50% or less tumor cells rose from 68% (OR of 6.5) to 75% (OR of 12) upon application of the balanced signature. The improvement is incremental but significant for patients wishing to benefit from future diagnostic signatures, especially because this indicates that a much larger group of samples can be included in signature profiling by taking into account the possibility of skewed expression- and phenotype-distributions of signature genes. Another possible approach for adjusting the signature is by weighting the predictive correlations of individual signature components based on tumor cell percentage in the sample. This mathematical correction results in a similar improvement in predictive accuracy (Fig. 6.4 F).

Discussion

In this study we have investigated the effects of tumor composition on the performance of a predictive signature, dissected the signature into different components and show that loss of predictive accuracy on low tumor cell percentage samples is, at least in part, caused by a skewed distribution of signature genes within these different components. The results have implications for our understanding of how metastases arise, for treatment of metastases and suggest several ways in which expression signatures can be improved.

Functional category analyses of classifiers has previously already indicated the presence of both tumor cell specific and stromal expressed genes in such signatures (9, 25, 34). By directly comparing LCM stroma fields with tumor fields we show that for an exhaustive collection of over 600 HNSCC lymph node metastasis associated genes (34), 12% are predominantly expressed in stroma, 25% in tumor cells and the majority in both tumor and stroma. This agrees with recent discoveries highlighting the contribution of the surrounding microenvironment towards cancer development (35-37) and the interplay between tumor and stromal cells that leads to metastasis (22, 24, 38).

A striking finding is the skewed distribution of stromal and tumor cell expressed genes with regard to their association with the presence or absence of metastasis (Fig. 6.3 D). Compared to the primary tumors that show no metastasis, the metastasizing primary head neck tumor is characterized by exclusive upregulation of a subset of stroma specific genes concomitant with predominant inactivation of a subset of tumor specific genes. This is in agreement with the idea that tissue surrounding tumor cells is actively transformed into a metastasis supportive microenvironment (20, 22, 24). The fact that metastasis is more strongly associated with down-regulation of tumor cell specific genes than activation, suggests that in tumor cells loss-of-function plays a more dominant role in acquiring a metastatic phenotype than gain of

function. Future analyses will perhaps indicate which of the tumor cell metastasis associated genes are causal to the concomitant changes observed in stroma expression. This dissection of the very large set of over 600 metastasis associated genes (34) into much smaller groups of strongly metastasis associated genes with defined expression, should simplify the task of finding suitable therapeutic targets for treatment of metastasis.

The HNSCC metastatic signature consists for about two-thirds of genes with similar expression in tumor cells and stroma. On there own, these only marginally discriminate between N0 and N+ tumors, presumably due to lower differences in expression for these genes between the two tumor types. Because these genes are expressed in both stroma and tumor cells and exhibit less discriminatory power, such genes may be more of an indirect mark of genetic polymorphisms associated with the metastatic phenotype, than directly causal to metastasis. This idea is in line with indications that a metastasis expression signature is at least partly a product of genetic polymorphisms rather than changes caused during tumorigenesis (39). Another interesting feature of the signature genes is the absence of highly specific, individual-gene differential regulation between N0 and N+ tumor or stroma. This agrees with the difficulties in finding highly specific metastasis markers for primary tumors and the fact that successful signatures require contributions of large numbers of genes for accurate prediction. This also indicates that the metastatic phenotype is caused by relatively minor changes in expression of a large number of genes.

The skewed distribution of metastasis signature genes over the different components (Fig. 6.3) has important implications for design of expression signatures. Samples consisting of a lower than 50% tumor percentage are generally excluded from profiling studies. This is an important but not well-documented issue. For example, approximately 30% of tumors in our current collection of head-neck tumor samples do not fulfill this criteria (P. Roepman, unpublished results). Such samples have been excluded from many successful profiling studies and cannot be included in future implementation of diagnostic profiling unless approaches are devised to allow inclusion based on accurate predictions. Even a marginal decrease to 40% or 25% tumor percentage for inclusion in future studies is a significant step forward for the patients involved.

Here we first confirm that the metastatic status of samples with a lower proportion of tumor cells are indeed less accurately predicted (Fig. 6.1) and demonstrate that at least in part, this is due to the skewed distribution of metastasis associated genes over several different signature components (Fig. 6.3). Because the most strongly metastasis associated genes are stromal genes which become upregulated and tumor cell genes which are down-regulated (Fig. 6.3 D), the presence of a higher amount of stromal material will *a priori* predispose a metastatic signature to making a N+ prediction. The loss in discriminatory power observed on whole tumor sections is not always skewed towards making false N+ predictions for lower tumor percentage samples (Fig. 6.1 B), suggesting that other factors such as sample heterogeneity also play a role. Due to the large number of samples required to counter sample heterogeneity, it is at present not possible to determine unequivocally whether all the loss in predictive accuracy observed for lower tumor cell percentage samples (Fig. 6.1 A) can be

attributed to the skewed distribution of signature genes. Nevertheless, the improved outcome on artificial LCM generated samples (Fig. 6.4 E) and complete tumor sections (Fig. 6.4 F) indicates that if steps are taken to analyze signature compositions and correct for skewed distributions over the different components, then a larger number of patients will in future benefit from diagnostic signatures.

Here we present three methods for improved prediction of lower tumor percentage samples for skewed composition signatures. The first method involves selection of signature genes expressed similarly in both tumor cells and stroma. The weaker discriminatory power of such genes is perhaps related to having no specific role in either tumor or stroma. When used on their own, the signature lacks sufficient discriminatory power, even when all 426 such genes are used together (Fig. 6.3 F). The two other approaches do not exclude the skewed signature components, but compensate the bias by selecting either a balanced number of genes (Fig. 6.4 D), or by tumor cell percentage weighted correction of individual component predictions. Both improve predictive accuracy for low tumor cell percentage samples, without loss of overall accuracy. Analysis of significantly more low tumor percentage samples will be required to ascertain whether these are indeed the best approaches. Such a study could also investigate the possibility of designing two different independent signatures: one "stromal-related" signature based on low tumor percentage samples and one "tumor-related" signature based on high tumor percentage samples. Via this approach a biological characteristic, that is the interplay between tumor and stromal cells will be divided into two separate signatures. Moreover, due to splitting the sample set into two, at least twice as many samples will be needed to achieve similar statistical significance. Insufficient numbers of low tumor percentage samples in our collection, renders it as yet impossible to conclude whether this approach is feasible. Regardless of the issue of current sample availability, the importance of the present study is that it successfully dissects a clinically relevant diagnostic signature into separate components, and shows that skewed distribution of signature genes over the different components contributes to lower predictive accuracy for low tumor percentage samples. Balancing the skewed distribution of available signature genes improves predictive accuracy of low sample tumors. It will be important to determine whether other signatures have similar properties and future studies can now take the possibility of skewed distributions of signature genes into account, leading to inclusion of more samples and increasing the number of patients to which diagnostic signatures can be applied.

Methods

Tumor samples | Previously determined gene expression data of 66 primary HNSCC tumor samples was used in this study (25). In addition, 11 extra tumor samples were analyzed for their gene expression profile. Selection criteria for this additional set of samples were similar as for the previous set of 66, except that complete tumor sections of these 11 samples showed a tumor percentage of less than 50%. RNA processing, microarray hybridization and analysis of the for the 11 samples was performed similar as previously (25).

Synthetic tumor percentage samples | For seven primary tumors (3 N0, 4 N+) randomly selected from the previously analyzed set of 66 samples, five synthetic samples were generated with 0, 25, 50, 75 or 100% tumor cells and one synthetic samples in which the original tumor

percentage was retained. The synthetic tumor percentage samples were generated by LCM of in total 1 mm^2 tumor section tissue. The synthetic samples that differed in tumor percentage were made by combining multiple isolated tumor cell areas (Fig. 6.2 B) and multiple isolated stromal field (Fig. 6.2 E) in different ratios, e.g. an 75% sample was generated by LCM of 0.75 mm^2 tumor cells and 0.25 mm^2 stroma. The synthetic samples in which the original composition was retained were generated by isolation of random circled areas from the complete tumor section (Fig. 6.2 H).

LCM and RNA isolation | Frozen tumor sections (10 µm) were fixated on PALM MembraneSlides (PALM MicroLaser Systems) and colored with hematoxylin for 30 seconds. Laser capture microdissection (LCM) was performed using the PALM MicroBeam System. Total RNA from captured microdissected cells was isolated using the PicoPure™ RNA Isolation Kit (Arcturus). RNA quality was checked on the 2100 bioanalyzer (Agilent).

RNA amplification and fluorescent labeling | RNA isolated from LCM samples was amplified using 2 rounds of T7 linear amplification. The first round was performed as described elsewhere (25) except that T7 in vitro transcription (IVT) was performed for 2 instead of 4 hours and without incorporation of aminoallyl-UTP. The generated first round cRNA was used as a template for a second round of amplification. Samples were vacuum concentrated to 9 µl and 1 µl random primers (1 µg/µl, Invitrogen) was added. Subsequent first strand cDNA synthesis was performed as previously described (25) followed by incubation at 94ºC for five minutes. After cooling the samples on ice, 1 µl of the previously used double anchored T7-poly(dT) primer was added and the samples were incubated 5 min at 70°C and subsequently for 3 min at 48°C. Second strand cDNA synthesis, second round IVT and cRNA cleanup was preformed as described elsewhere (25). During the second amplification round aminoallyl-UTP was incorporated into the generated cRNA enabling direct coupling of fluophores before hybridization. Direct coupling of cy5 or cy3 fluophores was done as described previously (25). Yield, quality and label incorporation were quantified spectrophotometrically and on the 2100 Bioanalyzer (Agilent).

Gene expression analysis | Gene expression patterns were determined using home-made 70-mer oligonucleotide DNA microarrays (25). Before hybridization, the microarray slides were incubated in borohydrate buffer (2x SSC, 0.05% SDS and 0.25% sodium borohydrate (Aldrich)) for 30 minutes at 42°C. Three-hundred ng of cy5 or cy3 labeled sample target were combined with 300 ng reverse labeled reference cRNA (25) and fragmented using Ambion's Fragmentation kit. Microarray hybridization was performed as described elsewhere (40). The slides were scanned in the Agilent G2565AA DNA Microarray Scanner. Images were quantified and corrected for background using Imagene software (Biodiscovery). Quantified expression data was normalized as described previously (25).

Metastasis predictive signature outcome | The metastasis predictive signature outcome of each analyzed HNSCC sample was determined by calculating the correlation of its specific gene expression pattern with the previously determined typical metastatic (N+) and non-metastatic (N0) profiles, as described previously (25). Combined, the N+ and N0 profile correlations denoted a single predictive signature outcome for each analyzed sample for a specific set of predictive genes. Positive correlation indicated an N+ profile, negative correlation an N0 profile. From the previously identified comprehensive set of 825 predictive genes (34), 685 gene were analyzed here which showed a robust profile when including the LCM and double amplification procedures.

References

1. Huang, E, et al., Gene expression phenotypic models that predict the activity of oncogenic pathways. Nat Genet, 2003. 34(2): p. 226-230.
2. Segal, E, et al., From signatures to models: understanding cancer using microarrays. Nat Genet, 2005. 37(6 Suppl): p. S38-45.
3. Bild, AH, et al., Oncogenic pathway signatures in human cancers as a guide to targeted therapies. Nature, 2006. 439(7074): p. 353-357.
4. Valk, PJ, et al., Prognostically useful gene-expression profiles in acute myeloid leukemia. N Engl J Med, 2004. 350(16): p. 1617-1628.
5. Perou, CM, et al., Molecular portraits of human breast tumours. Nature, 2000. 406(6797): p. 747-752.
6. Golub, TR, et al., Molecular classification of cancer: class discovery and class prediction by

gene expression monitoring. Science, 1999. 286(5439): p. 531-537.
7. Alizadeh, AA, et al., Distinct types of diffuse large B-cell lymphoma identified by gene expression profiling. Nature, 2000. 403(6769): p. 503-511.
8. Ma, XJ, et al., A two-gene expression ratio predicts clinical outcome in breast cancer patients treated with tamoxifen. Cancer Cell, 2004. 5(6): p. 607-616.
9. Ramaswamy, S, et al., A molecular signature of metastasis in primary solid tumors. Nat Genet, 2003. 33(1): p. 49-54.
10. Wang, Y, et al., Gene-expression profiles to predict distant metastasis of lymph-node-negative primary breast cancer. Lancet, 2005. 365(9460): p. 671-679.
11. Paik, S, et al., A multigene assay to predict recurrence of tamoxifen-treated, node-negative breast cancer. N Engl J Med, 2004. 351(27): p. 2817-2826.
12. Huang, E, et al., Gene expression predictors of breast cancer outcomes. Lancet, 2003. 361(9369): p. 1590-1596.
13. van 't Veer, LJ, et al., Gene expression profiling predicts clinical outcome of breast cancer. Nature, 2002. 415(6871): p. 530-536.
14. Tinker, AV, Boussioutas, A, and Bowtell, DD, The challenges of gene expression microarrays for the study of human cancer. Cancer Cell, 2006. 9(5): p. 333-339.
15. Simon, R, et al., Pitfalls in the use of DNA microarray data for diagnostic and prognostic classification. J Natl Cancer Inst, 2003. 95(1): p. 14-18.
16. Ransohoff, DF, Rules of evidence for cancer molecular-marker discovery and validation. Nat Rev Cancer, 2004. 4(4): p. 309-314.
17. Kallioniemi, O, Medicine: profile of a tumour. Nature, 2004. 428(6981): p. 379-382.
18. Alevizos, I, et al., Oral cancer in vivo gene expression profiling assisted by laser capture microdissection and microarray analysis. Oncogene, 2001. 20(43): p. 6196-6204.
19. Yamabuki, T, et al., Genome-wide gene expression profile analysis of esophageal squamous cell carcinomas. Int J Oncol, 2006. 28(6): p. 1375-1384.
20. Bissell, MJ and Radisky, D, Putting tumours in context. Nat Rev Cancer, 2001. 1(1): p. 46-54.
21. Forastiere, A, et al., Head and neck cancer. N Engl J Med, 2001. 345(26): p. 1890-1900.
22. Mueller, MM and Fusenig, NE, Friends or foes - bipolar effects of the tumour stroma in cancer. Nat Rev Cancer, 2004. 4(11): p. 839-849.
23. Hanahan, D and Weinberg, RA, The hallmarks of cancer. Cell, 2000. 100(1): p. 57-70.
24. Liotta, LA and Kohn, EC, The microenvironment of the tumour-host interface. Nature, 2001. 411(6835): p. 375-379.
25. Roepman, P, et al., An expression profile for diagnosis of lymph node metastases from primary head and neck squamous cell carcinomas. Nat Genet, 2005. 37(2): p. 182-186.
26. Reid, BC, et al., Head and neck in situ carcinoma: incidence, trends, and survival. Oral Oncol, 2000. 36(5): p. 414-420.
27. Bray, F and Moller, B, Predicting the future burden of cancer. Nat Rev Cancer, 2006. 6(1): p. 63-74.
28. Robbins, KT, et al., Neck dissection classification update: revisions proposed by the American Head and Neck Society and the American Academy of Otolaryngology-Head and Neck Surgery. Arch Otolaryngol Head Neck Surg, 2002. 128(7): p. 751-758.
29. Jones, AS, et al., Occult node metastases in head and neck squamous carcinoma. Eur Arch Otorhinolaryngol, 1993. 250(8): p. 446-449.
30. Woolgar, JA, Pathology of the N0 neck. Br J Oral Maxillofac Surg, 1999. 37(3): p. 205-209.
31. Schmalbach, CE, et al., Molecular profiling and the identification of genes associated with metastatic oral cavity/pharynx squamous cell carcinoma. Arch Otolaryngol Head Neck Surg, 2004. 130(3): p. 295-302.
32. Cromer, A, et al., Identification of genes associated with tumorigenesis and metastatic potential of hypopharyngeal cancer by microarray analysis. Oncogene, 2003.
33. Chung, CH, et al., Molecular classification of head and neck squamous cell carcinomas using patterns of gene expression. Cancer Cell, 2004. 5(5): p. 489-500.
34. Roepman, P, et al., Multiple robust signatures for detecting lymph node metastasis in head and neck cancer. Cancer Res, 2006. 66(4): p. 2361-2366.
35. Kalluri, R and Zeisberg, M, Fibroblasts in cancer. Nat Rev Cancer, 2006. 6(5): p. 392-401.
36. Pollard, JW, Tumour-educated macrophages promote tumour progression and metastasis. Nat Rev Cancer, 2004. 4(1): p. 71-78.
37. Balkwill, F, Cancer and the chemokine network. Nat Rev Cancer, 2004. 4(7): p. 540-550.

38. Joyce, JA, Therapeutic targeting of the tumor microenvironment. Cancer Cell, 2005. 7(6): p. 513-520.
39. Hunter, K, Welch, DR, and Liu, ET, Genetic background is an important determinant of metastatic potential. Nat Genet, 2003. 34(1): p. 23-24; author reply 25.
40. van de Peppel, J, et al., Monitoring global messenger RNA changes in externally controlled microarray experiments. EMBO Rep, 2003. 4(4): p. 387-393.

7

General discussion

Challenges of microarray studies for cancer research

General Discussion

Challenges of microarray studies for cancer research

During the last few years, microarray technology has rapidly become the main technique for studying gene expression. DNA microarrays have proven valuable for a better understanding of the biology of human cancer (1, 2) and have the potential to improve diagnosis and treatment (3). Cancer class discovery and prediction studies have identified new (sub)types of cancer (4-6). Diagnostic gene expression signatures have been discovered for analysis of disease progression, treatment response and survival rate (7-9) and will likely improve tailored patient therapy in the near future (4, 7, 10-12). Although the first diagnostic signature are becoming available for use in the clinic (3, 7), the full potential of DNA microarrays still needs to be realized.

While DNA microarray technology is continuously improving with regard to accuracy and precision, it remains difficult to combine and compare data that has been generated in different studies and using different microarray platforms. Besides practical constraints that are imposed due to the high costs of microarray studies and the difficulty in obtaining enough high-quality samples, important issues related to sample collection and study design are often overlooked. For optimal analysis and to prevent unwanted biases and confounding effects in the generated data, cancer genomics studies require sufficient attention to the study setup and sample collection (13, 14). Other important challenges of gene expression profiling studies are associated with data analysis pitfalls (15, 16). Here we discuss some important issues regarding study setup, data analysis, data and sample accessibility that limit the optimal use of DNA microarrays for design and implementation of cancer diagnostic signatures if insufficiently addressed. Next, an overview is given of the HNSCC metastatic gene expression profiling study described in this thesis, in which some challenging issues are illustrated. Finally, follow-up research needed to bring this signature to the clinic is discussed.

Study setup

An important task in setting up a DNA microarray study is to design the experiments in such a way that the generated data is most efficient and reliable for the objective at hand (17). Not paying sufficient attention to design issues such as sample selection and experiment design can lead to an experiment that gives satisfactory results but is less efficient than it could have been otherwise or, in the worst case scenario, is unable to answer the research question with the available data (14).

Due to heterogeneity between independent tumor samples and because microarray results are susceptible to large false discovery rates, cancer gene expression profiling studies require a sufficiently large number of samples for generating reliable and informative gene expression data. Optimal sample number differs per study and depends on the study objectives, the variation between the studied samples and the true difference between the analyzed sample

groups. Generally no less than 10-15 replicates per sample group should be used (18), but many cancer classification studies require many more samples for accurate analysis. The large biological variation between tumor samples calls for inclusion of enough biological replication, preferably from different patients, rather than many technical replicates. To avoid strong reduction in statistical power due to insufficient samples, it is desirable to perform a power analysis using a small number of representative tumor samples to estimate the sample size needed for a large-scale profiling study (19-21).

Dual-channel microarray experiments involve comparisons of two individual samples on a single microarray slide, in which both samples are labeled with different fluorophores (22). Unlike single-channel arrays in which absolute gene expression levels are estimated, dual channel microarray experiments are inherently comparative and lead to relative expression measurements. Generally, dual-channel experiment design can be divided into two types: direct and indirect design (14). In a direct experiment design, samples are compared directly within individual microarray slides. Direct comparison of a large number of samples with each other requires a very large number of hybridizations. Although a semi-direct loop design is able to reduce the number of microarray slides by comparing all samples via a looped pattern (23), an indirect study design by which all analyzed samples are compared to a common reference sample is most suitable for comparison of large numbers of tumor samples (17). This setup requires the lowest number of microarray slides and, unlike a loop design, makes insertion of additional samples possible without reanalysis of previous samples. The only drawback is the slight reduction in discriminatory power due to an indirect comparison of all samples with each other via a reference sample (14). For comparison of cancerous tissue with healthy samples, the optimal reference sample consists of mRNA from normal tissue, while for tumor class discovery and prediction studies the reference is preferably made of a pool of all analyzed samples to make sure that all analyzed gene transcripts are also present in the common reference pool.

Data confounding and sample annotation

Data confounding due to inappropriate sample selection are of particularly concern for cancer class comparison and prediction studies. Confounding refers to a lurking variable that is not known or acknowledged and can distort the relationship between the studied variable and the generated expression data (13). For example, in a study designed to identify a molecular signature for development of metastasis based on gene expression of the primary tumor, data confounding can take place if other (unknown) factors that influence the metastatic outcome, such as chemotherapy or anatomical location, are not equally distributed amongst the sample groups. As a result, the differences between tumors from patients with or without metastasis might not be caused by intrinsic metastatic properties but due to administered chemotherapy or differences in anatomical location. To avoid this problem, retrospectively collected samples should be balanced for known confounders by blindly selecting samples or by randomizing the samples across possible confounding variables. However, this may prove difficult if the available sample size is limited, making small-scale studies more susceptible for

data confounding. Besides intrinsic sample characteristics, differences in physical handling and processing within different sample groups can lead to biases in the measured expression data (24-26). The use of a prospective study design is a very effective way for controlling confounding and bias effects because in a prospective setup the status of the studied sample variable is initially unknown, thereby automatically randomizing possible confounding factors. Moreover, a prospective design can ensure that all samples are processed according to standardized protocols thus avoiding unnecessary heterogeneity due to variation in sample handling in the past.

To prevent data confounding, potential confounders such as age, gender, cancer stage, histology and administered treatment should be balanced across analyzed sample groups. This emphasizes the importance of accurate and comprehensive patient and sample annotation across clinical, histo-pathological and molecular biological features. Given the importance of adequate annotation, guidelines have been proposed for documenting the minimal clinical information for samples used in microarray studies (27) and standards for reporting diagnostic accuracy (28). Along the caveat "garbage in, garbage out", standards are also needed for assessment and documentation of the quality of the samples used for microarray analysis, such as RNA yield, quality and label incorporation efficiency (29). Samples that do not meet these annotative and quality criteria should be excluded from analysis to prevent abnormalities and biases in microarray data. Besides correct annotation of target samples, gene expression profiling also requires accurate annotation of the gene probes that are present on the microarray. Since the complete annotation of the human genome is still an ongoing process, optimal analysis of DNA microarray data necessitates the use of the latest genome annotation for identification of the probe spots on the array (30).

Data overfitting and validation

With the advances already made in DNA microarray technology, the bottleneck in genome-wide gene expression profiling studies has shifted from technical aspects to statistical analysis of the generated data. In a typical microarray experiment, thousands of genes are measured across a relative small number of samples (31). Next, all genes are individually subjected to a statistical test of significance to identify the differentially expressed genes between the analyzed sample groups. However, the standard *P*-value for significance of statistical testing was invented for testing individual hypotheses and will lead to a high number of false positives when applied in repeated testing of multilple genes, as is the case in microarray analysis (32). Standard multiple testing corrections, such as Bonferroni, are too conservative for microarray experiments since they control the probability of making at least one false positive. Therefore, less conservative methods have been developed that are able to control the number of false positives while retaining study power (21, 33, 34). Hitherto, it remains unclear which method is most appropriate for dealing with false negative results due to the lack of proper calibrated data sets (35).

Due to the high number of measured genes compared to the relative small amount of samples, cancer class discovery and classification studies run the risk of overfitting of a

specific gene expression profile (15, 16). By applying a supervised learning method on a large number of genes, there exists a substantial chance that a random subset of genes will correlate with the studied parameter. By definition, this association is arbitrary and does represent the true relationship between the different sample groups. Such data overfitting results in a expression signature with a very high accuracy on the training samples but is non-reproducible on independent samples. Consequently, it is essential to identify and assess predictive signatures by means of unbiased methods (15). The most commonly used methods for identification and assessment of an unbiased predictive signature are internal cross-validation procedures (36). These methods involve random splitting of the data set into a training and smaller test set. The predictive signature is built using the training samples and performance is assessed on the test set. Iteration of this procedure will result in the optimal predictive signature with the lowest bias towards the complete sample set.

Final validation of gene expression patterns should take place on a sufficiently large independent sample set. The danger of discovery-based research, in which large amounts of data are analyzed without prior hypothesis to discover discriminatory patterns among groups, lies in the true validity of the research results (37). Due to the complex and extensive nature of gene expression data, microarray research without an *a priori* hypothesis runs the risk of a "self-fulfilling prophecy" in which an apparent discrimination is caused by chance, even when using an unbiased cross-validation procedure. Although this phenomenon is less likely in cancer class prediction than in class discovery studies, proper rules of evidence are needed to evaluate the strength and validity of the results (37), preferably on independent samples that are collected and processed in different institutes.

Sample and data accessibility

As mentioned, sample size is one of the most important criteria for expression profiling studies. Increasing the number of analyzed samples reduces the risk for unwanted effects as well as data overfitting and increases the reproducibility and validity of an identified expression signature. Large sample numbers require the presence of a large collection of biological samples together with a comprehensive sample annotation that includes detailed histo-pathological, genetic and molecular biological data as well as information about the patient's medical history and life style. Such collections, also called biobanks, should preferably represent a large part of the population and need to be generally accessible to the research community to acquire sufficient samples for large-scale follow-up studies (38, 39). In order to combine samples from different biobanks and to link biobanks in the future, guidelines and standards are required for annotation and quality documentation of the stored samples. Preferably, such biobanks should be set up nationally to comprise sufficient samples for genomics studies, also for rare diseases (40).

Another way for robust independent validation of an identified signature without the need for a large number of additional samples, is by making use of gene expression data that has been generated by other studies. This procedure comprises validation on independent samples as well as for procedural differences between institutes. Moreover, general accessibility of

expression data allows large scale integrative profiling studies, or meta-analyses, to identify higher-level molecular signatures and processes that are shared across multiple cancer types (1). Unfortunately, the lack of microarray data management and accessibility is still a major problem in data sharing (41). Easy access to the increasing amount of microarray data requires publicly accessible databases and standards for presenting and exchanging data. Standards for annotation, such as MIAME (27), MAGE-ML (42), and public microarray databases, e.g. GEO (43) and ArrayExpress (44), are starting to be setup and used. However, to fully utilize generated microarray data, peer-reviewed scientific journals must oblige submission of properly annotated data to these public databases for manuscripts that include microarray experiments.

Gene expression signature for diagnosis of lymph node metastasis in HNSCC patients

In this thesis we have investigated the use of DNA microarrays for diagnosis of neck lymph node metastasis in patients with head and neck cancer (HNSCC). Due to problems in accurate detection of neck node metastasis many patients currently receive unnecessary or inappropriate treatment of the neck (45, 46). Instead of direct assessment of neck node metastases, gene expression measurements of primary HNSCC tumors were used to discriminate between patients with (N+) and without (N0) lymph node metastasis. For this study, a large set primary HNSCC tumors was selected that was balanced for tumors from N0 and N+ patients. To prevent that metastasis was caused by other tumors than the ones studied here, only patients were selected who did not show previous lesions in the head and neck region and who received no treatment before surgery. To reduce the large heterogeneity between HNSCC tumors, this study focused on two sub locations with the head and neck region, oral cavity and oropharynx. By means of a reference design, primary tumor samples were compared against a common reference that consisted of a pool of RNA from all individual samples. Although this study setup resulted in gene expression measurements that are dependent on the limited available reference sample, the big advantage of this design is the relative limited number of arrays that are needed. The reference design also allows straightforward comparisons between all currently and future analyzed samples (14).

Using an unbiased supervised cross-validation procedure, a primary tumor gene expression signature was identified that was associated with presence of lymph node metastasis. The metastatic signature outperformed current clinical diagnosis of lymph node biopsies on an independent validation set (chapter 3 and ref. 47). Moreover, no false negative predictions were made, which is most important for achieving clinical relevance. Surprisingly, we noticed a decrease in predictive accuracy for samples that were stored over longer periods of time. Although this confounding effect was likely caused by degradation of frozen tumor material over time, no direct evidence for RNA degradation could be found and all samples passed quality control (29). This example illustrates the effect that a confounding variable can have

on the generated gene expression data and, if not identified, can dramatically reduce or falsify the signature outcome and performance.

The heterogeneity in gene composition of expression signatures associated with specific cancer classes is generally becoming acknowledged (intermezzo and ref. 48). Several class predictive studies have derived equally predictive and valid signatures which showed only minimal overlap in gene lists (8, 11). Although this lack in overlap could be contributed to by differences in microarray platforms, it is probably caused by the sample composition of the training and test sets that were used for identification of the signatures (49, 50). Due to redundancy in predictive genes, different sample compositions result in multiple signatures that are composed of different predictive genes but which show an identical predictive outcome (50). In the case of the HNSCC metastatic signature, the initially identified 102 predictive genes are only a subset from a larger group of metastasis associated genes (chapter 4 and ref. 51). Since multiple predictive signatures with similar predictive outcome may be practically interchangeable, this characteristic is not harmful for accurate class prediction but does pose a problem for development of a unique diagnostic tool and for protection of intellectual property. Unstable gene lists may also thwart studies aimed at elucidating the underlying biology of a unique predictive gene signature. One option to tackle gene list instability is to focus on the subset of genes that are most stably selected across multiple predictive signatures (49). However, another approach for studying the biology behind a predictive signature is not by focusing on the smallest list possible but by taking a broader view of the underlying processes within the set of predictive genes. As described in this thesis, such functional category analysis is most powerful when based on a large set of signature associated genes instead on the smallest list possible (chapter 4).

The HNSCC metastatic signature was identified using complete primary tumor sections that comprised both tumor cells and surrounding stroma and, as a result, included predictive genes from both compartments. Direct investigation of the tumor cell and tumor stroma contributions indicated that tumor samples with low tumor percentage were more difficult to predict accurately due to an overrepresentation of stromal genes that are upregulated and tumor cell genes that are downregulated in N+ tumors (chapter 6). Adjustment for this skewed selection of predictive genes improved the accuracy of the signature, especially for samples with low tumor percentage. This finding indicates that samples with low tumor percentage (<50%) should not be disregarded *a priori* for gene expression signature analysis, an assumption which was initially used to make sure that a signature is mainly based on tumor cells (8, 47). Since both tumor and stromal related gene expression contribute significantly to the HNSCC metastatic signature, targeting both the tumor cells and the tumor stroma is a rational approach for diagnosis and treatment of lymph node metastatic disease (52, 53). Moreover, this indicates that identification of an optimal cancer gene expression signature requires close examination of the tumor and stromal contribution. An approach similar to the laser micro dissection procedure described in this thesis (chapter 6) should preferably be implemented in future studies to prevent tumor percentage related confounding effects that could lead to a reduced sensitivity and specificity.

Large-scale validation study

The identified HNSCC metastatic gene expression signature outperformed the current clinical diagnosis on an independent validation set of 22 samples, indicating that the identified metastatic signature is not biased to the training samples used here but also works for additional new samples. In addition, robustness was furthermore confirmed by the fact that the metastatic signature was maintained in the lymph node metastases (chapter 5). Extrapolation of the increased accuracy on the independent samples suggests that treatment of HNSCC patients can be substantially improved by using the gene expression signature for assessment of lymph node metastasis (chapter 2 and ref. 47). Although statistically significant, validation of the HNSCC signature was performed on a relatively small independent validation set. The real value of the metastatic signature will have to be determined using a large-scale validation study (37) in which the patients are diagnosed in parallel using current techniques and using microarray gene expression profiling. Such a large-scale validation study of the HNSCC signature is currently being set up across multiple institutes. After completion of this study, it can be decided whether to implement this molecular signature for better assessment of lymph node metastasis in patients diagnosed with HNSCC.

However, before clinical implementation, the validity of the signature must be confirmed on preoperatively clinical biopsies instead of retrospective analysis of surgically removed primary tumor samples. Also, a diagnostic microarray has to be developed for easy and robust assessment of the HNSCC metastatic signature. A designated array should contain the identified 825 predictive genes in triplicate together with a set of control features. Another option is to continue using a full-genome array for diagnostics. While containing no replicates for the identified signature genes, using a full-genome array for diagnostics maintains the possibility of future adjustment of the signature and additional transcriptional research of HNSCC tumors. The work described in this thesis provides a solid basis for improved diagnosis of neck node metastasis and will hopefully lead to a more tailored therapy of cancer patients thereby reducing the number individuals who receive inaccurate or unnecessary treatment. Such studies vindicate the large investments that have been made nationally and internationally in genomics research and form an example of the many benefits that such research will undoubtedly bring about in the future.

References

1. Segal, E, et al., From signatures to models: understanding cancer using microarrays. Nat Genet, 2005. 37(6 Suppl): p. S38-45.
2. Adler, AS, et al., Genetic regulators of large-scale transcriptional signatures in cancer. Nat Genet, 2006.
3. Kallioniemi, O, Medicine: profile of a tumour. Nature, 2004. 428(6981): p. 379-382.
4. Valk, PJ, et al., Prognostically useful gene-expression profiles in acute myeloid leukemia. N Engl J Med, 2004. 350(16): p. 1617-1628.
5. Chung, CH, et al., Molecular classification of head and neck squamous cell carcinomas using patterns of gene expression. Cancer Cell, 2004. 5(5): p. 489-500.
6. Perou, CM, et al., Molecular portraits of human breast tumours. Nature, 2000. 406(6797): p. 747-752.
7. Paik, S, et al., A multigene assay to predict recurrence of tamoxifen-treated, node-negative breast cancer. N Engl J Med, 2004. 351(27): p. 2817-2826.
8. van 't Veer, LJ, et al., Gene expression profiling predicts clinical outcome of breast cancer. Nature, 2002. 415(6871): p. 530-536.
9. Ramaswamy, S, et al., A molecular signature of metastasis in primary solid tumors. Nat Genet,

2003. 33(1): p. 49-54.
10. van de Vijver, MJ, et al., A gene-expression signature as a predictor of survival in breast cancer. N Engl J Med, 2002. 347(25): p. 1999-2009.
11. Wang, Y, et al., Gene-expression profiles to predict distant metastasis of lymph-node-negative primary breast cancer. Lancet, 2005. 365(9460): p. 671-679.
12. Dave, SS, et al., Prediction of survival in follicular lymphoma based on molecular features of tumor-infiltrating immune cells. N Engl J Med, 2004. 351(21): p. 2159-2169.
13. Potter, JD, Epidemiology, cancer genetics and microarrays: making correct inferences, using appropriate designs. Trends Genet, 2003. 19(12): p. 690-695.
14. Yang, YH and Speed, T, Design issues for cDNA microarray experiments. Nat Rev Genet, 2002. 3(8): p. 579-588.
15. Simon, R, et al., Pitfalls in the use of DNA microarray data for diagnostic and prognostic classification. J Natl Cancer Inst, 2003. 95(1): p. 14-18.
16. Miller, LD, et al., Optimal gene expression analysis by microarrays. Cancer Cell, 2002. 2(5): p. 353-361.
17. Churchill, GA, Fundamentals of experimental design for cDNA microarrays. Nat Genet, 2002. 32 Suppl 2: p. 490-495.
18. Pavlidis, P, Li, Q, and Noble, WS, The effect of replication on gene expression microarray experiments. Bioinformatics, 2003. 19(13): p. 1620-1627.
19. Dobbin, K and Simon, R, Sample size determination in microarray experiments for class comparison and prognostic classification. Biostatistics, 2005. 6(1): p. 27-38.
20. Wang, SJ and Chen, JJ, Sample size for identifying differentially expressed genes in microarray experiments. J Comput Biol, 2004. 11(4): p. 714-726.
21. Pawitan, Y, et al., False discovery rate, sensitivity and sample size for microarray studies. Bioinformatics, 2005. 21(13): p. 3017-3024.
22. DeRisi, J, et al., Use of a cDNA microarray to analyse gene expression patterns in human cancer. Nat Genet, 1996. 14(4): p. 457-460.
23. Kerr, MK and Churchill, GA, Experimental design for gene expression microarrays. Biostatistics, 2001. 2(2): p. 183-201.
24. Piper, MD, et al., Reproducibility of oligonucleotide microarray transcriptome analyses. An interlaboratory comparison using chemostat cultures of Saccharomyces cerevisiae. J Biol Chem, 2002. 277(40): p. 37001-37008.
25. Puskas, LG, et al., RNA amplification results in reproducible microarray data with slight ratio bias. Biotechniques, 2002. 32(6): p. 1330-1334, 1336, 1338, 1340.
26. Dobbin, KK, et al., Characterizing dye bias in microarray experiments. Bioinformatics, 2005. 21(10): p. 2430-2437.
27. Brazma, A, et al., Minimum information about a microarray experiment (MIAME)-toward standards for microarray data. Nat Genet, 2001. 29(4): p. 365-371.
28. Bossuyt, PM, et al., Towards complete and accurate reporting of studies of diagnostic accuracy: The STARD Initiative. Ann Intern Med, 2003. 138(1): p. 40-44.
29. Tumor Analysis Best Practices Working Group, T, Expression profiling-best practices for data generation and interpretation in clinical trials. Nat Rev Genet, 2004. 5(3): p. 229-237.
30. Curwen, V, et al., The Ensembl automatic gene annotation system. Genome Res, 2004. 14(5): p. 942-950.
31. Brown, PO and Botstein, D, Exploring the new world of the genome with DNA microarrays. Nat Genet, 1999. 21(1 Suppl): p. 33-37.
32. Dudoit, S, et al., Statistical methods for identifying differentially expressed genes in replicated cDNA microarray experiments. Stat. Sinica, 2002. 12: p. 111-139.
33. Reiner, A, Yekutieli, D, and Benjamini, Y, Identifying differentially expressed genes using false discovery rate controlling procedures. Bioinformatics, 2003. 19(3): p. 368-375.
34. Storey, JD and Tibshirani, R, Statistical significance for genomewide studies. Proc Natl Acad Sci U S A, 2003. 100(16): p. 9440-9445.
35. van Bakel, H, Genome-wide analyses of copper metabolism and its regulation across species. PhD Thesis. 2005: Utrecht University, NL.
36. Ambroise, C and McLachlan, GJ, Selection bias in gene extraction on the basis of microarray gene-expression data. Proc Natl Acad Sci U S A, 2002. 99(10): p. 6562-6566.
37. Ransohoff, DF, Rules of evidence for cancer molecular-marker discovery and validation. Nat Rev Cancer, 2004. 4(4): p. 309-314.
38. Kaiser, J, Genomic medicine. African-American population biobank proposed. Science, 2003. 300(5625): p. 1485.

39. Oosterhuis, JW, Coebergh, JW, and van Veen, EB, Tumour banks: well-guarded treasures in the interest of patients. Nat Rev Cancer, 2003. 3(1): p. 73-77.
40. Koninklijke Nederlands Akademie van Wetenschappen, Multifactoriële aandoeningen in het genomics-tijdperk. 2006.
41. Sarkans, U, et al., The ArrayExpress gene expression database: a software engineering and implementation perspective. Bioinformatics, 2004.
42. Spellman, PT, et al., Design and implementation of microarray gene expression markup language (MAGE-ML). Genome Biol, 2002. 3(9): p. RESEARCH0046.
43. Edgar, R, Domrachev, M, and Lash, AE, Gene Expression Omnibus: NCBI gene expression and hybridization array data repository. Nucleic Acids Res, 2002. 30(1): p. 207-210.
44. Brazma, A, et al., ArrayExpress--a public repository for microarray gene expression data at the EBI. Nucleic Acids Res, 2003. 31(1): p. 68-71.
45. Don, DM, et al., Evaluation of cervical lymph node metastases in squamous cell carcinoma of the head and neck. Laryngoscope, 1995. 105(7 Pt 1): p. 669-674.
46. Jones, AS, et al., Occult node metastases in head and neck squamous carcinoma. Eur Arch Otorhinolaryngol, 1993. 250(8): p. 446-449.
47. Roepman, P, et al., An expression profile for diagnosis of lymph node metastases from primary head and neck squamous cell carcinomas. Nat Genet, 2005. 37(2): p. 182-186.
48. Roepman, P and Holstege, FC, Tumor profiling turmoil. Cell Cycle, 2005. 4(5): p. 659-660.
49. Michiels, S, Koscielny, S, and Hill, C, Prediction of cancer outcome with microarrays: a multiple random validation strategy. Lancet, 2005. 365(9458): p. 488-492.
50. Ein-Dor, L, et al., Outcome signature genes in breast cancer: is there a unique set? Bioinformatics, 2005. 21(2): p. 171-178.
51. Roepman, P, et al., Multiple robust signatures for detecting lymph node metastasis in head and neck cancer. Cancer Res, 2006. 66(4): p. 2361-2366.
52. Mueller, MM and Fusenig, NE, Friends or foes - bipolar effects of the tumour stroma in cancer. Nat Rev Cancer, 2004. 4(11): p. 839-849.
53. Joyce, JA, Therapeutic targeting of the tumor microenvironment. Cancer Cell, 2005. 7(6): p. 513-520.

S

Summary

Samenvatting

Summary

Head and neck squamous cell carcinoma (HNSCC) consists of a group of neoplasms that arise in the epidermis of the oral cavity and upper aerodigestive tract. HNSCC is the fifth most common malignancy worldwide and is associated with high tobacco and alcohol use. Although our knowledge about this type of cancer has increased significantly, the 5-year survival rate of patients with HNSCC has not improved over the last 20 years and remains constant at about 50%. As with most forms of cancer, treatment depends largely on the progression of the disease and relies on the use of prognostic factors. Metastasis is the leading cause of cancer-related deaths and the presence of metastases can predict the survival rate for most cancer patients. For HNSCC, development of distant metastases is greatly dependent on the presence of regional lymph node metastasis. It is therefore crucial to determine whether a patient with HNSCC has developed lymph node metastases. Based on this assessment, the most appropriate therapy can be chosen.

Due to difficulties in detecting cervical lymph node metastases reliably, many patients currently receive inappropriate or unnecessary treatment which is accompanied by severe discomfort and complications such as shoulder disability. Assessment of the absence of metastasis is most challenging, since about one-third of the clinically negative (N0) patients actually show positive neck nodes after examination of removed neck tissue. Due to the high prevalence of clinically false negative patients, many clinics therefore also treat clinically assessed N0 patients. This treatment involves removal of the neck lymph nodes that are at highest risk for metastasis, a surgical procedure which is unnecessary for the nearly two-thirds of accurately diagnosed N0 patients.

To improve the diagnosis of lymph node metastasis and to relieve a significant number of patients from unnecessary neck surgery, current diagnostic methods need to be improved or new technologies need to be implemented. The primary goal of the work described in this thesis was to investigate the use of DNA microarray gene expression profiling of the primary tumor for assessment of lymph node metastasis in patients with oral cavity or oropharynx cancer. Secondly, examination of the gene expression patterns in primary and metastatic tumors was also undertaken to improve our understanding of how metastasis develops in patients with head and neck cancer.

Following an introduction (*Chapter 1*) about HNSCC and the use of DNA microarrays for cancer research, *Chapter 2* describes a pilot study that was performed to set up and validate all necessary experimental protocols and procedures for a large-scale tumor profiling study. The finalized procedures were tested for reproducibility and a high-throughput microarray hybridization platform was set up for quick and robust analysis of a large number of tumor samples. Furthermore, the proposed reference sample experiment design and statistical analyses were validated for discriminatory power between different HNSCC samples.

To identify a gene expression signature capable of predicting the presence of lymph node metastasis, 82 primary HNSCC tumor samples were analyzed, 45 from patients with lymph

node metastatic disease (N+) and 37 from patients known to be lymph node negative (N0). Using a supervised classification procedure, a set of 102 genes was identified that showed optimal predictive accuracy (c*hapter 3*). The accuracy was validated on 22 independent samples and the metastatic status of 19 samples was accurately predicted. The predictive gene signature outperformed the current clinical diagnosis of lymph node biopsy in this set of patients. Most importantly for clinical relevance, no false negative predictions were made in this independent test of the signature. These results strongly indicate that treatment of HNSCC patients can substantially be improved by applying the DNA microarray predictor and forms the basis for a large-scale multi-center trial that is currently underway.

The results described in c*hapter 3* are an example of the potential that gene expression profiling studies have for clinical application. Despite these benefits, genome-wide expression studies have come under severe criticism with respect to the lack in gene composition overlap between different expression signatures that set out to characterize identical sample properties. In the *intermezzo*, it is explained that while proper care does need to be taken in setting up and validating such studies, the nature of the criticism on different gene compositions is largely misplaced. This is further exemplified in c*hapter 4* where the stability in gene composition of the identified HNSCC metastatic signature was investigated thoroughly. Using a multiple training approach, numerous predictive gene sets were identified, which all differed in gene composition but showed identical performance. As predicted in the *intermezzo*, the initially identified 102 signature genes are a subset of a larger set of 825 metastasis associated genes from which multiple predictive signatures can be generated. While no specific subset is shown to be essential for accurate prediction, some genes are more suited for inclusion in signatures composed of a minimal number of genes. The lack of overlap between similarly predictive signatures can therefore be explained by the fact that there are more predictive genes than the number strictly required to design an accurate predictor and that these genes are interchangeable.

The function of the genes whose specific expression patterns are associated with the presence or absence of metastasis offers unique insights into the molecular processes that take place upon metastasis (*Chapter 3* and *4*). Two interesting functional categories within the set of predictive genes are binding to the extracellular matrix and protease activity for degradation of the extracellular matrix. Both categories are up-regulated in tumors that metastasize to the lymph nodes and support the theory that tumor cells gain mobility by an interplay between anchoring to the extracellular matrix and degradation of this matrix.

Comparison of whole genome expression profiles from primary tumors with their corresponding lymph node metastasis samples (*chapter 5*) sheds further light on oncogenesis. Gene expression patterns in lymph node metastases were most similar to the primary tumor from which they originate. Remarkably, both general and metastasis specific primary tumor gene expression patterns are maintained upon spread to the lymph nodes. These findings agree with the concept that disseminated cancer cells can alter their surrounding tissue into a metastatic microenvironment and underscore the importance of the metastatic gene expression signature early during and across multiple steps of cancer development. Apparently, disseminated

primary tumor cells do not need to undergo additional developmental changes for survival and proliferation in metastatic sites. This supports the theory that metastatic properties are acquired early during tumorigenesis and sustained throughout cancer progression.

Traditionally, cancer research focuses mainly on processes within tumor cells, such as oncogenes and tumor suppressor genes. *Chapter 6* describes work aimed at investigating the contribution of the surrounding, stromal cells towards the predictive signature. Generally, only primary tumor sections with at least 50% tumor cells are used for gene expression studies. Despite the fact that many of the signature genes are expressed in the stroma, metastasis of primary tumor samples with lower amounts of tumor cells were more difficult to predict accurately. Laser capture microdissection was used to generate samples with varying ratios of tumor versus stromal cells. It is shown that the decreased predictive accuracy for samples with lower tumor cell percentage is caused by an overrepresentation within the predictive signature of stromal genes that are upregulated in metastatic tumors and tumor cell genes that are downregulated in metastatic tumors. Adjustments for this skewed signature composition improved the accuracy of the signature and, importantly, makes the signature potentially useful for accurate prediction of tumor samples with less than 50% tumor cells, a subset that has previously been considered unsuited for expression profiling.

Finally, *chapter 7* discusses some important issues that need to be considered for optimal design of DNA microarray expression profiling studies in general and for implementation of diagnostic gene expression signatures in the clinic. This is worth pursuing for the HNSSC metastasis predictive signature presented here. Extrapolation from the independent validation set indicates that applying the signature would substantially improve the treatment of patients with head and neck cancer.

Samenvatting (ook voor niet-vakgenoten)

Het hoofd-halsplaveiselcelcarcinoom (Engels: head and neck squamous cell carcinoma, HNSCC) bestaat uit een groep tumoren die ontstaat in het slijmvlies van de mondholte en de keel. Wereldwijd is HNSCC één van de meest voorkomende vormen van kanker. Deze tumor ontstaat voornamelijk bij personen die veel roken en/of veel alcohol consumeren. Hoewel de kennis over deze aandoening aanzienlijk is toegenomen, zijn de overlevingskansen voor patiënten met HNSCC de afgelopen 20 jaar niet substantieel verbeterd en overlijdt ongeveer de helft van de patiënten binnen 5 jaar nadat bij hen de diagnose hoofd-hals kanker is gesteld. De behandeling van patiënten met HNSCC is afhankelijk van de uitgebreidheid van de ziekte en het bepalen hiervan is van essentieel belang voor een optimale behandeling.

De aanwezigheid van uitzaaiingen (metastasen) is een belangrijke doodsoorzaak bij kankerpatiënten en het al dan niet aanwezig zijn hiervan is de belangrijkste voorspellende factor voor de overlevingkans van een patiënt. Voor een optimale behandeling is het daarom van groot belang om een juiste diagnose ten aanzien van de aanwezigheid van halslymfeklier metastasen te stellen. Ook neemt de kans op de ontwikkeling van HNSCC metastasen op afstand, in bijvoorbeeld de longen en de lever, toe naarmate er in de hals meer tumorpositieve lymfeklieren aanwezig zijn.

Met de huidige diagnostiek wordt bij één op de drie patiënten ten onrechte vastgesteld dat er géén halslymfeklier metastasen (N0 patiënten) aanwezig zijn terwijl deze patiënten wel halsklier metastasen hebben (N+ patiënten). Vanwege dit grote aantal fout-negatieve diagnosen, geven veel klinieken de voorkeur aan operatieve behandeling van álle N0 patiënten. Deze operatieve ingreep, waarbij een deel van de halslymfeklieren verwijderd wordt, is overbodig voor bijna twee op de drie N0 patiënten. Zodoende ondergaat een groot gedeelte van de patiënten een met pijn en ongemak gepaard gaande onnodige operatie aan de nek. De hieruit voortvloeiende vermindering van de schouderfunctie, heeft ernstige gevolgen voor het dagelijks functioneren.

Om het aantal patiënten dat onnodig deze behandeling ondergaat in de toekomst te verminderen, moeten de huidige diagnostische methoden verbeterd worden of moeten nieuwe nauwkeurigere technieken worden ontwikkeld zodat beter onderscheid gemaakt kan worden tussen N0 en N+ patiënten. Het hoofddoel van het onderzoek dat beschreven is in dit proefschrift was het onderzoeken van de potentiële waarde van de nieuwe DNA microarray technologie voor het verbeteren van de huidige diagnostiek. Met DNA microarrays is het mogelijk om de activiteit van duizenden genen in een bepaald celtype of weefsel tegelijkertijd te meten. Met deze techniek kan gezocht worden naar groepen genen die verschillen in activiteit (genexpressie) tussen wel en niet-uitgezaaide tumoren. Zo kan een genexpressie profiel geïdentificeerd worden dat beide type tumoren kan onderscheiden. Tevens geven de verschillen in genexpressie ook meer inzicht in de cellulaire en moleculaire processen die leiden tot het ontstaan van uitzaaiingen.

Na een algemene introductie (*hoofdstuk 1*) over de ontwikkeling van hoofd-hals kanker en

het gebruik van DNA microarrays voor kankeronderzoek, beschrijft *hoofdstuk 2* het opzetten van alle benodigde protocollen en procedures voor het analyseren van tumor samples met DNA microarrays. Tevens wordt de opzet van een 'high-throughput' microarray systeem beschreven waarmee binnen een kort tijdbestek veel tumor samples geanalyseerd kunnen worden.

In *hoofdstuk 3* werden 82 primaire tumoren gebruikt, 45 van N+ patiënten en 37 van N0 patiënten, om een genexpressie profiel te identificeren dat in staat is om de halslymfeklier status (N0 of N+) van patiënten met HNSCC te voorspellen. Een expressie signatuur bestaande uit een set van 102 genen bleek de onderzochte groep patiënten optimaal te kunnen splitsen naar aanwezigheid van halslymfeklier metastasen. Het genexpressie profiel is bovendien gevalideerd op een onafhankelijke set tumoren. Binnen deze validatieset werden 86% van de tumoren goed geclassificeerd met dit genexpressie profiel tegenover 68% met de huidige klinische diagnose. Bovendien werd geen enkele fout-negatieve voorspelling gemaakt. Deze resultaten duiden erop dat de diagnose en dus de behandeling van patiënten met HNSCC sterk verbeterd zou kunnen worden. Dit resultaat vormt dan ook de basis van een geplande grote prospectieve studie waaraan meerdere ziekenhuizen binnen Nederland zullen gaan deelnemen.

Ondanks de uitgebreide toepassingsmogelijkheden van DNA microarrays voor gebruik in de kliniek, hebben microarray studies recentelijk veel kritiek ontvangen. De meeste kritiek betrof de geringe overeenkomsten tussen genexpressieprofielen die gevonden zijn in vergelijkbare studies evenals dat ook bínnen studies verschillende profielen gevonden kunnen worden die een zelfde voorspellende waarde hebben. Hoewel het plaatsen van kanttekeningen bij nieuwe technologieën van belang voor degelijk wetenschappelijk onderzoek wordt in het *intermezzo* uitgelegd waarom deze recente kritiek op microarray studies grotendeels onrechtvaardig en misplaatst is. Dit wordt verder uiteengezet in *hoofdstuk 4* waarin de stabiliteit van de selectie van genen voor het HNSCC metastase genexpressie profiel wordt onderzocht. De oorspronkelijke set van 102 voorspellende genen blijkt een subset te zijn van 825 genen welke allen geassocieerd zijn met de aanwezigheid van halsklier uitzaaiingen. Uit deze grotere groep genen kunnen meerdere voorspellende profielen worden gemaakt die elk een vergelijkbare nauwkeurigheid hebben. Hoewel sommige genen belangrijker zijn en een grotere voorspellende waarde hebben, blijkt geen enkele specifieke groep genen essentieel voor de diagnose naar uitzaaiingen in de onderzochte groep patiënten. Het gebrek aan overeenkomsten tussen verschillende genexpressie profielen kan dus verklaard worden doordat er meer voorspellende genen bestaan dan strikt noodzakelijk voor het maken van een genexpressie profiel. Hierdoor zijn de genen onderling uitwisselbaar zonder dat dit invloed heeft op de voorspellende waarde van het profiel en kunnen dus verschillende combinaties van genen tot waardevolle genexpressie profielen leiden.

Naast eventuele toekomstige verbetering van de diagnose van patiënten met HNSCC, biedt het onderzochte genexpressie profiel inzicht in moleculaire processen die een rol spelen in de ontwikkeling van uitzaaiingen (*hoofdstuk* 3 en 4). Twee interessante processen die naar voren zijn gekomen uit het genexpressie profiel is de binding van cellen aan de omringende extracellulaire matrix en de specifieke afbraak van deze matrix door proteasen. Activatie van

beide processen in uitgezaaide tumoren zou erop kunnen duiden dat tumor cellen zich actief kunnen verplaatsen door het omringende weefsel door middel van een samenspel tussen binding aan en afbraak van de extracellulaire matrix.

In *hoofdstuk 5* is het genexpressie profiel van de primaire tumor vergeleken met het profiel van de lymfeklier uitzaaiingen en het blijkt dat deze uitzaaiingen in sterke mate hetzelfde profiel hebben als de primaire tumor. Omdat het expressieprofiel zowel genactiviteit in de tumorcellen als in het omgevende stroma omvat is deze bevinding in overeenkomst met de theorie dat uitgezaaide tumor cellen het omringende weefsel kunnen veranderen in een 'metastase ondersteunende' omgeving die sterk lijkt op de situatie in de primaire tumor. Dit resultaat bevestigt de belangrijke rol van het gevonden HNSCC genexpressie profiel voor de ontwikkeling van uitzaaiingen, zowel voor processen in de primaire tumor alsmede voor de verdere ontwikkeling van uitzaaiingen in de halslymfeklieren. Blijkbaar heeft een cel van een uitzaaiende primaire tumor cel geen extra veranderingen in genexpressie meer nodig om zich te nestelen in de halslymfeklieren en uit te groeien tot een uitzaaiing.

Traditioneel richt kanker onderzoek zich voornamelijk op processen in tumorcellen. Over het algemeen worden voor microarray studies dan ook alleen samples gebruikt die voor tenminste 50% bestaan uit tumor cellen. Het wordt echter steeds duidelijker dat ook de stromale componenten van een tumor, zoals bindweefselcellen en cellen van het immuun systeem, een grote rol spelen bij de ontwikkeling van kanker. In *hoofdstuk 6* is de specifieke rol van deze stroma cellen in het HNSCC metastase profiel onderzocht. Tevens hebben we het genexpressie profiel aangepast zodat het ook potentieel geschikt is voor diagnose van samples die relatief veel stroma bevatten. Ondanks dat een aanzienlijk deel van de genen van het metastase genexpressie profiel voornamelijk tot expressie komt in het stroma, zijn samples met een laag tumor percentage moeilijker te classificeren met dit profiel. Met behulp van laser microdissectie werden samples gegenereerd met verschillende tumor percentages. en Hiermee kon worden aangetoond dat de verminderde nauwkeurigheid van het expressie profiel voor samples met een lager tumorpercentage wordt veroorzaakt door een onevenredige verdeling van tumor en stroma gerelateerde genactiviteit. In uitzaaiende tumoren worden 'tumor-genen' voornamelijk gedeactiveerd en worden 'stroma-genen' exclusief geactiveerd. Het corrigeren van een onevenredige verdeling van genen leidde tot een verbetering van het voorspellend genexpressie profiel, met name voor samples met een laag tumor percentage. Dit resultaat toont aan dat microarray genexpressie analyse ook geschikt gemaakt kan worden voor samples met minder dan 50% tumor cellen, waardoor deze nieuwe techniek hopelijk toegepast kan worden op een grotere groep patiënten.

Als laatste worden in *hoofdstuk 7* enkele aandachtspunten besproken die van groot belang zijn voor het optimaal identificeren en valideren van microarrays genexpressie profielen in het algemeen, en voor diagnostische profielen in het bijzonder. De resultaten beschreven in dit proefschrift lijken een sterke verbetering van de diagnose van patiënten met hoofd-halstumoren door DNA microarray analyse mogelijk te maken. De toepasbaarheid van dit genexpressie profiel in de kliniek zal gevalideerd worden in een grote prospectieve studie die binnenkort zal worden opgezet door meerdere onderzoeksinstituten en ziekenhuizen. De verwachting is dat toekomstige implementatie van het gevonden genexpressie profiel in de

Dankwoord

Curriculum vitae

List of publications

Dankwoord

Zoals het geval is voor de meeste proefschriften wordt na het bekijken van het omslag vluchtig doorgebladerd naar schijnbaar het meest belangrijkste deel van het boekje: het dankwoord. Waarschijnlijk bent u dan ook één van de weinigen die wel de tijd heeft genomen om in ieder geval de samenvatting door te nemen. (of toch niet?) Dit bevestigt dan ook de uitspraak die ik een tijdje terug hoorde: "een proefschrift is er om geschreven te worden en niet om te lezen". Maar aangezien de komende twee pagina's door de meesten wel gelezen wordt is dit de juiste plaats om iedereen te bedanken die bijgedragen heeft aan het tot stand komen van dit proefschrift.

Als eerste wil ik mijn twee promotoren bedanken zonder wie dit promotieonderzoek nooit tot stand was gekomen, Frank Holstege en Piet Slootweg. Frank, erg bedankt dat je vanaf het begin af aan veel vertouwen in me hebt gesteld voor het uitvoeren van een belangrijk onderzoeksproject binnen jou groep. Piet, erg bedankt voor alle tijd en moeite die je gestoken hebt om mij wegwijs te maken in alle pathologisch en klinisch belangrijke zaken. Beide erg bedankt voor het opzetten van dit project. Ook wil ik Peter van de Vliet bedanken voor het mogelijk maken van dit project binnen de afdeling Fysiologische chemie.

De collega's waarmee ik het meeste te maken heb gehad zijn natuurlijk mijn (voormalige) kamergenoten, Nienke, Jeroen, Ellen, Alike, Maike, Sake en Tineke. Het was in 'onze' kamer vaak een gezellige drukte was (ja, die drukte kwam dan ook met name door mij…). Nienke, naast dat je altijd een spontane gezellige collega bent geweest heb ik je hulp aan mijn project erg op prijs gesteld. Hopelijk krijg je het in Lelystad net zo naar je zin als bij ons. Jeroen, erg bedankt voor al je hulp, discussie en gezelligheid die we de afgelopen 4 jaar gedeeld hebben, en nu ook ik klaar ben met het schrijven van mijn proefschrift weet ik wat je bedoelde met "eindelijk af". Ellen, thank you for your company during the year you were working in our group. Good luck with your further scientific career in Norway. Alike, erg bedankt voor jou werk dat je in totaal 14 maanden hebt uitgevoerd voor mij (wat een verdubbeling van de tumor groep betekende) wat (hopelijk) geleid heeft tot een wetenschappelijk artikel. Naast dat je goed praktisch werk hebt verricht was je ook een zeer gezellig en sociale collega. Veel succes met het voltooien van je studie. Maike, ook jij was een gezellige (studenten-)collega en ondanks dat je zelf vond dat je afstudeerproject wat tegenviel hoop ik wel dat je een plezierige tijd hebt gehad. Sake, de komende tijd zal hopelijk alle 'tam-tam' van mijn project overgeheveld wordt naar jou. Gisteren hoorde ik dat jij samen met Philip in het UMC koor bent beland en dat jullie nu druk aan het oefenen zijn voor een kerstconcert. Ik verwacht dus op mijn promotiefeest een generale repetitie! Tineke, als student bij Sake wens ik ook jou veel succes met je afstudeerproject en het vervolg van je studie.

Een belangrijk deel van mijn promotieonderzoek heeft in het lab plaatsgevonden. Als eerste wil ik dan ook de pioniers binnen ons lab, Dik, Nynke en Theo bedanken voor het degelijk opzetten van het lab en mij wegwijs maken toen ik hier begon. Dik, zonder jou was dit project waarschijnlijk nooit echt van de grond gekomen. Door het kritische optimaliseren van de productie van DNA microarrays heb ik de afgelopen 4 jaar zo'n 800 microarrays met succes kunnen analyseren. Nynke en Theo, onze Friezen, ook al heb ik voor mijn praktisch

labwerk weinig (zeg maar geen) dezelfde technieken gebruikt wil ik jullie toch erg bedanken voor het goed organiseren van het lab en natuurlijk ook voor alle gezellige koffie-uurtjes en andere nevenactiviteiten. Theo, veel succes verder in Groningen en Nynke veel succes in je verdere wetenschappelijke carrière. Tony, over jou veelzijdigheid binnen het lab ben ik erg onder de indruk. Veel succes met het opzetten van nieuwe technieken, en natuurlijk helemaal met je golf-cursus. Joris, de mass-spec goeroe van ons lab, veel succes binnen onze groep en hopelijk krijg je het net zo naar de zin als ik het heb gehad. Jean-Christophe, I wish you good luck with your own research group in Marseille. Eveline, Esther, Geert, Koen, Maike, Maurice en Linda, ook jullie bedankt voor alle levendigheid binnen de groep. Zoals al genoemd heeft de microarray faciliteit een grote rol gespeeld in het succes van mijn promotieonderzoek. Joop, Marian en Diana ook erg bedankt. Ik ben er van overtuigd dat met jullie inzet de kwaliteit van onze arrays steeds beter zal worden.

Patrick, Philip, Harm, Erik, Thessa en (wederom) Marian, erg bedankt voor jullie hulp met alle data analyse en voor mij enthousiast te maken voor dit vakgebied! Philip, veel succes met jou komende promotie en Harm veel succes in Toronto. And Marijana, as I'm now taking about bioinformatics I'd like to thank you for all the joy and energy you brought into our lab. Since we both decided to continue our careers in the field of bioinformatics, I'm sure we will meet again. Verder wil ik ook Arnaud en Yumas bedanken voor het in het gareel houden van alle computers en servers. Nu ik als laatste van de eerste lichting van AIOs bij Frank mijn proefschrift af heb, wil ik graag het stokje doorgeven aan de twee nieuwe AIO binnen onze groep, Loes en Eva. Both good luck with your PhDs and keep up the good work.

Naast de collega's binnen onze eigen afdeling, inclusief de mensen 'achter de schermen', Mirjan, Lilian, Marojeine, Marjoleine, Kees en Marcel, en iedereen van de 3e verdieping die mij geholpen heeft, wil ik ook graag enkele mensen bij de afdeling pathologie bedanken voor hun medewerking aan dit project. Alain, erg bedankt voor je hulp sinds Piet naar Nijmegen is vertrokken. Marina en Sabrina bedankt voor het selecteren en uitzoeken van de tumor samples. Erica en Roel erg bedankt voor het helpen opzetten van de laser microdissectie procedure. Lodewyk en Marcel erg bedankt voor de eerste belangrijke data analyse.

Pap, Mam, (schoon)familieleden, vrienden ('Wageningse biologen' en Brabanders), teamgenoten en kennissen, jullie ook allemaal erg bedankt voor jullie steun en interesse gedurende de afgelopen 4½ jaar. Door jullie ben ik op de hoogte gebleven van het leven buiten het lab en kon ik de nodige afleiding vinden van mijn werk. Erik en Martijn, erg bedankt dat jullie als paranimf me willen bijstaan tijdens mijn promotie. Erik, als tweelingbroer ben ik benieuwd wat jij van de hele academische 'poppenkast' vindt en Martijn, goede vriend en mede AIO 'slachtoffer' binnen de biologen-groep, hopelijk krijg je alvast een goede indruk van wat jou in de nabije toekomst ook te wachten staat in Amsterdam aan de UvA.

Suzanne, door al jou steun en hulp de afgelopen jaren is mijn promotieonderzoek soepeler verlopen dan dat ik ooit had verwacht. Erg bedankt voor al jou steun in moeilijke tijden maar ook voor het delen van de vreugde wanneer het goed ging. Nu mijn promotie bijna achter de rug is, kunnen we ons gaan voorbereiden op jou promotie en op onze nieuwe banen, waarna we een begin kunnen gaan maken aan de rest van ons leven samen. Ik hou van jou.

Curriculum vitae

Paul Roepman werd geboren op 18 augustus 1979 te Oosterhout. Na het halen van zijn eindexamen VWO atheneum aan het Cambreurcollege te Dongen begon hij met de studie Biologie aan de toenmalige Landbouw Universiteit Wageningen waar hij in 1998 *cum laude* zijn propedeuse behaalde. Binnen de doctoraal opleiding Biologie, met als specialisatie cel- en moleculaire biologie, vond zijn eerste afstudeerproject plaats in 2000 bij de vakgroep Moleculaire Biologie onder beleiding van dr. ir. Rene Geurts. Het hoofddoel van dit project was het genetisch lokaliseren van het *hcl*-gen (root hair curling) dat betrokken is bij de vorming van wortelknolletjes van de plant *Medicago truncatula* (rolklaver). Voor zijn stage verhuisde hij in 2001 voor 7 maanden naar Minneapolis-St.Paul in de Verenigde Staten waar hij bij het Department of Plant Biology aan de University of Minnesota, onder leiding van prof. dr. Kate VandenBosch, werkte aan het opzetten van een DNA microarray platform voor het analyzeren van genoom-brede genexpressie van *Medicago truncatula*.

Terug in Nederland vond zijn tweede afstudeerproject plaats binnen het departement Biomolecular Sciences van TNO Kwaliteit van Leven, te Zeist, onder begeleiding van dr. ir. Marjan van Erk. Hier werkte hij aan het analyseren van DNA microarray data voor het onderzoeken van de beschermende effecten van de flavenoide quercetine voor colon kanker. Op 24 juni 2002 studeerde hij *cum laude* af aan de Wageningen Universiteit en begon in september 2002 met zijn promotieonderzoek aan het Universitair Medisch Centrum Utrecht bij de afdeling Fysiologische Chemie in samenwerking met de afdeling Pathologie. De resulaten van het promotieonderzoek, gedaan in de periode van september 2002 tot september 2006 onder beleiding van prof. dr. Frank Holstege en prof. dr. Piet Slootweg, zijn beschreven in dit proefschrift.

List of publications

Roepman P, Wessels LFA, Kettelarij N, Kemmeren P, Miles AJ, Lijnzaad P, Tilanus MGJ, Koole R, Hordijk GJ, Vliet van der PC, Reinders MJT, Slootweg PJ, Holstege FCP. An expression profile for diagnosis of lymph node metastases from primary head and neck squamous cell carcinomas. *Nat. Genet.* 2005 Feb; **37** (2): 182-186

Roepman P, Kemmeren P, Wessels LFA, Slootweg PJ and Holstege FCP. Multiple robust signatures for detecting lymph node metastasis in head and neck cancer. *Cancer Res.* 2006 Feb; **66** (4): 2361-2366

Roepman P, and Holstege FCP. Tumor profiling turmoil. *Cell Cycle.* 2005 May; 4 (5): 659-660

Slootweg PJ, **Roepman P**, Takes R, Holstege FCP. Genexpressieprofielen en halskliermetastasen bij hoofd-halsplaveiselcelcarcinoom, *Nederlands Tijdschrift voor Oncologie*. 2006 Apr; **3** (2): 66-72

Roepman P, Jager de A, Groot Koerkamp MJA, Kummer JA, Slootweg PJ and Holstege FCP. Maintenance of head and neck gene expression profiles upon lymph node metastasis. *Cancer Res.* 2006, in press

Roepman P. Koning de E, Leenen van D, Kummer JA, Weger de RA, Slootweg PJ and Holstege FCP. Dissection of a metastasis expression signature into stromal and tumor cell components for improved predictive accuracy and sample scope. *Submitted*

van Erk MJ, **Roepman P**, van der Lende TR, Stierum RH, Aarts JM, van Bladeren PJ, and van Ommen B. Integrated assessment by multiple gene expression analysis of quercetin bioactivity on anticancer-related mechanisms in colon cancer cells in vitro. *Eur J. Nutr.* 2005 Mar; **44** (3):143-56.

A

Appendix

Appendix

Appendix Table 4.1 is available online and can be downloaded via:
http://www.genomics.med.uu.nl/publications/pr/hnscc/data/Table2.xls

Appendix Table 3.1
Clinical and histological parameters of the tumor collection

Characteristic	training set		validation set	
Sex – no. (%)				
Male	45	(55%)	15	(68%)
Female	37	(45%)	7	(32%)
Location - no. (%)				
oral cavity	67	(82%)	20	(91%)
oropharynx	15	(18%)	2	(9%)
Age group at initial diagnosis – no. (%)				
<50 yr	6	(7%)	1	(5%)
50-60 yr	36	(44%)	5	(23%)
60-70 yr	25	(30%)	12	(54%)
≥70 yr	15	(18%)	4	(18%)
Age median	59		64	
Age range	38 - 87		42 - 83	
Year of initial diagnosis – no. (%)				
1996 - 1997	38	(46%)	0	(0%)
1998 - 1999	32	(39%)	1	(5%)
2000 - 2001	12	(15%)	21	(95%)
Primary tumor size – no. (%)				
Maximal diameter (cm)				
0 - 2.5	24	(29%)	9	(41%)
2.5 - 5.0	40	(49%)	9	(41%)
≥5.0	18	(22%)	4	(18%)
Infiltrative (mm)				
0 - 10	23	(23%)	7	(32%)
10 - 20	40	(40%)	8	(36%)
≥20	19	(19%)	7	(32%)
Tumor-% - no. (%)				
50-70	38	(46%)	4	(18%)
70-90	37	(45%)	10	(46%)
≥90	7	(9%)	8	(36%)
Tumor-% median	*70*		*80*	
Tumor-% range	*68*		*77*	
Clinical N-status classification (pre-operatively) – no. (%)				
N0	45	(55%)	15	(68%)
N+	37	(45%)	7	(32%)
Histological N-status classification (post-operatively) - no (%)				
N0	37	(45%)	12	(55%)
N+	45	(55%)	10	(45%)

Appendix Table 3.2
Clinical and histological parameters of individual patients

Training set
Patients are ordered according to the ranking in Fig. 3.2 A

Tumor	M/F	Year	Location	Clin	Hist	Sign	XRT
97-03434	F	1997	oropharynx	N0	N0	N0	yes
97-19374	F	1997	oral cavity	N0	N0	N0	no
98-07302	M	1998	oral cavity	N0	N0	N0	no
97-17037	M	1997	oral cavity	N0	N0	N0	yes
00-06316	F	2000	oral cavity	N0	N0	N0	no
98-05544	M	1998	oral cavity	N0	N0	N0	yes
97-06609	M	1997	oral cavity	N0	N+	N0	no
98-20741	F	1998	oral cavity	N0	N+	N0	yes
96-16684	F	1996	oral cavity	N+	N0	N0	yes
97-01621	F	1997	oropharynx	N+	N0	N0	no
97-22745	M	1997	oral cavity	N0	N0	N0	no
97-19712	F	1997	oral cavity	N0	N0	N0	no
96-18035	M	1996	oral cavity	N0	N0	N0	yes
00-02976	M	2000	oral cavity	N0	N0	N0	yes
98-14584	M	1998	oral cavity	N0	N0	N0	no
98-05095	M	1998	oral cavity	N0	N0	N0	yes
97-07915	F	1997	oral cavity	N0	N0	N0	yes
98-02073	F	1998	oral cavity	N0	N0	N0	no
97-14891	M	1997	oral cavity	N+	N+	N0	yes
98-22487	F	1998	oral cavity	N0	N+	N0	yes
98-08714	F	1998	oral cavity	N0	N0	N0	yes
96-19792	M	1996	oral cavity	N0	N+	N0	yes
98-06781	M	1998	oral cavity	N0	N0	N0	yes
96-19320	M	1996	oral cavity	N0	N+	N0	no
98-07751	F	1998	oral cavity	N0	N0	N0	no
97-02160	M	1997	oral cavity	N+	N0	N0	no
00-07858	M	2000	oropharynx	N+	N0	N0	yes
98-08979	M	1998	oral cavity	N+	N+	N0	yes
98-01095	F	1998	oral cavity	N0	N0	N0	no
97-18034	M	1997	oral cavity	N0	N0	N0	no
96-15250	M	1996	oral cavity	N0	N+	N0	yes
97-11093	M	1997	oral cavity	N+	N0	N0	yes
96-01268	F	1996	oral cavity	N0	N+	N+	yes
99-10495	F	1999	oral cavity	N0	N+	N+	no
97-21024	M	1997	oropharynx	N+	N+	N+	yes
00-06477	F	2000	oral cavity	N0	N0	N+	no
98-02651	F	1998	oral cavity	N+	N+	N+	yes
96-20218	M	1996	oral cavity	N+	N+	N+	yes
99-20272	F	1999	oral cavity	N+	N+	N+	yes
96-15806	F	1996	oral cavity	N0	N+	N+	yes
96-14125	F	1996	oral cavity	N0	N0	N+	no

Tumor	M/F	Year	Location	Clin	Hist	Sign	XRT
97-22395	M	1997	oral cavity	N+	N+	N+	yes
98-13755	F	1998	oral cavity	N+	N+	N+	yes
96-05586	F	1996	oral cavity	N+	N+	N+	yes
00-09251	F	2000	oral cavity	N+	N+	N+	yes
98-03374	F	1998	oropharynx	N+	N+	N+	yes
99-19057	F	1999	oropharynx	N0	N+	N+	yes
97-21657	F	1997	oral cavity	N+	N+	N+	yes
98-16925	M	1998	oral cavity	N+	N+	N+	yes
96-16887	F	1996	oral cavity	N0	N0	N+	no
96-17252	M	1996	oral cavity	N0	N0	N+	yes
98-10392	M	1998	oropharynx	N+	N+	N+	yes
97-11336	F	1997	oral cavity	N0	N0	N+	yes
99-20368	M	1999	oropharynx	N+	N+	N+	yes
98-13098	F	1998	oral cavity	N0	N0	N+	yes
98-14727	M	1998	oral cavity	N+	N+	N+	no
96-01054	F	1996	oral cavity	N+	N+	N+	yes
00-04428	F	2000	oropharynx	N+	N+	N+	yes
00-10305	F	2000	oral cavity	N+	N+	N+	yes
97-17905	M	1997	oral cavity	N+	N0	N+	yes
98-07499	F	1998	oropharynx	N+	N+	N+	yes
97-19866	M	1997	oropharynx	N+	N+	N+	yes
99-18862	M	1999	oral cavity	N+	N+	N+	yes
97-19014	M	1997	oral cavity	N0	N0	N+	yes
96-19491	M	1996	oropharynx	N0	N0	N+	yes
99-21712	M	1999	oral cavity	N0	N+	N+	yes
00-01713	M	2000	oropharynx	N+	N+	N+	yes
97-07298	M	1997	oral cavity	N0	N0	N+	yes
00-07596	M	2000	oral cavity	N0	N+	N+	yes
00-11195	M	2000	oral cavity	N0	N+	N+	yes
00-03459	F	2000	oral cavity	N0	N+	N+	yes
98-10136	M	1998	oral cavity	N0	N0	N+	yes
97-21995	M	1997	oropharynx	N+	N+	N+	yes
99-20557	F	1999	oral cavity	N0	N+	N+	yes
98-14182	M	1998	oral cavity	N+	N+	N+	yes
98-03124	M	1998	oral cavity	N+	N+	N+	yes
96-15039	M	1996	oral cavity	N+	N0	N+	no
98-09426	M	1998	oral cavity	N+	N+	N+	yes
97-22248	M	1997	oral cavity	N+	N+	N+	yes
00-00142	F	2000	oral cavity	N+	N+	N+	no
98-04323	M	1998	oropharynx	N+	N+	N+	yes
96-09293	F	1996	oral cavity	N0	N0	N+	no

year, year of initial diagnosis
Clin, clinical assessment (pre-operative)
Hist, histological assessment (post-operative)
Sign, assessment using the predictive sgnature
XRT, post-operative radiation therapy

Validation set

Patients are ordered according to the ranking in Fig. 3.2 C

Tumor	M/F	Year	Location	Clin	Hist	Sign	XRT
00-14673	F	2000	oropharynx	N+	N0	N0	yes
00-06216	F	2000	oral cavity	N0	N0	N0	no
00-13420	M	2000	oral cavity	N0	N0	N0	yes
00-14235	M	2000	oral cavity	N0	N0	N0	no
01-04383	F	2001	oral cavity	N+	N0	N0	yes
00-16834	M	2000	oral cavity	N0	N0	N0	yes
01-00605	M	2001	oral cavity	N0	N0	N0	yes
01-01713	F	2001	oral cavity	N0	N0	N0	no
00-11843	F	2000	oral cavity	N0	N0	N0	yes
00-12610	M	2000	oral cavity	N0	N+	N+	no
00-15451	M	2000	oral cavity	N0	N+	N+	yes
00-19274	M	2000	oral cavity	N0	N+	N+	yes
00-01958	M	2000	oral cavity	N0	N0	N+	yes
00-13232	M	2000	oral cavity	N+	N+	N+	no
00-01044	M	2000	oral cavity	N+	N+	N+	yes
00-00772	M	2000	oral cavity	N0	N+	N+	no
01-02275	M	2001	oral cavity	N0	N0	N+	yes
98-13562	M	1998	oropharynx	N+	N+	N+	yes
00-20731	F	2000	oral cavity	N0	N0	N+	yes
00-02445	F	2000	oral cavity	N+	N+	N+	yes
00-02909	M	2000	oral cavity	N0	N+	N+	no
00-02247	M	2000	oral cavity	N+	N+	N+	yes

year, year of initial diagnosis
Clin, clinical assessment (pre-operative)
Hist, histological assessment (post-operative)
Sign, assessment using the predictive sgnature
XRT, post-operative radiation therapy

Appendix Table 3.3

Complete list of the 102 HNSCC predictor genes

Gene	GenBank ID	Gene name	N+ corr
FTH1	NM_002032	ferritin, heavy polypeptide 1	0.726
COL5A1	NM_000093	COL5A1 protein (collagen 5 type A1 like)	0.627
NCOR2	NM_006312	Nuclear receptor co-repressor 2	0.617
P4HA1	NM_000917	proline 4-hydroxylase alpha polypeptide I	0.572
TNFAIP3	NM_006290	tumour necrosis factor, alpha-induced protein 3	0.536
PLAU	NM_002658	urokinase plasminogen activator (uPA)	0.535
COL5A3	NM_015719	Collagen, type V, alpha 3	0.521
SPOCK	NM_004598	Sparc/osteonectin, cwcv and kazal-like domains proteoglycan (testican)	0.500
FAP	NM_004460	fibroblast activation protein, alpha	0.498
ADAM12	NM_003474	a disintegrin and metalloproteinase domain 12 (meltrin alpha)	0.482
TPM2	NM_003289	tropomyosin 2 (beta)	0.470
MICAL2	NM_014632	flavoprotein oxidoreductase MICAL2	0.459
D2S448	XM_056455	D2S448 (Melanoma associated gene)	0.446
PAI-1	NM_000602	plasminogen activator inhibitor type 1	0.440
REN	NM_000537	renin	0.383
POSTN	NM_006475	periostin, osteoblast specific factor	0.367
CKTSF1B1	NM_013372	cysteine knot superfamily 1, BMP antagonist 1 (DRM/GREMLIN)	0.330
IER3	NM_003897	immediate early response 3	0.303
MMD	NM_012329	monocyte to macrophage differentiation-associated	0.300
CTDSP1	NM_021198	CTD (carboxy-terminal domain, RNA polymerase II, polypeptide A)	0.260
PSMD2	NM_002808	proteasome (prosome, macropain) 26S subunit, non-ATPase, 2	0.256
MAN1B1	NM_016219	mannosidase, alpha, class 1B, member 1	0.254
DKK3	NM_013253	dickkopf homolog 3 (Xenopus laevis)	0.140
NT5C3	NM_016489	5'-nucleotidase, cytosolic III	0.138
DAPK3	NM_001348	death-associated protein kinase 3	0.022
NDUFB4	NM_004547	NADH dehydrogenase (ubiquinone) 1 beta subcomplex, 4, 15kDa	0.012
UBA52	NM_003333	ubiquitin A-52 residue ribosomal protein fusion product 1	-0.002
C9orf5	NM_032012	chromosome 9 open reading frame 5	-0.075
COPG	NM_016128	Coat protein gamma-cop	-0.081
RGS5	NM_003617	regulator of G-protein signalling 5	-0.097
FLJ12236	AK022298	Homo sapiens cDNA FLJ12236 fis, clone MAMMA1001244	-0.104
IDI1	NM_004508	Isopentenyl-diphosphate delta isomerase	-0.126
RPL37A	NM_000998	ribosomal protein L37a	-0.162
ZDHHC18	NM_032283	Zinc finger DHHC domain containing protein 18	-0.175
MO30	M26463	Homo sapiens immunoglobulin mu chain antibody MO30 (IgM) mRNA	-0.194
FLJ20073	NM_017654	Hypothetical protein FLJ20073	-0.215
FLJ30814	AK055376	Homo sapiens cDNA FLJ30814 fis, clone FEBRA2001529	-0.222
PLK2	NM_006622	polo-like kinase 2	-0.230
MMPL1	NM_004142	Matrix metalloproteinase-like 1	-0.230
	Z95126	Human DNA sequence from clone RP1-30P20 on chromosome Xq21.1-21.3	-0.232
BAL	NM_031458	B aggressive lymphoma protein (BAL)	-0.234
OSBP2	NM_030758	Oxysterol binding protein 2	-0.244
PARVB	NM_013327	Parvin, beta	-0.286
CEBPA	NM_004364	CCAAT/enhancer binding protein (C/EBP), alpha	-0.290
ZNF533	NM_152520	zinc finger protein 533	-0.291
ABCA12	NM_015657	ATP-binding cassette, sub-family A (ABC1), member 12	-0.293
LOR	NM_000427	loricrin	-0.322
E2F5	NM_001951	E2F transcription factor 5, p130-binding	-0.356
APM2	NM_006829	Adipose specific 2	-0.360
CAPNS2	NM_032330	CAPNS2 (calpain small subunit 2)	-0.360
MGC13219	NM_032931	Hypothetical protein MGC13219	-0.367
FLJ22202	NM_024883	Hypothetical protein FLJ22202	-0.383

Appendix Table 3.3, continued

Gene	GenBank ID	Gene name	N+ corr
KRT23	NM_173213	keratin 23 (histone deacetylase inducible)	-0.409
PPT2	NM_005155	palmitoyl-protein thioesterase 2	-0.417
PGBD5	NM_024554	piggyBac transposable element derived 5	-0.469
SSH2	NM_033389	SSH2 (slingshot 2)	-0.475
ALOX12B	NM_001139	arachidonate 12-lipoxygenase, 12R type	-0.480
MAL2	NM_052886	mal, T-cell differentiation protein 2	-0.544
ZD52F1	NM_033317	Hypothetical gene ZD52F1	-0.562
EPPK1	AB107036	Epiplakin 1	-0.566
S100A7	NM_002963	S100 calcium binding protein A7 (psoriasin 1)	-0.580
FLJ22184	NM_025094	Hypothetical protein FLJ22184	-0.586
MAP17	NM_005764	membrane-associated protein 17 (MAP17)	-0.591
FLJ13497	AK023559	Homo sapiens cDNA FLJ13497 fis, clone PLACE14518	-0.603
ECM1	NM_022664	extracellular matrix protein 1	-0.610
TGM3	NM_003245	transglutaminase 3 (E polypeptide, protein-glutamine-gamma-glutamyltransferase)	-0.629
RAD17	NM_133344	RAD17 homolog (S. pombe)	-0.631
FLJ30988	AK055550	Homo sapiens cDNA FLJ30988 fis, clone HLUNG1000030	-0.650
C10orf26	NM_017787	chromosome 10 open reading frame 26	-0.653
PALM2	NM_053016	paralemmin 2	-0.655
C4.4A	NM_014400	GPI-anchored metastasis-associated protein homolog (C4.4A)	-0.665
ECG2	NM_032566	Esophagus cancer-related gene-2 protein precursor (ECRG-2)	-0.670
PPL	NM_002705	periplakin	-0.672
HPCAL1	NM_002149	hippocalcin-like 1	-0.674
SLPI	NM_003064	secretory leukocyte protease inhibitor (antileukoproteinase)	-0.677
PI3	NM_002638	protease inhibitor 3, skin-derived (SKALP)	-0.680
FLJ25911	AK098777	Hypothetical protein FLJ25911 [Fragment]	-0.680
CLIC3	NM_004669	chloride intracellular channel 3	-0.691
BENE	NM_005434	BENE protein	-0.698
FLJ00074	AK024480	FLJ00074 protein [Fragment]	-0.699
DKFZp547F134	AL512697	Homo sapiens mRNA; cDNA DKFZp547F134 (from clone DKFZp547F134)	-0.706
PLA2G4B	NM_005090	phospholipase A2, group IVB (cytosolic)	-0.707
	AF339799	Homo sapiens clone IMAGE:2363394, mRNA sequence	-0.708
TRGV9	BC062761	T cell receptor gamma variable 9	-0.710
DSG3	NM_001944	desmoglein 3 (pemphigus vulgaris antigen)	-0.711
FLJ12787	NM_032175	Hypothetical protein FLJ12787	-0.734
LLGL2	NM_004524	lethal giant larvae homolog 2 (Drosophila)	-0.738
SMC5L1	NM_015110	SMC5 structural maintenance of chromosomes 5-like 1	-0.741
ODCP	NM_052998	Ornithine decarboxylase-like protein (EC 4.1.1.17) (ODC-paralogue) (ODC-p)	-0.741
FLJ31161	AK055723	Homo sapiens cDNA FLJ31161 fis, clone KIDNE1000028	-0.747
FLJ21214	AK024867	Homo sapiens cDNA: FLJ21214 fis, clone COL00523	-0.748
SPINK5	NM_006846	serine protease inhibitor, Kazal type, 5	-0.749
KIAA0350	XM_290667	KIAA0350 protein	-0.760
PGLYRPL	NM_052890	peptidoglycan recognition protein L precursor	-0.764
S100A9	NM_002965	S100 calcium binding protein A9 (calgranulin B)	-0.773
DNAH11	NM_003777	Dynein, axonemal, heavy chain-11	-0.776
LAGY	NM_032495	lung cancer-associated Y protein; homeodomain-only protein	-0.793
IVL	NM_005547	involucrin	-0.801
TNFRSF5	NM_001250	tumor necrosis factor receptor superfamily, member 5 (CD40)	-0.802
SRP19	NM_003135	signal recognition particle 19kDa	-0.814
KLK12	NM_019598	kallikrein 12	-0.837
IL22RA1	NM_021258	interleukin 22 receptor, alpha 1	-0.885